MPhil in School of Electronic Electrical and System Engineering

University of Birmingham

A Study of Smart Grids for Railways

Author : **Ms. Sunghee Cho**

Date Submitted : **27 August 2018**

Supervisors : **Dr. Stuart Hillmansen**

& Prof. Felix Schmid

Abstract

The smart grid is a next-generation electric power supply grid in which IT technologies are applied to optimise energy efficiency through the exchange of power information between suppliers and consumers in real time. To date, smart grid research has been focussed on the home and domestic sectors, while little progress has been made in developing smart grids for railways. This likely stems from the complexity of electric railway traction systems, which must supply multiple electrical trains with variable electrical loads depending on varying combinations of trains and train operation requirements including maintaining constant speed and reducing speed. Furthermore, during a daily cycle there are typically variations in the overall total traction demand arising from transitions between operational peak and off-peak periods. Although many attempts have been made to develop smart grids covering both the entirety and sections of railways, it has proven difficult to develop systems to provide rail traction power using renewable energy sources. Therefore, this thesis proposes to assess the hypothesis that renewable energy, which is one of the representative technologies used in smart grids, can in fact be applied in railway traction power systems. This is also a motivation of this thesis for the author; the author wants to suss out this hypothesis.

As a grounding for addressing this hypothesis, this paper begins with a discussion of smart grids and an analysis of trends relating to such grids and railway technologies worldwide in terms of rail way traction, PV array, wind power, energy storage and management systems.

Each related technology is simulated across a number of operational methods using a MATLAB model involving the operation of trains over a 100-km railway powered by a 1,000 MW photovoltaic (PV) array system, a 1,000 MW wind power generation system and a 1,000 MW energy storage system (ESS). It is found that two trains requiring a combined 6,539 MW can be powered by a combination of 7,833 MW of distributed generation and 2,520 MW from the national grid, with 3,280 MW returned to the national grid and 2,216 MW charged to the ESS.

In addition, an economic analysis of a smart grid comprising 45 cases involving combinations of 1,000, 2,000 and 3,000 MW PV array, wind power generation and energy

storage systems and assuming operational start dates in 2020, 2025 and 2030 is carried out. While the smart grid project for a railway starting operation in 2020 is found to not generate business profits, starting the project in 2025 can result in business profits when the ESS capacity is equal to or larger than the distributed generation capacity. Starting the project in 2030 results in business profits if large ESS and PV array systems are use do wing to the significant decrease in the levelised cost of PV electricity generation by that date. In short, projects starting after 2025 are projected to have several advantages, with nearly half of such projects able to obtain economic profit depending on the costs of distributed generation and ESS capacity.

Finally, future work on the use of smart grids for railways and their expected advantages and effects are discussed at the end of this study.

This thesis is also an oriented study that provides guidance in the advance planning of grid systems to be implemented in the near future. In addition to contributions to the development of railway traction systems, it is also hoped that the results will help in intensifying the international competitiveness of railways in terms of greenhouse gas reduction and the reduction of energy imports.

Table of Contents

List of Figures

List of Tables

Glossary of Terms / List of Abbreviations

Term	Explanation / Meaning / Definition
A	Diode Ideal Constant
AC	Alternating Current
ARRA	American Recovery and Reinvestment Act of 2009
ASP	Advanced Supercritical Plant
AT	Autotransformer
ATS	Auto Train Supervision
BCRRE	Birmingham Centre for Railway Research and Education
Capex Cost	Capital Expenditures Cost
CCGT	Closed-Cycle Gas Turbine
CCS	Carbon Capture and Storage
CERTS	Consortium for Electric Reliability Technology Solution
$C_p(\lambda, \beta)$	Power Coefficient of the wind turbine
D	Diode Diffusion Factor
DC	Direct Current
DER	Distributed Energy Resource
DERMS	Distributed Energy Resource Management System
DG	Distributed Generation
DOE	U.S. Department of Energy
DSR	Demand-Side Response
EDLC	Electric Double Layer Capacitor
EREC	European Renewable Energy Council
ESS	Energy Storage System
ETP	European Technology Platform
F	Viscous Friction Coefficient
FERC	Federal Energy Regulatory Commission
G	Actual Irradiance (W/m^2)
GMI	Grid Modernisation Initiative

Term	Explanation / Meaning / Definition
I	Output Current (A)
I_0	Reverse Saturation or Leakage Current of the Diode (A)
I_d	Saturation Current of the first Diode (A)
I_p	Shunt Current (A)
I_{ph}	Solar-induced Current (A)
IGCC	Integrated Gasification Combined Cycle
IHS	Information Handling Service
J	Moment of Inertia
JNR	Japan National Railway
K	The Boltzmann constant (1.381×10^{-23} J/K)
K_i	Temperature Coefficient of I_{sc} (A/K)
KR	Korea Rail Network Authority
Li-ion	Lithium-Ion
LRV	Light Rail Vehicle
MPPT	Maximum Power Point Tracking
MYPP	Grid Modernisation Multi-Year Program Plan
Ni-MH	Nickel-Metal Hydride
NIST	National Institute of Standards and Technology
N_s	Number of series connected cells
OCGT	Open-Cycle Gas Turbine
Ofgem	Office of Gas and Electricity Markets
OLE	Overhead Line Electrification
Opex Cost	Operational Expenditures Cost
P&O	Perturbation and Observation
P_{blade}	Mechanical Power of the wind turbine (N·m/s)
PTD	Power-Transferring Device
PV	Photovoltaic
Q	The Elementary Charge on an Electron (1.602×10^{-19} C)
R	a Rotor Radius or Blade Length (m)

Term	Explanation / Meaning / Definition
R&D	Research and Development
R_p	Parallel Impedance (Ω)
RSPMS	Railway Smart Power Management System
R_s	Series Impedance (Ω)
RTRI	Railway Technical Research Institute
SCADA	Supervisory Control and Data Acquisition
SDMT	Strategic Decision Making Tool
SP	Sectioning Post
SS	Substation
SSP	Sub-Sectioning Post
STC	Standard Test Condition
STS	Single Train Simulator
T	Operating temperature (K)
T&D	Transmission and Distribution
T_{blade}	Rotor Torque
T_g	Generator Torque
T_n	Nominal Temperature (25+273 K)
UHVDC	Ultra-High Voltage Direct Current
V	Voltage imposed on the diode (V)
VSI	Voltage Source Inverter
V_{wind}	Wind Speed (m/s)
λ	Tip Speed Ratio
β	Pitch Angle
η	Efficiency of the generator and the converter
ρ	Air Density (1.225 kg/m^3)
ω_{blade}	Blade's Angular Speed (rad/s)

1   Introduction

In today's highly technological world, the generation and delivery of electricity is a universally important issue. Although energy consumption has historically tracked economic growth, many countries are now attempting to reduce energy consumption on both the customerside by, for instance, developing energy-saving products and cutting off standby power, and the supplier side through the growth of renewable energy generation. In spite of these efforts, electricitygenerationaccounts for 38% of global greenhouse gas emissions in the energy sector (although it represents only 17% of total world fuel consumption owing to the high dependence on fossil fuels and continuing grid inefficiencies [1]). Smart grids, in which multiple technologies are combined and managed using information technology to integrate the generation, transmission and consumption of electricity, have the potential to improve the efficiency of essential energy sources significantly. In this context, smart grids have proven vital in the development of 'green' energy systems and their use has increased rapidly, particularly in the home sector. In the railway sector, however, there has been limited effort to use smart grids owing to the load variabilities characterising this sector. Even though they are latecomers to this effort, railway systems can still be rapidly adapted because they use dedicated systems such as transmission and distribution lines, which means that updating will not require significant overhaul of infrastructure but rather simply finding suitable connection points between railway traction systems and a smart grid.

1.1 Background

A smart grid is a next-generation electrical grid in which information communication technologies are used to exchange power information between suppliers and consumers in real time to enable optimisation of energy efficiency. Such systems are intelligent power systems that can support the efficient management of consumption and supply of power. As shown in Figure 1-1, smart grids combining multiple technologies to intelligently integrate the generation, transmission and consumption of electricity potential can significantly improve the efficiency of essential energy sources.
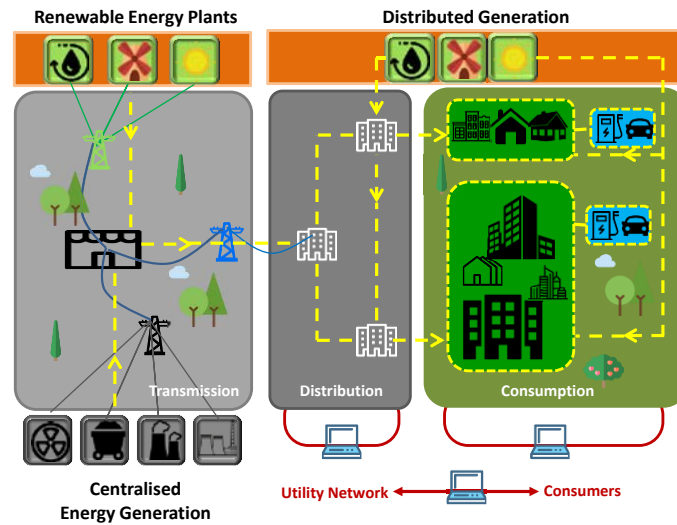
Figure 1-1: Outline of the smart grid

The concept of using techniques to improve the information-sharing relationship between distributed resources arose in the 1980s as 'modernisations of the grid' to allow greater diffusion of alternative and renewable energy sources [2]. The first references in the literature to 'the smart grid' appeared around 2001 in Amin and Wollenberg [2], [3], [4]. Since then, a wide range of research on and opinions regarding the definition, applications and technologies of smart grids have emerged, although the term has become more standardised to incorporate distributed generation, manageable loads, variable ranges of controllers and bidirectional information and telecommunication networks for providing energy reliability, security, efficiency and reduced greenhouse gas emissions [5], [6]. Table 1-1 shows the percentage use of renewable energy worldwide in 2000, 2010, 2014 and projected in to the future. In 2000, only 19.1% of electricity produced came from renewables; this was mostly hydro power, with wind and solar energy comprising only 0.6% of the total renewable electricity production. In 2010, the percentage of electricity generated from wind and solar had increased significantly to 2.1%, and by 2014 it had increased further to 4.0%. The most significant increases were seen in Europe, in which the 2010 renewable penetration was nearly10 times greater than in 2000. The EU have committed to using 100% renewable energy for electricity by 2050, while the US has announced has targeted 80% renewable energy for electricity by 2035. The details of these future plans are discussed later in this paper [7], [8], [9]. Given the significant advances in adapting power systems to the use of

renewable energy worldwide, the railway sector should make efforts to follow suit; this is the motivation for this study.

Table 1-1: Percentage of use of renewable energy in the world

Year	2000			2010			2014			Future	
Country	Total [TWh]	Renew% (Wind/ Solar%)	CO_2 [$MtCO_2$]	Total [TWh]	Renew% (Wind/ Solar%)	CO_2 [$MtCO_2$]	Total [TWh]	Renew% (Wind/ Solar%)	CO_2 [$MtCO_2$]	Renewable Energy %	
World	13,173	19.1% (0.6%)	22,805	18,553	20.2% (2.1%)	29,173	20,302	22.9% (4.0%)	31,220		
Europe	2,954	20.5% (0.9%)	4,151	3,381	25.7% (4.9%)	4,037	3,226	32.7% (10.1%)	3,629	100%	By 2050
N. America	4,093	15.9% (0.5%)	6,176	4,426	17.0% (2.5%)	5,929	4,368	20.0% (4.9%)	5,830	80%	By 2035 in US
S. America	801	62.0% (0.8%)	1,211	1,125	57.6% (1.1%)	1,561	1,275	52.7% (2.3%)	1,703		
Asia	3,345	13.5% (0.6%)	7,004	6,849	16.1% (1.2%)	12,177	8,439	19.5% (2.6%)	14,150		
Pacific	218	18.8% (1.2%)	376	264	18.5% (4.4%)	433	265	22.2% (7.6%)	432		
Africa	379	17.8% (0.2%)	730	531	17.6% (0.6%)	1,050	602	17.9% (0.6%)	1,120		
Mid-East	400	1.7% (0%)	990	743	2.0% (0%)	1,641	883	2.6% (0.2%)	1,880		

1.2 Structure of research

The main purpose of this study is to determine how railways can adopt smart grids and, if they can, when will be the most economical time to do so. Accordingly, this paper is structured as follows:

- Chapter 1 provides a general introduction to smart grids and renewable energy use.
- Chapter 2 reviews the trends in smart grids in Europe, the US, Asia and the railway sector.
- Chapter 3 introduces related technologies - electrical traction, PV array, wind power and energy storage systems (ESS) and management systems - and discusses their underlying theories and respective histories.
- A simulated railway system incorporating related technologies is presented in Chapter 4. To ensure that the energy consumption calculations are more complex, the case considers two trains. The power system is modelled as a simplified structure

- comprising a 1,000 MW PV array, 1,000 MV of wind power capacity and a 1,000 MW ESS.
- Chapter 5 presents a 45-case economic analysis of smart railway grids starting operation in 2020, 2025 and 2030.
- Finally, Chapter 6 provides a general summary of the study and introduces future study prospects along with the expected benefits of the present results.

2   Smart grid trends worldwide

2.1   The case of Europe

In 2006, the European Commission issued a green paper on 'A European Strategy for Sustainable, Competitive and Secure Energy'. The overriding objectives of European Union energy policy are sustainability, competitiveness and security of supply, and the bloc has attempted to craft a coherent and consistent set of policies and measures to achieve these. Around the same time as the green paper, the Commission published the European Smart Grids Technology Platform to set out a vision and strategy for Europe's future electricity networks. In this context, the European Technology Platform (ETP) for Smart Grids was set up in 2005 to create a joint vision for the European networks of 2020 and beyond. The platform includes input from representatives from industry, transmission and distribution system operators, research bodies and regulators. It has identified clear objectives and proposes an ambitious strategy to make their vision a reality for the benefit of Europe and its electricity customers [10], [11].

Meanwhile, in its 'RE-thinking 2050' report the European Renewable Energy Council (EREC) presented a pathway toward a 100% renewable energy system for the EU by 2050, examined the effects that achieving this goal would have on Europe's energy supply system and CO_2 emissions and portrayed the economic, environmental and social benefits of such a system. EREC provided policy recommendations for what would be needed to fully exploit the EU´s vast renewable energy potential. The largest project increase by 2050, in terms of both energy output and contribution to final energy, is in renewable electricity, in particular for pure power options such as wind and PV. The share of renewable electricity in the total final energy demand is projected to increase from 10% in 2020 to 18% in 2030 and finally to 41% by 2050. Overall, 'RE-thinking 2050' shows that, even without an aggressive

energy efficiency policy, the EU could achieve an effective share of 96% renewable energy in final energy consumption by 2050. This would correspond to reduced CO_2 emissions within the EU of 30% in 2020, 50% in 2030 and, finally, more than 90% relative to 1990 emissions in 2050 [12]. Currently, approximately 41 smart grid test beds are being operated or constructed in the EU with a focus on applying distributed generation, the diffusion of smart metering and the cultivation of IT infrastructure. The EU is unique in that it is attempting to develop an energy system integrated not only in terms of grid electrification but also gas, water and heating systems, and the bloc has taken a lead in the development of interoperability and standards [8]. The European smart grid can be characterised as customer–oriented in that is should be:

- Flexible: It should fulfil customers' needs while responding to the changes and challenges ahead.

- Accessible: Connection access to all network users should be possible. In particular, the smart grid should be available to renewable power sources and high-efficiency local generation with zero or low carbon emissions.

- Reliable: The grid should be secure and the quality of supply assured. It should be consistent with the demands of the digital age and resilient to hazards and uncertainties.

- Economical: The best possible value should be attained through innovation, efficient energy management and ensuring a level playing field in terms of competition and regulation [13].

In 2014, the Department of Energy and Climate Change (DECC) in the United Kingdom prepared a 'Smart Grid Vision and Route Map' that describes the vision, benefits, commercial and regulatory frameworks, technological innovation and growth needed for the UK to implement a smart grid. It forecasts that smart grids would be able reduce the cost of the additional distribution reinforcement needed to accommodate the connection of low carbon technologies by between £2.5 and £12bn (about a 20 to 30% reduction). The route map is the result of careful consideration of what investment would be required in the Low Carbon Networks Fund to facilitate a transition to a low carbon future from 2010. The new Revenue = Incentives + Innovation + Outputs (RIIO) framework, which is designed to set up distribution networks that help to decarbonise Britain, was developed as a response to a consultation on demand-side response (DSR) [14]. In 2013, the Office of Gas and Electricity

Markets (Ofgem) produced a detailed paper to summarise stakeholder views on the key challenges to the efficient system-wide use of DSR [15], [16].

2.2   The case of the United States

The Northeast blackout of 2003 was a widespread power outage that occurred throughout parts of the Northeast and Midwest of the US and Ontario in Canada on 14th August 2003 at 16:10. Although some power supplies were restored by 23:00, many customers did not recover power for another two days. It was the second most widespread blackout in history after a 1999 event in southern Brazil. The primary cause of the Northeast blackout was a software bug in the alarm system that caused an alarm to fail and left operators unaware of the need to re-distribute power after overloaded transmission lines hit unpruned foliage. As a result, a manageable local problem cascaded into massive widespread distress on the electric grid, which was exacerbated by decrepit grid facilities. About 55 million people were affected by the blackout [17].

After this severe manmade disaster, the US government announced the Energy Independence and Security Act of 2007 to support the modernisation of the electricity transmission and distribution system in the US and maintain a reliable and secure electricity infrastructure to meet future demand growth. The law also directed the National Institute of Standards and Technology (NIST) to develop smart grid standards that the Federal Energy Regulatory Commission (FERC) would publicise through official rulemakings. Smart grids received further support from the American Recovery and Reinvestment Act of 2009 (ARRA), which set aside $4.5 billion of funding for smart grid development, deployment and worker training [18]. Under the stipulations of these acts, the smart grid framework in the U.S. is ability-based [13]:

- It should be self-healing following a power disturbance event.
- It should enable active participation by consumers in enacting demand response.
- It should operate resiliently against physical and cyber-attacks.
- It should provide quality power to meet 21st century needs.
- It should accommodate all generation and storage options.

President Obama later set a goal of generating 80% of the nation's electricity from clean energy sources by 2035 and evolving consumer expectations to require a more resilient, reliable, sustainable and affordable grid. In this context, the U.S. Department of

Energy (DOE) coordinated the Grid Modernisation Initiative (GMI) and developed the Grid Modernization Multi-Year Program Plan (MYPP) to enact the GMI. The vision of the GMI is 'a future electric grid that provides a critical platform for U.S. prosperity, competitiveness, and innovation by delivering reliable, affordable, and clean electricity to consumers where they want it, when they want it, how they want it'. To help achieve the vision for this initiative, the DOE is targeting three national outcomes: a 10% reduction in the economic costs of power outages by 2025, a 33% decrease in the cost of reserve margins while maintaining reliability by 2025, and a 50% decrease in the net integration costs of distributed energy resources by 2025 [9]. To achieve these goals, there are currently 181 smart grid test sites in the US; the majority of these have been renewing obsolete transmission and distribution lines for use in smart grid systems applying, for instance, the diffusion of smart metering, cultivation of IT infrastructure, automation of distribution and transmission, monitoring for quality of electricity, distributed generations and energy storage systems [8].

2.3   The case of Asia

The South Korean government announced its 'vision of the smart grid' in 2009, representing a foundation for increasing low-carbon green growth though the cultivation of a smart grid. To achieve this vision, a national road map of the smart grid was prepared in 2010. The road map comprises five primary fields of action: smart power grids, smart places, smart renewables, smart transportation, and smart electrification services. The phased objectives of the smart grid are the construction of a top-class smart grid test city by 2012, the construction of a customer-oriented wide area smart grid by 2020 and the construction of the world's first national-scale smart grid by 2030 [19]. To implement these goals, the South Korean government enacted the 'basic act on low carbon green growth' in 2010 to define the administrative office, standards for running renewable energy companies and management processes for achieving the smart grid objectives. The first phased objective, called the 'Smart Grid Test Bed in Jeju' was completed in 2013. The test bed has two substations, four distribution lines and 3,000 customer houses and cost about £140 million to construct five action fields. The test bed uses smart meters located in all houses to exchange power data and control energy consumption for customers and suppliers. It is connected to renewable energy sources such as a PV array system, wind power capacity and electricity charging stations and uses an integrated management centre to monitor and control all of the smart grid equipment

from one location [20]. Sejong City, a special autonomous city and one of a wide range of smart grid cities, plans to increase the use of renewable energy sources from 0.01 to 9.5% by 2020 [21].

Following massive blackouts and meltdowns at a nuclear power plant caused by a tsunami in 2011, Japan moved its national energy policy toward a goal of an increasingly efficient energy supply, energy security and environmental protection. Smart grids have become a natural focus for achieving this policy [22], [23]. The country has become a world leader in smart grid investment, and there have been significant efforts to design a framework on which clean technologies can be utilised in the reorientation of many aspects of human life within a smart grid framework [23]. Japan has a number of reasons to use smart grids in its electricity system, including upgrading the voltage system, increasing the share of renewable energy and enhancing energy savings [24], [25]; however, the chief goal of smart grid employment is the complete shift from fossil fuels to renewable energy resources in developing a low-carbon society [23], [25]. The smart grid, which is defined as a 'next generation energy and community system' by the Japanese Ministry of Economy, Trade and Industry, is to cover various smart city functionalities such as sewage treatment, smart transportation, etc. Although Japan only started to seriously concentrate on smart grids in 2011 following change in the national energy policy, the country had tried to take some steps toward making its electrical grid smarter in 2008. The technical roadmap for smart grid development indicates that, from that year, work should be undertaken in four key areas: power system operation optimisation, distributed generation interconnection, electric vehicles and charging stations and novel buildings and houses. The process of developing a smart grid in Japan under these categories will be continued until 2030 [26].

China has the largest market in the world for electricity manufacturing development and power transmission and distribution (T&D). It has become the world`s major consumer of smart grid technologies, and the Chinese government has developed a long-term scheme for investment in smart grids [27], [28], [24]. In 2009, a strategic framework for smart grid development was outlined by the government at the International Conference on UHV Transmission with the goals of building a strong and powerful electricity grid with an ultra-high voltage transmission corridor and coordinating development at all levels.

There are two main managerial and technical guidelines for smart grid development: realising informationalised, automatic and interactive technological development; and

establishing intensified, concentrated and lean management codes. The Chinese government has planned three stages of smart grid development. In the first stage, which started in 2009 and finished in 2010, there was a focus on research and development (R&D) on smart grid pilot projects and technical innovations. During this stage, 21 demonstration projects, two construction programs and 10 research projects were accomplished. The second stage of the framework took place between 2011 and 2015, in which the emphasis was on promoting smart grids nationwide and, in particular, the acceleration in the construction of ultra-high voltage direct current (UHVDC) lines within the power distribution network. The last stage started in 2016 and will be completed in 2020. In this stage, source distribution stability and interactivity between utility and load will be enhanced and a smart grid will eventually be constructed. The systems to be employed in this project include a technical support system, a standard system, a fundamental grid system and an application system. Under the introduced framework, the under-construction smart grid should be clean, reliable, efficient, transparent and interactive with other grids. Within the smart grid development framework of China, all sections of the power system (generation, transmission, transformation, distribution, consumption and deployment) are considered [29].

2.4 Smart grid trends in the railway sector
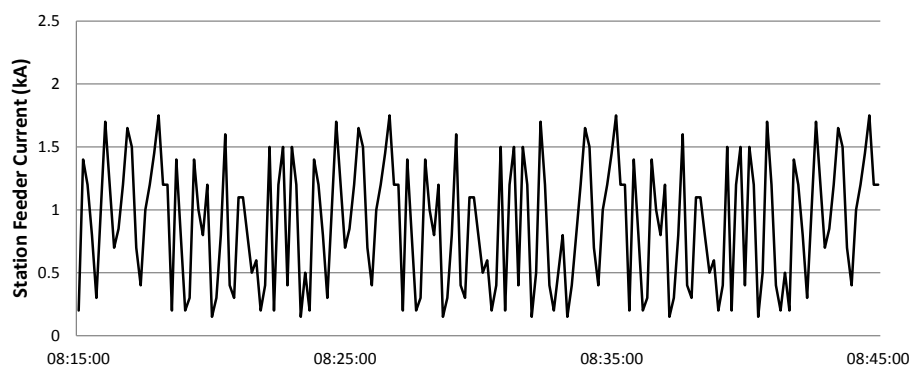
Figure 2-1: Typical electric railway traction loading profile

The difficulties in applying smart grids to railways stem from the unpredictable power requirements of rail networks. In the domestic sector, it is easy to predict required electric

loads throughout the day as well as seasonal fluctuations in heating and air conditioning demand. By contrast, the demand produced by a railway traction system varies significantly and is difficult to predict; this is illustrated in Figure 2-1, which shows a simplified reproduced graph of station feeder current in the UK Main Line Rail at the peak time from 8:15 to 8:45 A.M. [30]. Each section of a railway carriesmultiple trains producingvariable electrical loads that depend uponacombination of train location, mode of operation (acceleration, cruising, coasting and braking) and section gradient and curvature. Furthermore, variations in traction demand occur over a daily cycle spanning peak and off-peak periods, over which thetrain service levels can transition fromhigh/intensive tomoderate. Figure 2-2, which is also a simplified reproduction graph [30], shows this peaky characteristicclearly. From 6 A.M. to 11 P.M, a UK main line railway requires significant traction energy for running trains, with commuting hours requiring more traction energy than other times. Traction energy is also required at night to accommodate maintenance, moving trains to depots and other activities. An added complexity is that trains can be self-generating while braking and represent physically moving electrical loads within the traction [30]. Safety is another critical factor that must be considered and can becompromised during an electricity shortage; for this reason, railway electric traction systems use duplicateprivate lines. These unique characteristics and safety priorities have made adapting smart grids to railway use difficult.
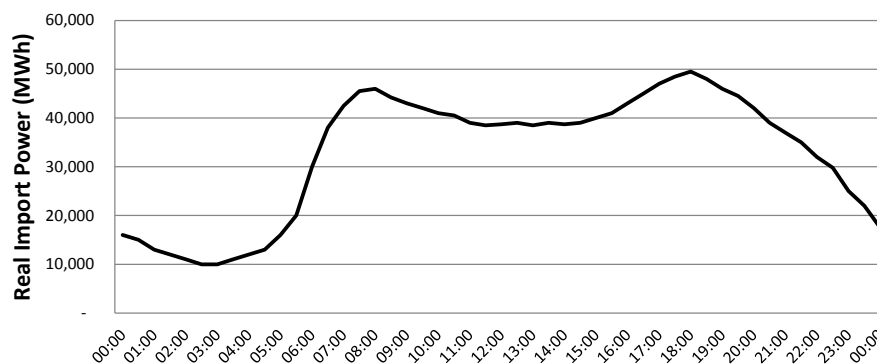
Figure 2-2 :24 hours of an AC traction energy profile of UK main line rail

The benefits of smart grids include grid loss reduction, enhanced system performance and asset utilisation, integration of renewable energy sources, active demand response and energy efficiency. In adapting smart grids to railways, these advantages should all be realised.

However, there are some challenges in the use of a smart grid for railways. The biggest smart grid railway project to date has been MERLIN, a 3-year R&D project co-funded by the European Commission under FP7 and finished in 2015. The overall objective of this project was to investigate and demonstrate the viability of an integrated management system in achieving a more sustainable and optimised energy usage in European electric mainline railway systems [31]. As shown in Figure 2-3, the MERLIN project had ten work packages (WP) [32]:

- (WP01) the analysis of the requirements of the operators and infrastructure managers and the elaboration of a global energy consumption map
- (WP02) reference architecture for smart energy use
- (WP03) the definition of real scenarios involving high speed, mainline and mixed passenger and flight lines by train operating companies and infrastructure managers
- (WP04) the development of new controllable components, modules and applications and protocols of the railway smart grid from the operational side
- (WP05) creation of specific optimisation tools reflecting the strategic point of view
- (WP06) evaluation of the strategic tool
- (WP07) recommendations for implementation and standardisation
- (WP08) dissemination and training
- (WP09) technical coordination
- (WP10) project management
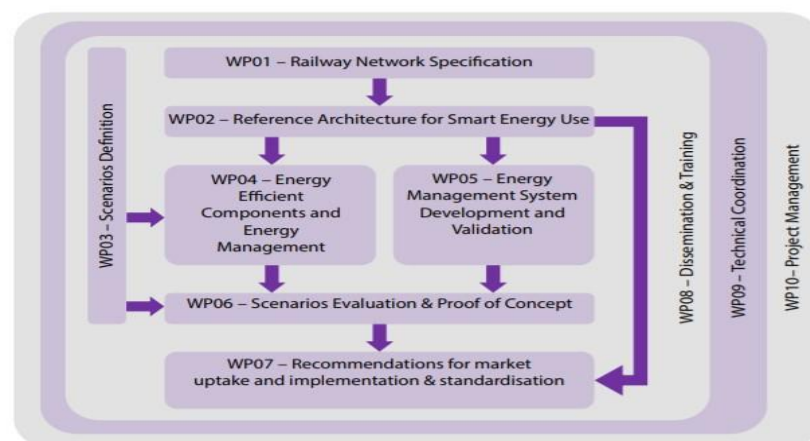
Figure 2-3 : Merlin project organisation [32]

In South Korea, there have been several attempts to incorporate smart grid technology into direct current (DC) railways. In these pilots, energy storage systems such as particularly super capacitors have been used to store regenerative energy from braking for reuse and thereby reduce peak power demand. Although some train and metro stations have installed PV array systems to generate energy for auxiliary facilities, such systems do not supply railway traction power [33], [34]. The East Japan Railway Company has been studying eco-friendly railway enhancements since 2009. Photo voltaic systems have been added to the roofs of high-speed railway stations and their use in the production of energy for railway distribution systems such as signalling systems and stations has been evaluated. In addition, the possibility of using PV power in DC traction power supply systems has been explored [35], [36]. The East Japan Railway also published a paper investigating the installation of a 'Railway Static Power Conditioner' to utilise regenerative energy in external phase lines. The Conditioner has since been installed in traction substations within their high-speed railway system [37]. Furthermore, 98% of railway station in India will be powered by PV array system in 2018. There are 7,137 railway stations in India and 7,000 stations will adapt this system, now 300 railway systems are already completed [38].

Energy management systems are another proposed modification [39] that involve the addition of a power-transferring device (PTD) that can transfer active and reactive power as specified by a control system from one feeding section to another for both the positive and negative phases.

2.5 Hypothesis Development

As discussed in Sections 2.1 to 2.4 above, there has been a good deal of effort expended in developing smart grids to many sectors of the economy. In the context of the railway sector, however, it has proven difficult to tailor renewable generation to railway traction systems. The motivations for the use of smart grids in the overall energy system and in railway systems are shown schematically in Figures 2-4 and 2-5, respectively. This thesis proposes the following hypothesis: renewable energy, which is one of the representative technologies used in smart grids, can in fact be applied in railway traction power systems. This is also a motivation of this thesis for the author; the author wants to suss out this hypothesis.
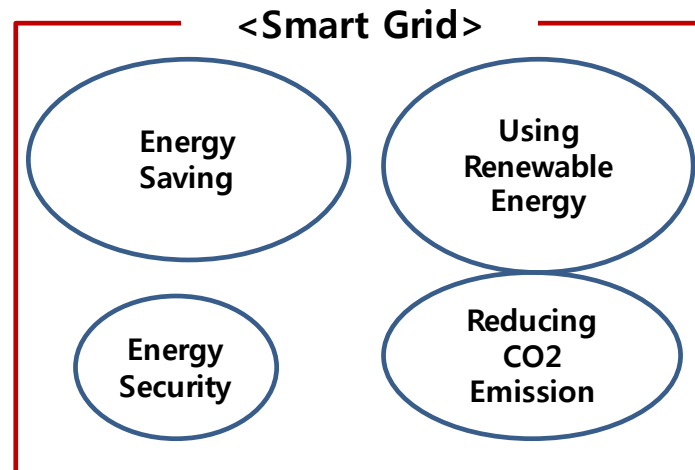
Figure 2-4 : The purpose of a Smart grid usage
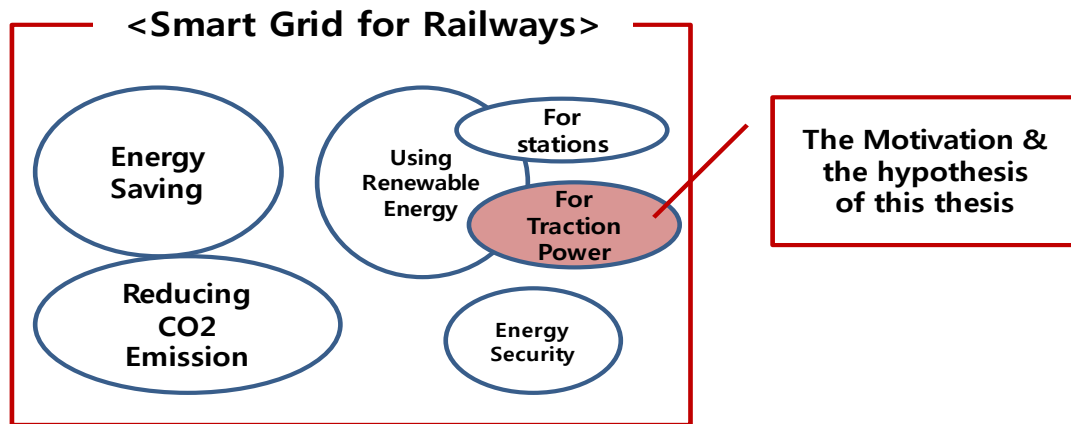
Figure 2-5: The purpose of a smart grid usage for railways

To validate the hypothesis, technologies relating to railway electrical traction systems and renewable energy sources such as wind and solar power system were assessed and simulated in the context of developing a railway smart grid.

2.6   Summary

In this chapter, trends in the development of smart grids in major world regions were discussed and strategies and characteristic definitions relating to the development of smart grids were introduced. Although the evolution of such systems has varied somewhat by country, smart grids have been initially introduced within a context of power stabilisation and have been further developed with energy saving, increasing renewable energy usage and

reducing greenhouse gas emissions in mind. In particular, the smart grid framework in Europe is customer-oriented in that the grid is being designed to be flexible, accessible, reliable and economical for customers, while the smart grid framework in the US is ability-based. Meanwhile, China intends to combine large-scale power generation with a smart grid. In the railway sector, smart grid development has been limited to the production of renewable energy for use in railway stations. The goal of this paper, as outlined in Section 2.5, is to derive a pathway for the application of smart grids to railway traction power systems.

Considering the characteristics of traction loads in railways, it is necessary for a railway smart grid to be:

- Reliable: It should provide quality power to electric trains. The electrical load of trains systems changes depending on the traffic situation and tracks the spatial movement of individual trains.
- Combinable: It should integrate distributed generation sources, including regenerative braking energy, and use these efficiently.
- Accessible and Predictable: It should be not only accessible to monitoring, managing and control systems but should also analyse data and forecast energy consumption.
- Eco-friendly: It should reduce greenhouse gas emissions.
- Economical: The best possible value should be attainable through innovation, efficient energy management and levelling the playing field in terms of competition and regulation.

3 Related technologies

3.1 Electrical traction system

3.1.1 Outline and theory

Electrical railway traction systems are powered by either direct current (DC) or alternating current (AC) supplies. Typically, urban rail services are powered by DC via a third rail or overhead line electrification (OLE), while mainline and high-speed railways are powered by AC supplies using OLE exclusively. Table 3-1 lists systems in common use around the world [40].

Table 3-1: Railway traction systems in common use

Railway	Current	Voltage, kV	Transmission	Countries
Urban	DC	0.6-1.2	Third rail	UK, Switzerland, Germany
		1.2	OLE	Spain
		1.5	Third rail	China
			OLE	UK
Mainline	DC	1.5	OLE	France, Netherlands, UK
		3	OLE	Widespread across Europe, South Africa
	AC	15, 16 2/3 Hz	OLE	Austria, Germany, Norway, Sweden, Switzerland
		11, 25 Hz	OLE	North America
		25, 50/60 Hz	OLE	World Standard
High Speed	AC	25, 50/60 Hz	OLE	World Standard

Both DC and AC supplies for rail are obtained from the public power supply network, which generally provides 132, 275 or 400 kV AC. In a DC network, three-phase duplicated input transformers step down the voltage to 11, 22 or 33 kV AC for input to substations along the line. Within the substation, the voltage is then reduced again before being rectified to the correct DC voltage for the third rail or OLE. In an AC network, no intermediary transformer is required; instead, the substations feed directly from the grid and reduce the voltage to 25 kV for OLE. However, as single-phase AC transformers are used in this case, the load on the grid is balanced by having substations along the route draw from different phases. The rails themselves provide the return path for the current drawn from the catenary. DC and ACsystems are illustrated in Figure 3-1 [41].
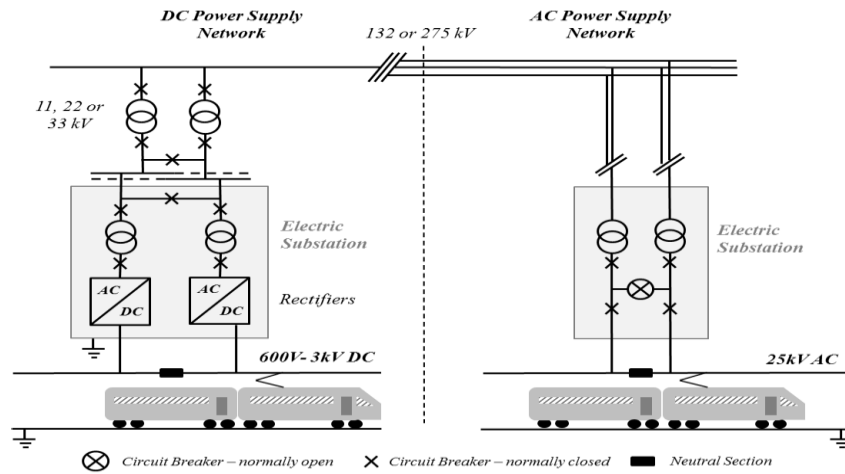
Figure 3-1: Power supply chains for AC and DC railway networks

Neutral sections are installed between substation supplies to electrically isolate live sections from one another; this ensures that there are no phase synchronisation problems between sections powered by different grids, which is particularly important for AC systems that draw from different supply phases. Sectioning posts (SPs), also known as mid-point track sectioning cabins, are also used to prevent contact between different phases, as shown in Figure 3-2 [41]. If the substation spacing is sufficiently long, further sub-sectioning post (SSPs), or intermediate track sectioning cabins, are used to reduce communication interference and separate faulted line sections.
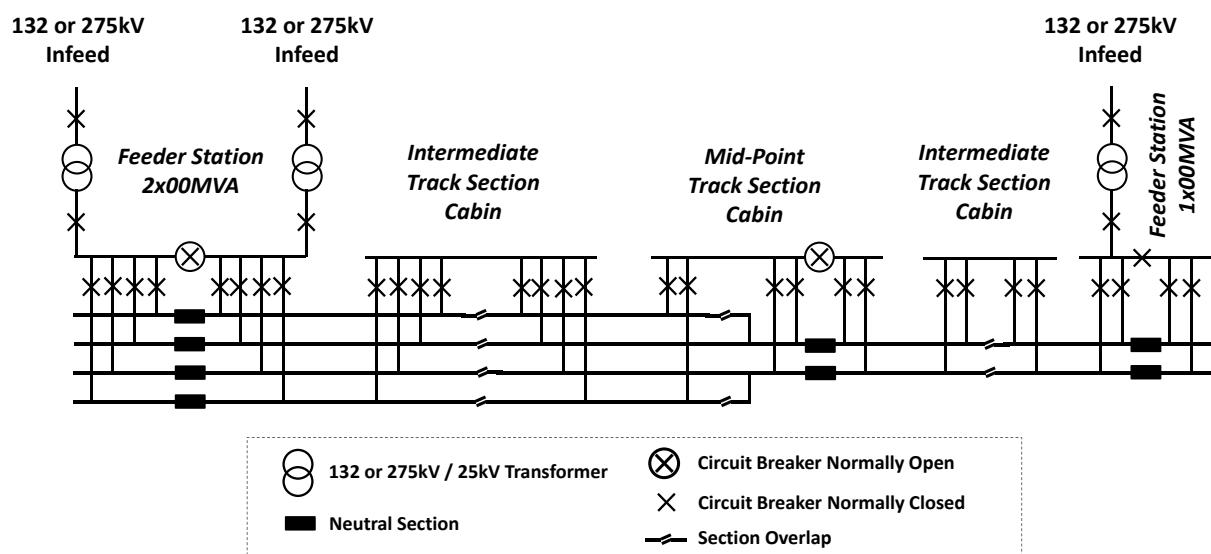
Figure 3-2: AC substation arrangement

Ordinarily, SPs are supplied from both substations; however, if one substation is under fault conditions or maintenance, the supply for that section is fed by extension from another substation, as shown in Figure 3-3.
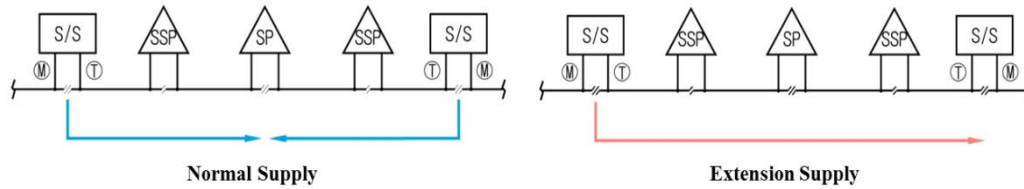
Figure 3-3: Application by Korea Railways

3.1.2 Calculation of electrical traction system

The typical current flow of anauto transformer (AT) system is shown in Figure 3-4. When a train is fed a current *I* from the contact wire, the current travels to both the left and right ATs, which thenreturn the current to the substation [31].
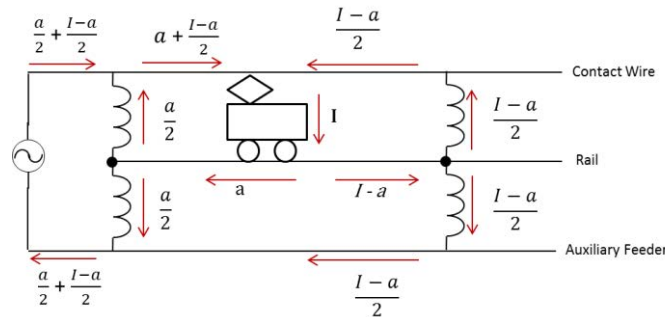
Figure 3-4: The current flow in the AT system

This AT supply system comprises several complicated applications such as transmission lines, catenary systems and ATs. In addition, as trains are moving loads it is not a simple task to analyse the power flow mathematically. A schematic of a simple AT supply system is shown in Figure 3-5.
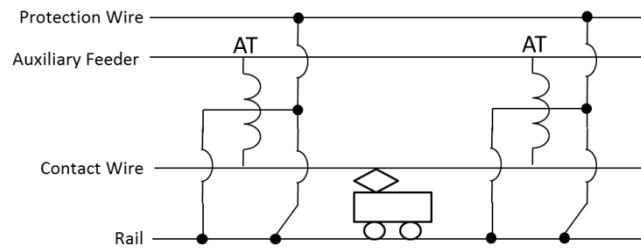
Figure 3-5: Configuration of the AT supply system

The problem of modelling the power flow of an electric railway system can be simplifed by applying multi-terminal modelling using precise electrical characteristics such as points of self- and mutual impedance and changing moving loads. Figure 3-6 shows a multi-terminal modeling of an electric railway traction system in which there is one train operating between a substation (SS) and an SSP. The modelling is divided into three large conductor groups: anauxiliary feeder conductor group, a contact wire conductor group, and a rail conductor group. Correspondingly, it can be defined using a six-terminal model [33].
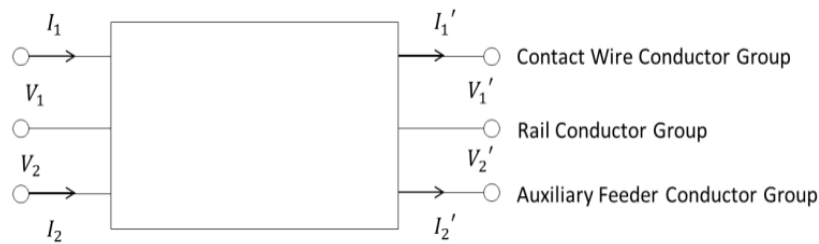
Figure 3-6: The 6-terminal catenary model

3.1.2.1   Equivalent circuit model at the SS
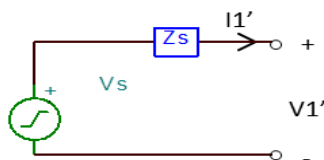
Figure 3-7: Equivalent circuit model for electric power source

There are two circuits modelsused in the SS: an electric power source and an AT. The equations for these twocircuits are developed in advance to produce a representative equation for the SS. Figure 3-7 shows a schematic of the power source from a main transformer at the SS [33], in which Z_S is an equivalent impedance containingthebus impedance of the conventional grid, a transmission impedance and a main transformer impedance at the railway substation. The assembly has a p.u. value of 55 kV.

$$V_s = V_1' + Z_s \cdot I_1' \tag{1}$$

$$V_s = \begin{bmatrix} 1 & Z_s \end{bmatrix} \cdot \begin{bmatrix} V_1' \\ I_1' \end{bmatrix} = M_{zs} \cdot \begin{bmatrix} V_1' \\ I_1' \end{bmatrix} \tag{2}$$
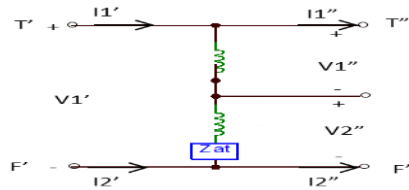
Figure 3-8: Equivalent circuit model for AT at SS

As shown in Figure 3-8, the AT at the SS is fed 55 kV from the source and the secondary side of the AT provides 27.5 kV to the contact-rail andrail-auxiliary feeders,as represented in the two following equations [33]:

$$(a) \begin{cases} V_1' = V_1'' + V_2'' \\ I_1' - I_1'' = -I_1' - I_2'' \end{cases}$$

$$\tag{3}$$

$$(b) \begin{cases} V_1' = 2V_1'' + \dfrac{Z_{at}}{2} I_1'' + \dfrac{Z_{at}}{2} I_2'' \\ I_1' = \dfrac{1}{2} I_1'' - \dfrac{1}{2} I_2'' \end{cases}$$

These can be rewritten as follows:

$$(a)\begin{bmatrix}V_1'\\I_1'\end{bmatrix}=\begin{bmatrix}1&1&0&0\\0&0\frac{1}{2}&-\frac{1}{2}\end{bmatrix}\begin{bmatrix}V_1''\\V_2''\\I_1''\\I_2''\end{bmatrix}$$

(4)

$$(b)\begin{bmatrix}V_1'\\I_1'\end{bmatrix}=\begin{bmatrix}2&0\frac{Z_{at}}{2}&\frac{Z_{at}}{2}\\0&0\frac{1}{2}&-\frac{1}{2}\end{bmatrix}\begin{bmatrix}V_1''\\V_2''\\I_1''\\I_2''\end{bmatrix}$$

Using (1) and (3), the power source equations are derived as

$$\begin{cases}V_s=V_1''+V_2''+Z_s\left(\frac{1}{2}I_1''-\frac{1}{2}I_2''\right)\\V_s=2V_1''+\dfrac{Z_{at}+Z_s}{2}I_1''+\dfrac{Z_{at}-Z_s}{2}I_2''\end{cases}$$

(5)

$$\begin{bmatrix}V_s\\V_s\end{bmatrix}=\begin{bmatrix}1&1&\dfrac{Z_s}{2}&-\dfrac{Z_s}{2}\\2&0\dfrac{Z_{at}+Z_s}{2}&\dfrac{Z_{at}-Z_s}{2}\end{bmatrix}\begin{bmatrix}V_1''\\V_2''\\I_1''\\I_2''\end{bmatrix}=M_{zs}\cdot\begin{bmatrix}V_1''\\V_2''\\I_1''\\I_2''\end{bmatrix}$$
, (6)

from which the source and AT matrix, M_{zs}., for the SS is obtained.

3.1.2.2 Equivalent circuit model for the catenary
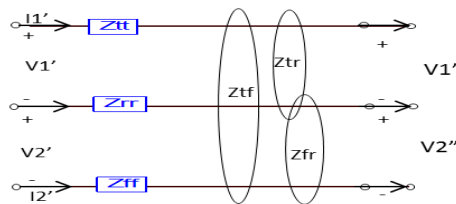
Figure 3-9: Equivalent circuit model for catenary

As shown in Figure 3-9, each conductor has a self-impedance (Z_{tt}, Z_{rr}, Z_{ff}), and; in addition,mutual impedances (Z_{tr},Z_{fr}, Z_{tf}) are present betweeneach conductor [33].

Thus circuit can be represented using the followingequation:

$$\begin{cases} V'_1 = V''_1 + (Z_{tt} + Z_{rr} \text{-} 2Z_{tr})I''_1 + (Z_{rr} + Z_{tf} \text{-} Z_{tr} \text{-} Z_{fr})I''_2 \\ V'_2 = V''_2 + (Z_{tr} \text{-} Z_{rr} \text{-} Z_{tf} + Z_{fr})I''_1 + (2Z_{fr} \text{-} Z_{rr} \text{-} Z_{ff})I''_2 \\ \qquad\qquad I'_1 = I''_1 \\ \qquad\qquad I'_2 = I''_2 \end{cases} \qquad (7)$$

$$\begin{bmatrix} V'_1 \\ V'_2 \\ I'_1 \\ I'_2 \end{bmatrix} = \begin{bmatrix} 1 & 0 & Z_{tt} + Z_{rr} \text{-} 2Z_{tr} & Z_{rr} + Z_{tf} \text{-} Z_{tr} \text{-} Z_{fr} \\ 0 & 1 & Z_{tr} \text{-} Z_{rr} \text{-} Z_{tf} + Z_{fr} & 2Z_{fr} \text{-} Z_{rr} \text{-} Z_{ff} \\ 0 & 0 & 1 & 0 \\ 0 & 0 & 0 & 1 \end{bmatrix} \cdot \begin{bmatrix} V''_1 \\ V''_2 \\ I''_1 \\ I''_2 \end{bmatrix} = M_{cat} \cdot \begin{bmatrix} V''_1 \\ V''_2 \\ I''_1 \\ I''_2 \end{bmatrix} , (8)$$

from which the catenary system matrix, $M_{cat.}$, is derived.

3.1.2.3 Equivalent circuit model for the train

The main reason for using a constant impedance model for a train is usability, as it enables calculation of both sides of the train voltage from the inverse of the impedance matrix, as shown in Figure 3-10 [33].
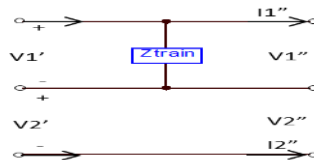
Figure 3-10: Constant impedance model for the traction load (train)

$$
\begin{bmatrix} V_1' \\ V_2' \\ I_1' \\ I_2' \end{bmatrix} = \begin{bmatrix} 1 & 0 & 0 & 0 \\ 0 & 1 & 0 & 0 \\ \dfrac{1}{Z_{train}} & 0 & 1 & 0 \\ 0 & 0 & 0 & 1 \end{bmatrix} \cdot \begin{bmatrix} V_1'' \\ V_2'' \\ I_1'' \\ I_2'' \end{bmatrix} = M_{train} \cdot \begin{bmatrix} V_1'' \\ V_2'' \\ I_1'' \\ I_2'' \end{bmatrix}
\tag{9}
$$

From (9), the train matrix, M_{train}., is derived. However, because trains are dynamic loads this equation, which uses a constant impedance model, might have some tolerance issues. Further dynamic analysis using aconstant-current train model will be required to further validate this formulation.

3.1.2.4   Equivalent circuit model for the AT at the SSP

The AT at the SSP is shown schematically in Figure 3-11 [33].
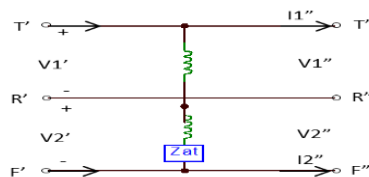
Figure 3-11: Equivalent circuit model for AT at the SSP

This can be then represented using the following equations:

$$
\begin{cases}
V_1' = V_1'' \\
V_2' = V_2'' \\
I_1' - I_1'' = I_2' - I_2'' \\
V_2'' = V_1'' + \left(I_2'' - I_2' \right) Z_{at}
\end{cases}
\tag{10}
$$

$$
\begin{bmatrix} V_1' \\ V_2' \\ I_1' \\ I_2' \end{bmatrix} = \begin{bmatrix} 1 & 0 & 0 & 0 \\ 0 & 1 & 0 & 0 \\ \dfrac{1}{Z_{at}} & -\dfrac{1}{Z_{at}} & 1 & 0 \\ \dfrac{1}{Z_{at}} & -\dfrac{1}{Z_{at}} & 0 & 1 \end{bmatrix} \cdot \begin{bmatrix} V_1'' \\ V_2'' \\ I_1'' \\ I_2'' \end{bmatrix} = M_{ssp} \cdot \begin{bmatrix} V_1'' \\ V_2'' \\ I_1'' \\ I_2'' \end{bmatrix}
\tag{, (11)}
$$

from which the matrix of AT at the SSP, M_{ssp}., is obtained.

3.1.2.5 Equivalent circuit model for the AT at the SP

As shown in Figure 3-12, the SP is the end of the circuit and receives the final voltage and current. Because the AT is a 1:1 transformer, $I_1^{'}$ and $I_2^{'}$ arehave the same values, thecatenary-rail voltage value is the same as the AT winding voltage and the rail-feeder voltage value is a smaller than the AT winding voltage value, which is equal to the voltage drop resulting from the AT initial impedance [33].
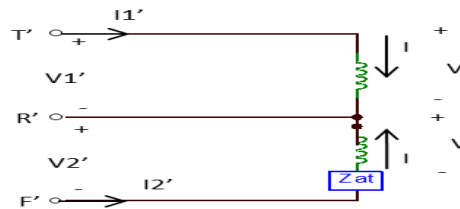
Figure 3-12: Equivalent circuit model for AT at the SP

Mathematically, this is represented as

$$\begin{cases} V_1' = V \\ V_2' = V - Z_{at} \cdot I \\ I_1' = I \\ I_2' = I \end{cases} \tag{12}$$

$$\begin{bmatrix} V_1' \\ V_2' \\ I_1' \\ I_2' \end{bmatrix} = \begin{bmatrix} 1 & 0 \\ 1 & -Z_{at} \\ 0 & 1 \\ 0 & 1 \end{bmatrix} \cdot \begin{bmatrix} V \\ I \end{bmatrix} = M_{sp} \cdot \begin{bmatrix} V \\ I \end{bmatrix} \tag{13}$$

from which the matrix of AT at the train SP, M_{sp}, is obtained.

3.1.2.6 Analysis of the electrical railway traction system
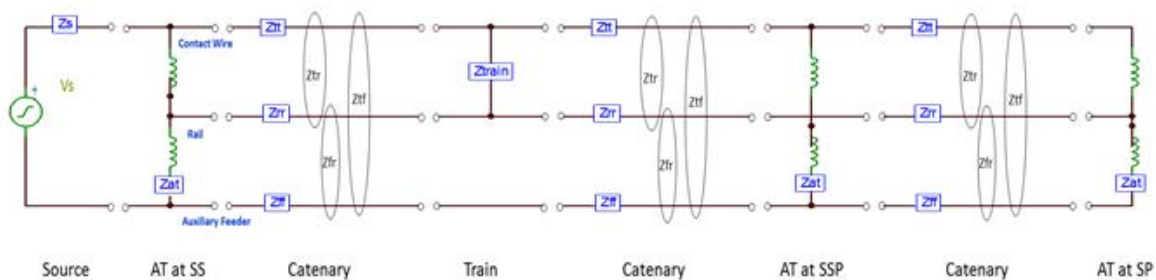
Figure 3-13: A power flow of an electric railway traction system

As shown in Figure 3-13, all circuitsexpressed in the preceding parts of this chapter can be assembled to easily analyse the power flow in an electrical railway traction system. To analyse a model with more than one train, individual copies of the circuit in the figure can simply be connected. Figure 3-13can be expressed by the following equation:

$$\begin{bmatrix} V_s \\ V_s \end{bmatrix} = M_{zs} \cdot M_{cat} \cdot M_{train} \cdot M_{cat} \cdot M_{ssp} \cdot M_{cat} \cdot M_{sp} \cdot \begin{bmatrix} V \\ I \end{bmatrix} \tag{14}$$

The railway traction system power flow circuit shown Figure 3-14 was simulated using MATLAB, with Eq. (14) used to express the circuit values atpoints 1 to 8 in the figure.
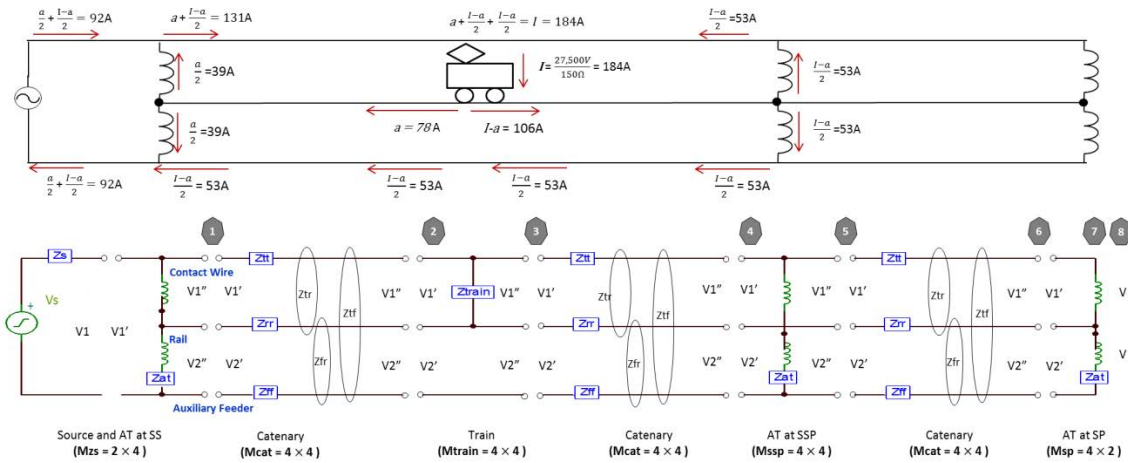
Figure 3-14: Total circuit model for the electric railway traction circuit

Table 3-2: Input Value of Impedance

Name	Value	Name	Value
V_s	55kV	Z_{rr}	0.009+j0.467 Ω
Z_{at}	0.0287+j0.4491 Ω	Z_{ff}	0.122+j0.587 Ω
Z_s	0.1+j0.15 Ω	Z_{tr}	0.053+j0.373 Ω
Z_{train}	150 Ω	Z_{fr}	0.058+j0.369 Ω
Z_{tt}	0.194+j0.731 Ω	Z_{tf}	0.051+j0.361 Ω

Table 3-3: The result of each point of circuit

Point	V_1 [V]	V_2 [V]	I_1[A]	I_2 [A]
1	27,494- j17	27,497+ j3	131+ j3	-53+ j3
2	27,480- j71	27,488- j2	131+ j3	-53+ j3
3	27,480- j71	27,488- j2	-53+ j3	-53+ j3
4	27,484- j43	27,489-j24	-53+ j3	-53+ j3
5	27,484- j43	27,489-j24	-14+ j2	-14+ j2
6	27,486- j36	27,488- j29	-14+ j2	-14+ j2
7	27,486- j36	-	-14+ j2	-
8[1)]	27,450- j135	-	-59+ j5	-

[1)] The value of the point 8 is when one more train is added in this circuit

The input impedance values used in the modelling were obtained from Chang's thesis [33]. As seen in Table 3-3, the numerical and MATLAB-derived current values were identical, validating the use of Eq. (14) equations in modelling the electrical properties of a railway grid for railways. The representative grid-side model developed in this section will be used later on in this paper in conjiunction with single and multi-train simulation models developed primarily at the University of Birmingham.

3.2   Distributed generation

Unlike conventional power stations, distributed generation (DG) systems are small-scale assemblages of generators that operate parallel to or independently of conventional power stations. DG typically uses renewable energy sources such as wind, solar and geothermal power. ESSs can also be included in DG systems. Using an appropriate interface, DG can be coordinated and managed within a smart grid. According to [42], DG can enable the merging of energy supply from many different sources to improve the security of supply. Although the magnitude of power supplies is often considered first, it is also vital to focus on how to merge DG to ensure stability and efficient use of variable sources. Thus,successful operation of DG requires an energy management system, a forecasting system for load and renewable energy unitsgeneration and a data management system. In addition, a powerful front end is required to enablebidirectional communication within the energy management system [43].

3.2.1 Solar cells, panels and arrays and photovoltaic (PV) system

Although the solar cell was invented in 1876, the technology only became commercially viable following the fabrication of the first silicon cell in 1956. Following their use in satellites from the late 1960s, the popularity of solar cells has continued to increase. The Southern Railway first installed solar modules in a power warning lights at a railway crossing in the state of Georgia, USA in 1974. The governments of developing countries began to fund solar energy programmes in the 1980s to enable individual buildings to act as their own electrical power plants. The price of solar cells has continued to decrease, and they have become the cheapest and cleanest power source for small-scale loads located off the grid. The first large-scale solar cell assembly, or solar farm, was built in 1982 at Lugo in the United States and has a1 MW capacity [44]. India is now constructing the world's largest solar farm at Sambhar Lake; its capacity of 4,000 MW is eight times larger than the largest solar farm currently operating in the US [45]. Solar cells are not restricted to land [46], and the world's largest floating solar farm currently helps power London. It contains 23,000 solar panels and its capacity of 6.3 MW can supply electricity to about 1,800 houses [47]. Trackside sound-insulated walls with solar cells are now commercialised in Germany and Switzerland, and solar cells are also of great value for use in railways [48].

3.2.1.1 Outline and theory

A solar cell is an electronic device that directly converts sunlight into electricity. Light shining on the solar cell produces both a current and a voltage to generate electric power. The solar-induced current, I_{ph}, which is directly created by photons from the sun, depends on both the irradiance and temperature, making these the most important factor in electricity generation. The output current I is equal to I_{ph} minus the diode exception losses and the series and parallel resistance losses, R_s and R_p from, respectively. A solar module combines several solar cells, while several solar panels combine to form a solar or PV array. The outputs of the individual panels are combined using components that manage and control the PV array as a unified PV system, as shown in Figure 3-15 [49].
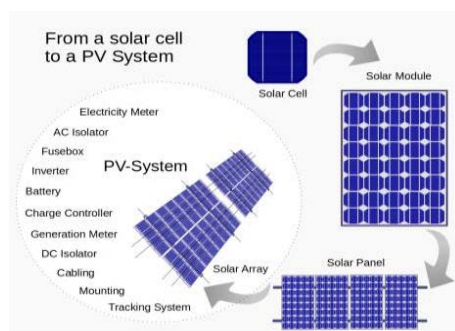
Figure 3-15: Components of photovoltaic system

3.2.1.2   Calculation of PV array system values

(a) The ideal model   (b) With R_s (c) With R_s , R_p
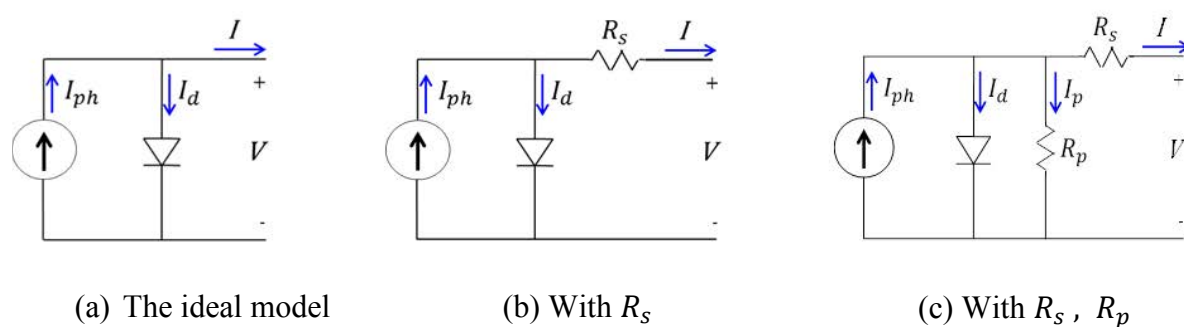
Figure 3-16: The equivalent circuit of a solar cell

Figure 3-16 shows the equivalent circuit of a solar cell; Where,

I_{ph}			I_d	
I_p				
			N_s	
I_0			R_s	Series Impedance (Ω)
		10^{-23}	R_p	Parallel Impedance (Ω)
			K_i	I_{sc}
	10^{-19}		N_s	
T_n			T	
G		m^2		

a) Ideal single model

As the ideal single model as seen in Figure 3-16 (a) does not take into account internal losses of current, the output current I can be obtained using the Kirchhoff law:

$$I = I_{ph} - I_d \qquad\qquad , (15)$$

where the diode current I_d is proportional to the saturation current and given by

$$I_d = I_0 \left[\exp\left(\frac{K \cdot V \cdot T}{A \cdot N_s \cdot q}\right) - 1 \right] \qquad (16)$$

$$a = \frac{N_s \cdot A \cdot K \cdot T}{q} \qquad (17)$$

where a is the thermal voltage, which depends on operating temperature.

b) With R_s

However, it is impossible to ignore the series and parallel resistances R_s and R_p, respectively, because all circuits have losses. When R_s is considered, as shown in Figure 3-16 (b), the circuit equation becomes

$$I_d = I_0 \left[\exp\left(\frac{V + I \cdot R_s}{a}\right) - 1 \right] \qquad (18)$$

c) With R_s, and R_p

When the parallel resistance R_p, is considered, as shown in Figure 3-16 (c), the current is given by

$$I = I_{ph} - I_d - I_p \qquad (19)$$

Combining Eq. (16) into Eq. (19) then gives

$$I = I_{ph} - I_0 \left[\exp\left(\frac{V + I \cdot R_s}{a}\right) - 1 \right] - \frac{V + I \cdot R_s}{R_p} \qquad (20)$$

d) Determination of the parameters

(1) I_{ph}

The quantity of photovoltaic power generated depends on irradiance and temperature; thus, I_{ph}, I_0 and A are used as the PV array parameters.

As seen in Figure 3-17 (a), the output current at the standard test conditions (STC) is

$$I = I_{ph,ref} - I_{0,ref}\left[\exp\left(\frac{V}{a_{ref}}\right) - 1\right]$$ (21)

When the PV cell is short-circuited, this becomes

$$I_{sc,ref} = I_{ph,ref} - I_{0,ref}\left[\exp\left(\frac{V + I \cdot R_s}{a}\right) - 1\right] - \frac{V + I \cdot R_s}{R_p} \cong I_{ph,ref}$$ (22)

The photocurrent depends on both the irradiance and temperature and is given by

$$I_{ph} = \frac{G}{G_n}(I_{ph,ref} + K_i \cdot (T - T_n))$$ (23)

(2) I_0

Because R_p is generally very large, the final term of Eq. (20) should be ignored. There are three primary points under the STC:

First, the open circuit point ($I = 0$, $V = V_{oc,ref}$), where

$$0 = I_{ph,ref} - I_{0,ref}\left[\exp\left(\frac{V_{oc}}{a_{ref}}\right) - 1\right]$$ (24)

Second, the short circuit point ($V = 0$, $I = I_{sc,ref}$), where

$$I_{sc,ref} = I_{ph,ref} - I_{0,ref}\left[\exp\left(\frac{I_{ph,ref} \cdot R_s}{a_{ref}}\right) - 1\right]$$ (25)

Third, the maximum power point ($V = V_{mp,ref}$, $I = I_{mp,ref}$), where

$$I_{mp,ref} = I_{ph,ref} - I_{0,ref}\left[\exp\left(\frac{V_{mp,ref} + I_{mp,ref} \cdot R_s}{a_{ref}}\right) - 1\right]$$ (26)

Here, the (-1) term can be neglected because it is significantly smaller than the exponential term. Eq. (24) can be combined with Eq. (22) to obtain

$$0 \cong I_{sc,ref} - I_{0,ref} \cdot \exp\left(\frac{V_{oc,ref}}{a_{ref}}\right) \tag{27}$$

Therefore,

$$I_{0,ref} = I_{sc,ref} \cdot \exp\left(\frac{-V_{oc,ref}}{a}\right) \tag{28}$$

The reverse saturation current is defined by

$$I_0 = D \cdot T^3 \cdot \exp\left(\frac{-q \cdot \varepsilon_G}{A \cdot K}\right) \tag{29}$$

To eliminate the diode diffusion factor D, this equation is computed at two points in time, T and T_n. The ratio of the two expressions of the equation is then given as

$$I_0 = I_{0,ref} \cdot (\frac{T}{T_n})^3 \cdot \exp[\left(\frac{-q \cdot \varepsilon_G}{A \cdot K}\right) \cdot \left(\frac{1}{T_n} - \frac{1}{T}\right)] \tag{30}$$

Eq. (28) can then be integrated into this to give I_0 as

$$I_0 = I_{sc,ref} \cdot \exp\left(\frac{-V_{oc,ref}}{a}\right) \cdot (\frac{T}{T_n})^3 \cdot \exp[\left(\frac{-q \cdot \varepsilon_G}{A \cdot K}\right) \cdot \left(\frac{1}{T_n} - \frac{1}{T}\right)] \tag{31}$$

A model of the PV array based on the above equations was validated using MATLAB, with I_{ph}, I_0 is calculated using Eqs. (23) and (31), respectively, and Eq.(21) used to calculate I. However, as these equations apply to a single PV cell, they had to be multiplied by factors of N_s, N_p, and N_{sm}, N_{pm} for series and parallel cells and series and parallel arrays, respectively, to iteratively construct a 100kW PV array. In addition, V_{PV_module} is getting was assumed to be equal to V_{oc} with for each iteration. The total output of the PV array system was then iteratively calculated using Eqs. (32) to (36) using the procedure in Figure 3- 17:

$$V_{PV\_module} = V_{oc} \tag{32}$$

$$I_{PV\_module} = N_p \cdot I \tag{33}$$

$$I_{PV\_array} = N_{pm} \cdot I_{PV\_module} \tag{34}$$

$$V_{PV\_array} = N_{sm} \cdot V_{PV\_module} \tag{35}$$

$$P_{PV\_array} = V_{PV\_array} \cdot I_{PV\_array} \tag{36}$$
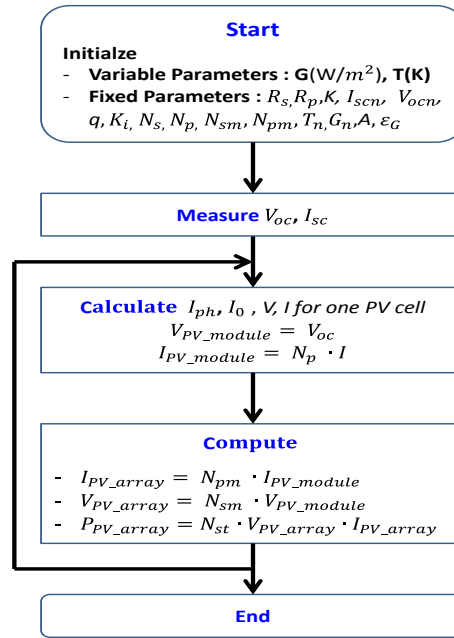
Figure 3-17: The method of calculation of PV array system

e) P&O Maximum Power Point Tracking (MPPT) algorithm for maximum power
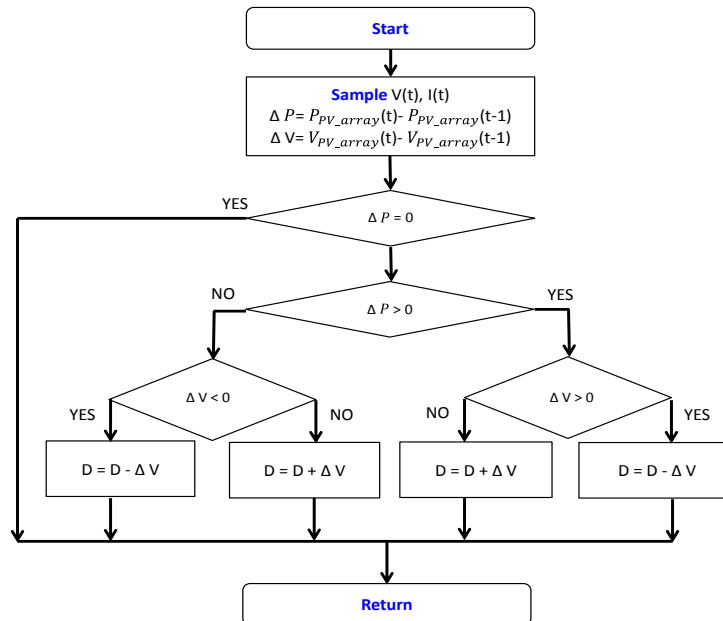
Figure 3-18: The method of a P&O MPPT algorithm

Many maximum power point tracking (MPPT) approaches have been developed to maximise PV array power. MPPT algorithms are commonly used to maximise power extraction from intermittent, renewable sources. In this study, Perturbation and Observation (P&O), the most commonly used algorithm for tracking maximum power owing to its simplicity and limited parameter requirements [50], was used in Figure 3-18. P&O follows a simple iterative approach in which the voltage is varied and the resulting power level measured. If the new power level is higher than the previous value, the voltage is kept constant; if it is reduced, the voltage is incremented and the process is repeated.

3.2.2 Wind power system

Wind is the oldest renewable energy source. It was used to propel boats along the Nile River in 5,000 BC and by the Persians to pump water and grind grain between 900 and 500 BC. Wind power technology spread to Northern Europe around 1,000 AD, and the Netherlands adapted windmills to help drain lakes and marshes in the Rhine River Delta [51]. The first windmill for electricity production was built in Glasgow, Scotland in 1887 by Professor James Blyth of Anderson's College and was run for 25 years to power his home. At nearly the same time, Professor Charles F. Brush built a 12 kW wind turbine to charge 408 batteries stored in the cellar of his mansion [52]. Today, wind power generators range from tiny plants used for battery charging at isolated residences to near giga watt-size offshore and onshore wind farms that supply electricity to national electrical grids. The largest onshore wind farm, called Gansu Wind Farm, is located in China; it had a capacity of over 6,000 MW in 2012 and will be increased to 20,000 MW by 2020. The 630 MW London Array, which was built in 2013, is the largest offshore wind farm. Many large wind farms are under construction, including the 700 MW Sinus Holding Wind Farm in Romania and the 420 MW Macarthur Wind Farm in Australia [53].

In a rail context, it has been proposed that wind power can be harnessed from moving trains. However, equipping fast-moving trains to do so would also increase their air resistance (drag), requiring more energy to overcome the drag. However, such setups could be used to assist in train braking, as the extra drag would increase deceleration. More research is required in this area.

3.2.2.1   Calculation of wind power generation parameters

Figure 3-19 [54] shows a wind generation system in which a wind turbine drives an electrical generator to produce electricity. Wind passing over the turbine blades exerts a turning force that rotates a shaft within a nacelle coupled to a gearbox. The gearbox increases the rotational speed to a level compatible with a generator, which uses magnetic fields to convert the rotational energy into electrical energy [55].
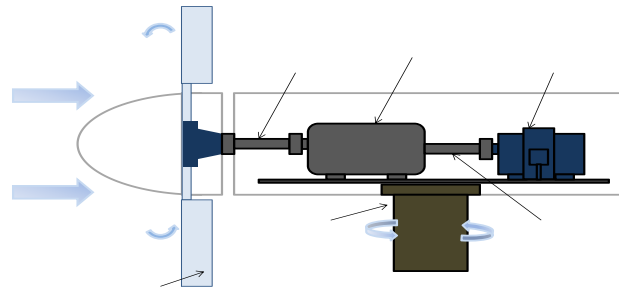
Figure 3-19: The shape of a wind turbine
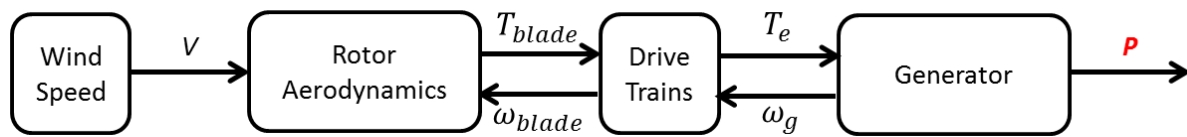
Figure 3-20: Wind turbine scheme

Figure 3-20 shows a schematic of a typical turbine-based wind energy conversion system [56] comprising an aerodynamic system, a drive train and an electrical generator. The static characteristics of a wind turbine can be described in terms of the relation between total power extracted from the wind and the mechanical power generated by the turbine. Using this formulation, a basic model for a wind turbine in electric power system can be constructed [57]:

$$P_{wind} = \frac{1}{2}\rho\pi R^2 V_{wind}^3 \tag{37}$$

Where ρ is air density (1.225 kg/m^3), R is the rotor radius or blade length (m) and V_{wind} is the wind speed (m/s). However, it is impossible to extract all of the wind's kinetic energy, and the fraction of power extracted by the turbine is a function of the power coefficient

$C_p(\lambda, \beta)$ of the wind turbine in terms of the tip speed ratio λ, and the pitch angle β.of the wind turbine [57] given by

$$P_{blade} = C_p(\lambda, \beta)P_{wind} \tag{38}$$

where P_{blade} is the mechanical power of the wind turbine (N·m/s). Although the ideal power coefficient is given as $C_p(\lambda, \beta) = \frac{16}{27} = 0.59$, realistic values of is about up to 0.44 [58] (Betz' limit [57]) can be obtained.

The tip speed ratio λ is defined as

$$\lambda = \omega_{blade} R/V_{wind} \tag{39}$$

Where ω_{blade} is the blade's angular speed (rad/s), R is the rotor radius (m) and V_{wind} is the wind speed (m/s). Assuming a constant V_{wind}, λ will be equivalent to the rotational speed of the wind turbine rotor [57].The highest value of C_p is typically obtained for λ values in a range of eight to nine (i.e., when the tips of the blades move eight to nine times faster than the incoming wind).

The rotor torque T_{blade} is given by

$$T_{blade} = \frac{P_{blade}}{\omega_{blade}} = \frac{C_p(\lambda, \beta)P_{wind}}{\omega_{blade}} = \frac{C_p(\lambda, \beta) \cdot \frac{1}{2}\rho\pi R^2 V_{wind}^3}{\omega_{blade}} \tag{40}$$

and the dynamic equation of the wind turbine is given as

$$\frac{d\omega_{blade}}{dt} = \frac{1}{J}\left[T_{blade} - T_g - F \cdot \omega_{blade}\right] \tag{41}$$

where J is the moment of inertia, F is the viscous friction coefficient and T_g is the generator torque.

The power output of a wind energy conversion system is given by

$$P_{out} = P_{blade} \cdot \eta = (\frac{1}{2} C_p(\lambda, \beta) \rho\pi R^2 V_{wind}^3) \cdot \eta \tag{42}$$

where· η is the net efficiency of the combined generator and converter system.

Using λ, P_{out} can be written as

$$\lambda = \omega_{blade} R/V_{wind} \tag{43}$$

$$P_{out} = (\frac{1}{2} C_p(\lambda, \beta) \rho\pi\omega_{blade}^3 R^5\lambda^3) \cdot \eta \tag{44}$$

3.3 Energy Storage System (ESS)

ESSs are used in distributed generation to provide power to loads in the manner of other types of distributed generation sources and also to merge various generation sources. At the grid side, ESSs are used to mitigate grid variability and uncertainty; at the generation side, they are used to convert uncontrollable variables and partially unpredictable resources into controlled and predictable energy flow [59]. By matching generation for loads with time-variable power density and load-following energy density, an ESS can smooth the output from individual distributed generation sources. Because different renewable generation sources have differing and often hybrid characteristics, an ESS must be capable of operating over a wide range of power and energy densities; as no single energy storage technology has this capability, an ESS will comprise combinations of technologies including batteries, super capacitors, fuel cells and flywheels [60].

3.3.1 Outline and theory

ESS technologies have advanced significantly and provide benefits such as peak load demand smoothing while reducing energy consumption and initial system cost. Metrics used to characterise storage systems include the energy-to-weight ratio (Wh/kg, or E) and the energy-to-volume ratio (Wh/L, or energy density). However, the power density of a storage system (W/kg, or P) is the most important factor in hybrid traction applications. Whereas energy density corresponds to the ability to supply power for a prolonged length of time, power density reflects the ability to deliver pulse power at increased levels for short periods of time. In application, pulse power delivery can last up to 30 s. The classical relationship between energy density E and power density P is given by the Ragone plot, in which a set of data points is plotted by specific energy density E on the Y-axis and by specific power density P on the X-axis [61], as shown in Figure 3-21. Using a Ragone plot, the energy characteristics of several storage devices can be directly compared. Although such characteristics are well established at single cell level, it is not clear how they are modified at the module and storage device levels. To address the lack of comparative analysis in the literature on power and energy densities achieved by practical railway energy storage applications, a Ragone plot showing the characteristic relationship between power and energy density in recent and past systems is provided in Figure 3-22. Because electric double layer capacitors (EDLCs) discharge faster than flywheels or batteries, they are more suitable for

use in light rail vehicles (LRVs) in terms of running catenary-free systems and saving energy. Flywheels have an operating discharge time that falls between those of batteries and EDLCs, which makes them acceptable for use in electrified railways; however, as they are generally larger than either batteries or EDLCs they are unsuitable for use in on-board systems. Furthermore, although adapted batteries can be installed in substations and at track sides, their limited life cycles can be a disadvantage in a railway context [62].
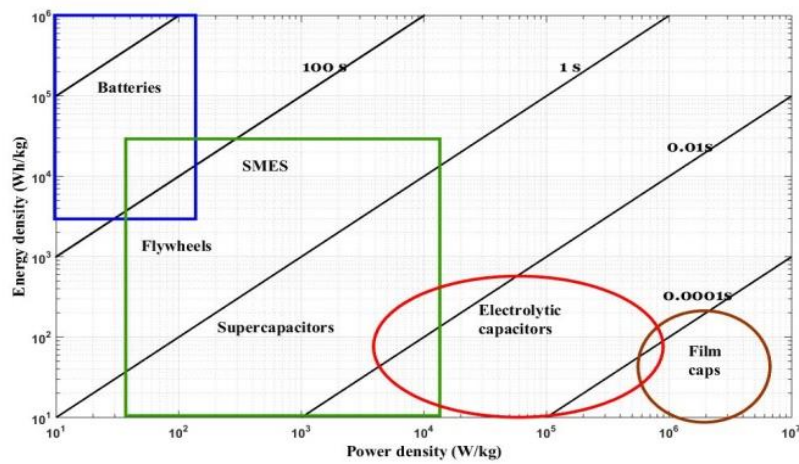
Figure 3-21: A Ragone plot
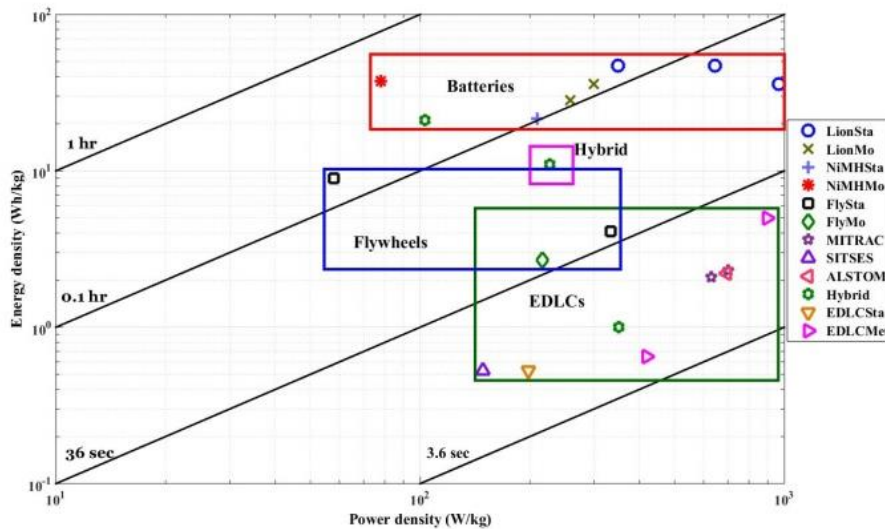
Figure 3-22: A Ragone plot of real energy storage devices for electrified railways

The most wide spread form of energy storage is the battery, which has long been used to save energy for use in fault situations and to reduce peak power, Similarly, batteries have

been adapted for use in catenary-free operating systems. Whereas conventional lead-acid batteries have been extensively studied, modified and deployed in railway systems, lithium-ion (Li-ion) and nickel-metal hydride (Ni-MH) batteries are now emerging as technologies for transport applications owing to their high energy densities. Lead-acid batteries were first used in 1912 in Japan to reduce energy demand and support the power supply system during short-term fault cases. These batteries were in use for 15 years before new substations were built [63], [64]. In 1980, the Japan National Railway (JNR) installed a lead-acid battery post at Nakajima station in Kobe as part of a study analysing their usefulness in voltage drop compensation; they were found to be very effective [63], [64]. In 2005, the Kobe Municipal Transportation Bureau tested Li-ion batteries installed at the Myodani substation of the Seishin-Yamate line, which has an average slope of 2.9% over a distance of 4 km. Many attempts have also been made to develop catenary-free systems, starting in 2003 when the Japanese Railway Technical Research Institute (RTRI) installed Li-ion batteries on a remodelled tram, which was tested at a maximum speed of 40 km/h over a total distance of17.4 km with an inter-station spacing of 250 m. The on-board Li-ion battery unit comprised168 cells connected in series and had a rated capacity of 33 kWh at 605 V.

In 1988, Japan's Keihin Electric Express Railway installed flywheels for storing regenerative energy at Zushi station. The flywheels were capable of saving up to 12% of the total energy, and the system is still operating [63]. The London Underground installed flywheels to recover voltage drops in 2000. Although the nominal voltage in the Underground is 630 V, prior to the installation the voltage drop varied from 180 to 450 V during rush hour. The use of flywheels increased the average voltage by up to 530 V [65].

As mentioned above, EDLCs have good performance in terms of high power densities, reduced charging and discharging times, long life cycles, reduced maintenance costs and lower internal resistance and are therefore widely used for storing regenerative braking energy in public transportation [66]. These advantages have led to a significant amount of attention in both the academic literature and the industrial sphere. One significant product of this research is the MITRAC Energy Saver by Bombardier. From 2003 to 2008, a 300 kW MITRAC was installed onboard a light rail vehicle (LRV) by the German operator Rhein-Neckar-Verkehr Gmbh in Mannheim. It reduced the consumption of traction energy by 30% [66], [67] and the current peak and voltage drop by 50% each. The 1 MW SITEAS SES developed by Siemens can also save nearly 30% of energy while regulating voltage.

While there has no shortfall in active interest in adapting energy storage systems to the railway sector, the available energy storage systems have been limited in size relative to the state-of-the-art technologies. According to the Information Handling Service (IHS), the global pipeline of planned battery and flywheel projects had reached 1.6 GW by the end of 2015, with a nearly 3-GW energy storage portfolio planned for rollout in the near future [68]. Many railway companies still firmly believe that sufficient reliability can only come via private main electric lines from conventional substations; however, ESSs can be a big part of ensuring reliable power, as will be shown in the simulation model results in Chapter 4.

3.4   Management system

Distributed generation systems (DGs) are smaller than conventional power stations and often operate either independent or in parallel with them. DGs typically use renewable energy sources such as wind, solar and geothermal power and often include ESSs. Using an interface, a DG can be coordinated and managed within a smart grid. DGs can enable the merging of power produced from many different sources, thereby improving security of supply. Although the focus has generally been on the quantity of power delivered, stability concerns have spurred interest in using DGs with merging capability to ensure efficient power system use. For successful operation, a DG requires an energy management system, a system for forecasting the load and power generation of renewable energy units and a data management system. DGs also require a powerful front end for bidirectional communication within the energy management system [42], [69],[70], [71], [72], [73] .

3.4.1 Outline and theory

Much of the research on smart grid management systems has been focused on micro grids, which are defined as low- or medium-voltage systems with distributed energy sources, storage devices and controllable loads that can be either isolated or connected to the main power system. Micro grids are vital components of smart grid architecture and represent microcosms of such grids [74] in the form of cells or nodes that can constitute a hierarchical grid architecture [75]. Many studies on micro grid management systems have been undertaken and, in this chapter, micro and smart grids are considered to be the same technologies. In 2002, the Consortium for Electric Reliability Technology Solution (CERTS) published a white paper on the integration of distributed energy resources using the 'CERTS

Micro Grid Concept' [76]. The paper introduced a micro grid structure in which loads and micro grid sources are integrated into a single system that can provide both power and heat. The micro sources that comprise the DGs within a smart grid must apply power electronics to provide the flexibility required to ensure controlled operation as a single aggregated system. This control flexibility allows a micro grid to insert itself into the bulk power system as a single controlled system, with plug-and-play simplicity for all sources ensuring that local customers' needs are met.

A micro grid has two typical operational modes: grid-connected mode and islanded mode. In the former, a micro grid operates within a utility grid and, when the utility grid fails the micro grid must be automatically disconnected from the utility grid and converted to islanded mode to ensure a continuous supply of power to important loads within the micro grid [77], [78]. Accordingly, the micro grid's control system is a vital element in supplying power in are liable, stable and seamless manner [79]. Micro grid controllers must ensure the following:

- that micro sources work properly at either the predefined operating point or close enough to it to satisfy operating limits;
- that active and reactive power is transferred to meet the requirements of the micro grid and/or the distribution system;
- that disconnection and reconnection processes are conducted seamlessly;
- that market participation is optimised through the optimised production of local micro sources and power exchange with the utility;
- that in cases of general failure the micro grid is able to operate through a black-start;
- that the ESSs can support the micro grid and enhance system reliability and efficiency.

Based on the above requirements and controller coordination needs, several different control systems are used, namely, master-slave control, peer-to-peer control and multi-agent control [77], [78].

The master-slave control system is used by micro sources control to control other micro sources via a voltage source inverter (VSI). In this scheme, the master inverter adopts an active and reactive power (PQ) control method to perform power management and variable renewable energy suppression in grid-connected mode, in which the voltage and frequency of the micro sources are governed by the utility grid. In islanded mode, the master

inverter adopts a voltage/frequency (V/f) control method to provide simulated grid voltage references for slave inverters that adopt a PQ control method [77], [78], [80].

In a peer-to-peer control system, all micro sources have equal status in terms of control and there is no hierarchy among controllers. In this scheme, each micro source controls itself using its own controllers. Micro grid plug-and-play can only be implemented through peer-to-peer control. Because micro sources are controlled using local information in peer-to-peer systems, no communication line is needed [78]. When a micro grid is in islanded mode under peer-to-peer control, each micro source is controlled through via a droop control strategy that regulates the voltage and frequency within the micro grid using real power from the micro sources to calculate the ideal operating frequency. However, this method has several weaknesses that limit its applicability; in particular, it is not suitable for use in paralleled systems that must share nonlinear loads, as the control units in such systems must take harmonic currents into account to balance active and reactive power [74]. Several attempts have been made to offset this problem, including the use of novel control loops that adjust the output impedance of the units by adding output effective resistors or reactors [74], [81], [82]. Although the droop method does not require communication between sources, there are many issues in terms of system stability, backup of power-frequency droop operation and grid-interactive operation that require further investigation [74].
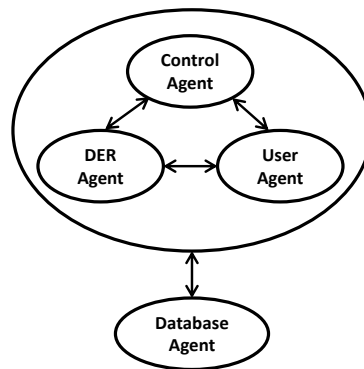
Figure 3-23: The multi-agent system architecture

Multi-agent control systems are very similar to traditional grid control systems and apply the concept of breaking down complex problems and large entities into smaller and simpler problems handled by several entities, as shown in Figure 3-23 [83]. A multi-agent system comprises four agents: a control agent, a distributed energy resource (DER) agent, a user agent, and a database agent. The control agent is responsible for monitoring voltage and

frequency to detect contingency situations or utility grid failure and for sending signals to the main circuit breaker to change to islanded mode. It also receives real-time electricity prices from the utility grid. The DER agent is responsible for storing DER information and monitoring and controlling the DER power level and its connect/disconnect mode. The user agent delivers real-time information from a user to the micro grid and monitors energy consumption, enabling users to control the status of loads. The database agent is responsible for storing system information and recording the messages and data shared among agents.
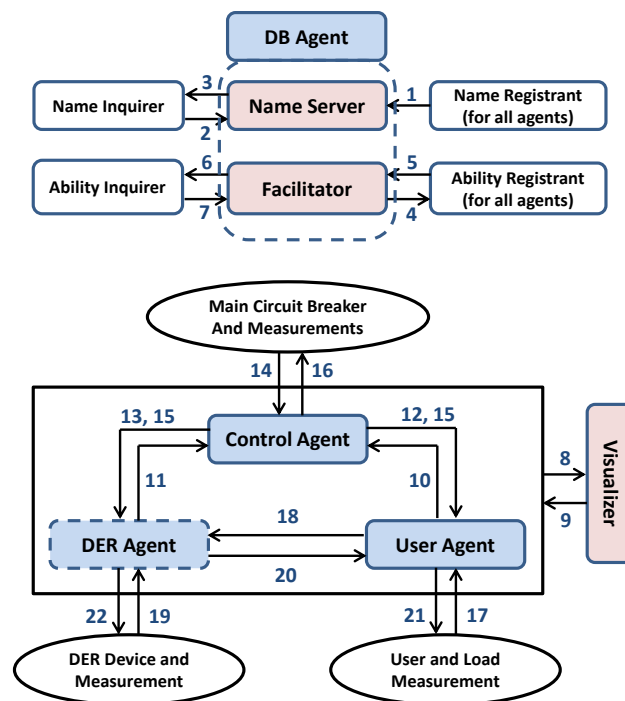
Figure 3-24: A diagram of a multi-agent system

Figure 3-24 shows a schematic multi-agent system [83]. From steps 1 to 7, all agents relay their names, IP addresses, facilitators and abilities to the database agent. From steps 8 to 13, the user and DER agents register with their associated control agents. In step 14, the control agent receives measurements from the main grid, and instep 15 it publishes that information to its registered agents. If the utility grid fails, the control agent sends a signal to the main circuit breaker in step 16, and the user agent receives power requirement information from the loads and sends commands to the DER agent in steps 17 and 18, respectively. In step 19, the DER agent receives information from the DER, and in step 20 it

sends this information to the user agent. The user and DER agents react to their environment using rules predetermined by the user in steps 21 and 22, respectively. The visualiser collects all messages exchanged among all agents in steps 8 and 9, allowing these messages to be displayed [83].

Figure 3-25 illustrates the operation an ESS. If the amount of energy generated by the DGs is larger than the load, the system works in charge mode. In charge mode, an ultra-capacitor is charged to full, after which a battery system and then a fuel cell water electrolyser are charged. If the system is still in charge mode following full charging of all of these storage systems, power is fed back to the grid. If the amount of energy generated by the DGs is smaller than the load, the storage system changes to discharge mode, in which the ultra-capacitor, then the battery system and, finally, the fuel cells are drained in turn. If, the system is still in discharge mode following draining of all of these sources, power is extracted from the grid to fulfil the load. The system checks the amount of distributed energy and the load each second to enable rapid mode change. Overall, this scheme is a very stable and efficient method for utilising the characteristics of ESSs through a skilful balance of the respective components, i.e., an ultra-capacitor has a very quick response, while a small capacitor can manage rapid, sudden, and small changes in power and a battery system with a large capacitor can handle long-term and large-scale power changes. Although this study looks at ESSs with ultra-capacitors, battery systems and fuel cells, a railway system smart grid can have many energy storage configurations.
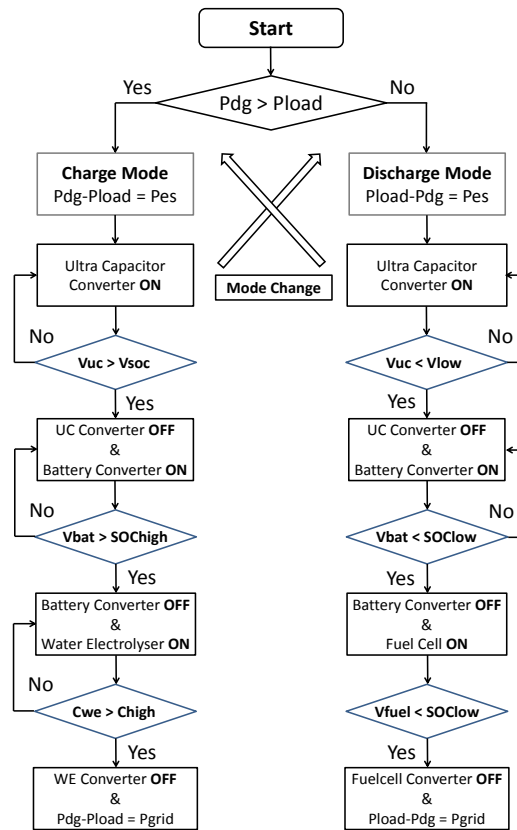
Figure 3-25: The operation method of an energy storage system

This chapter discussed the technologies used in smart grids and traction systems and outlined their under lying theories. Methods for calculating the parameters of electrical traction, PV array, wind power, ESSs and management systems were presented. Multi-terminal modelling was presented as a method for determining the exact electrical characteristics of electric railway traction systems characterised by moving load features. An ESS tailored to use in railways and a detailed multi-agent control system for use in a smart grid were also presented. In the next chapter, a simulation in which these technologies are applied together will be presented to validate their usefulness in a railway smart grid environment.

A Study of Smart Grids for Railways

4   Simulation of a smart grid for a railway
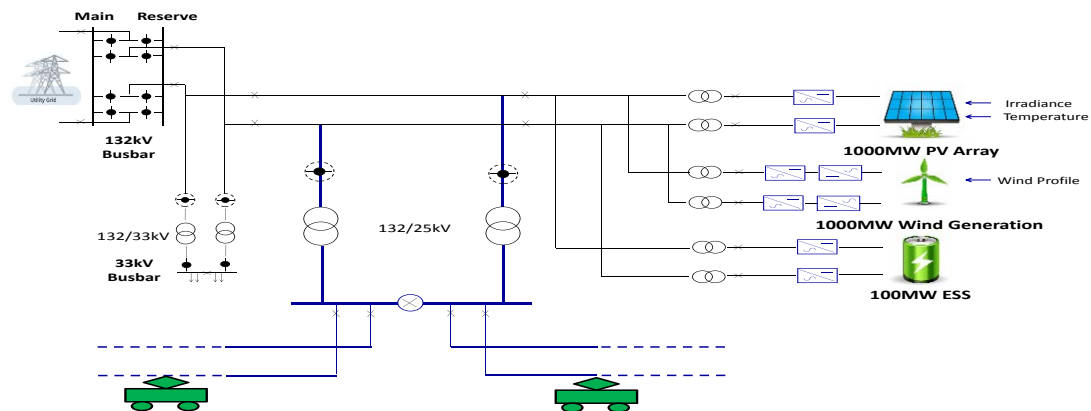
Figure 4-1: Schematic arrangement of a smart grid for railways

Figure 4-1 shows a schematic of a railway simulation that uses a smart grid comprising three DGs—a PV array system (1,000 MW), a wind power system (1,000 MW) and an ESS (1,000 MW)—to supply a 100-km-long railway traction system. This configuration is used because it is representative of the most commonly used renewable generation systems while applying realistic capacities to these.

4.1   Simulation of loads (trains)

Figure 4-2 shows a basic layout and model of a 100-km-long railway that was validated against draft BS EN 50641 25-0-25 kV [84]. In this schema, four trains travel between stations A and F following the timetable presented in Table 4-1. The model was selected to enable comparison between the results of this thesis and draft BS EN 50641.
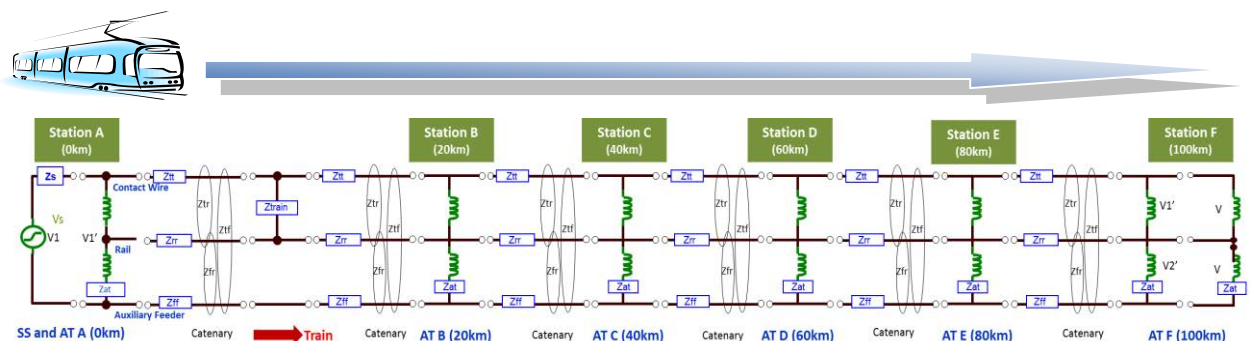
Figure 4-2: A 100km long railway model for simulation

Table 4-1: Time table description for trains

Train	Departure Position	Departure Time	Stopping Position	End Position
HS (High Speed Train)	Station A	0:00	-	Station F
SUB (Suburban Train)	Station A	00:15	Station B Station C Station D Station E	Station F

Tables 4-2 and 4-3 contain input data specifying the train and track parameters, respectively. Figures 3 and 4 show the route, live characteristics and traction power of each train as measured on train. The simulation was performed using the University of Birmingham's single train simulator (STS). Figures 4-5 and 4-6 show voltage, current and power parameters of the model, which is measured at the railway substation. Table 4-4 shows the results obtained using maximum and minimum voltages; all values are within the average voltage over the zone of BS EN 50641.

Table 4-2: Input data of trains in the model (1)

Item / Train	HS	SUB
Total Mass [T]	580	400
Max Speed [km/h]	220	160
Maximum Tractive Effort [kN]	250	320
Davis Equation Coefficients [kN] [kN·s/m] [kN·s²/m²]	9.23 0.0158 0.00123	24.3 0.0847 0.00403
Efficiency	85 [%]	85

Table 4-3: Input data of track in the model

Item / Track		Value
Max Speed		200 [km/h]

Gradient Description				Station Location	
Position [km]		**Gradient [‰]**		**Station**	**Position (km)**
Start	End				
0	41	0		Station A	0
41	59	5		Station B	20
59	61	0		Station C	40
61	69	10			
69	71	0		Station D	60
71	81	-10		Station E	80
81	99	-5		Station F	100
99	104	0			
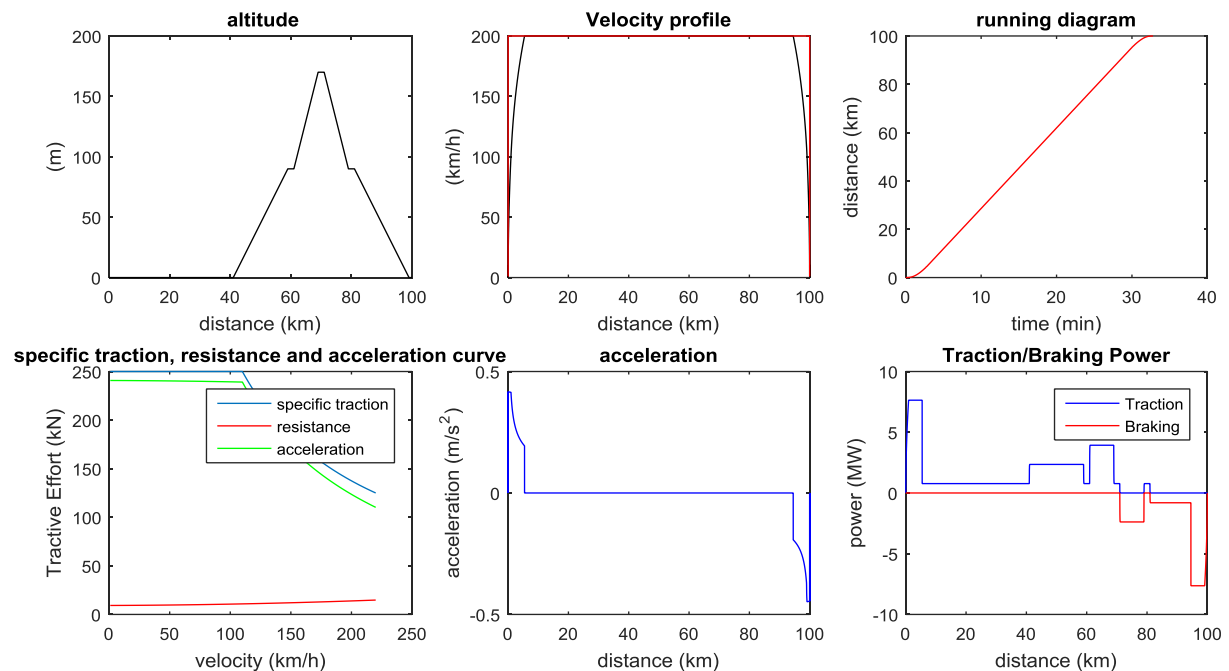
Figure 4-3: The live characteristics and traction power of the HS train and the route
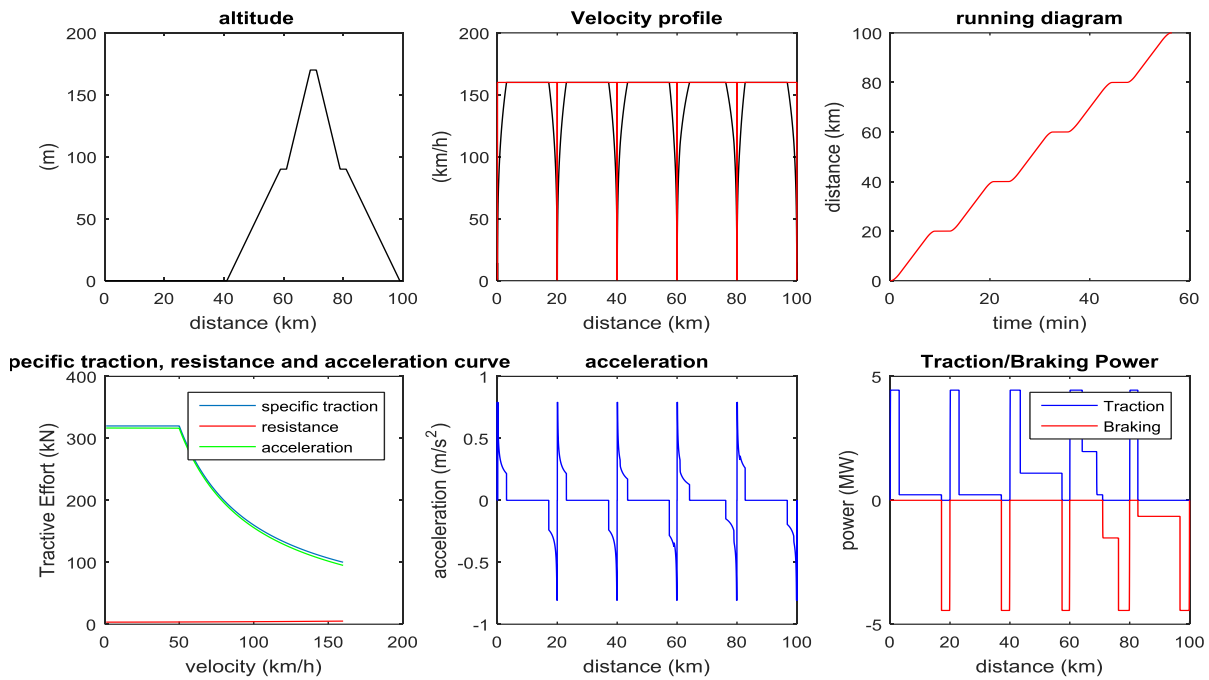
Figure 4-4: The live characteristics and traction power of the SUB train and the route
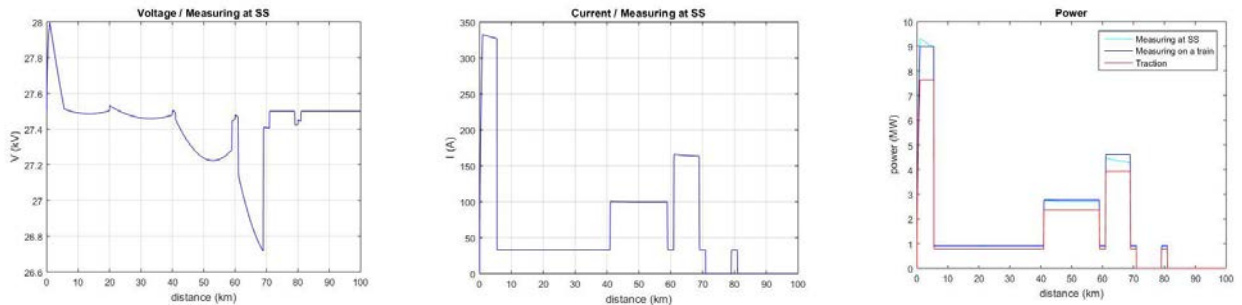
Figure 4-5: Voltage, current and power of the HS train at the railway substation
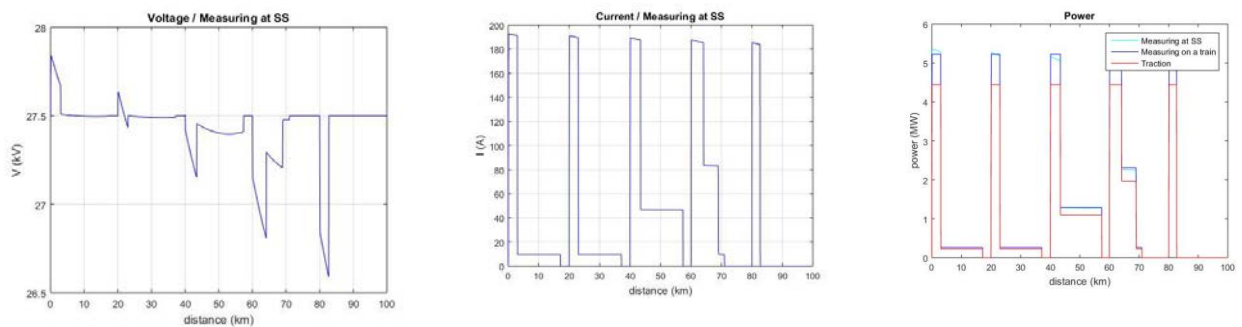
Figure 4-6: Voltage, current and power of the SUB train at the railway substation

Table 4-4: Results of maximum and |minimum voltage

Train	Maximum Voltage		Minimum Voltage	
	BS EN 50641	Result	BS EN 50641	Result
HS	29,171	27.995	23,075	26,716
SUB	28,934	27,841	23,003	26,589
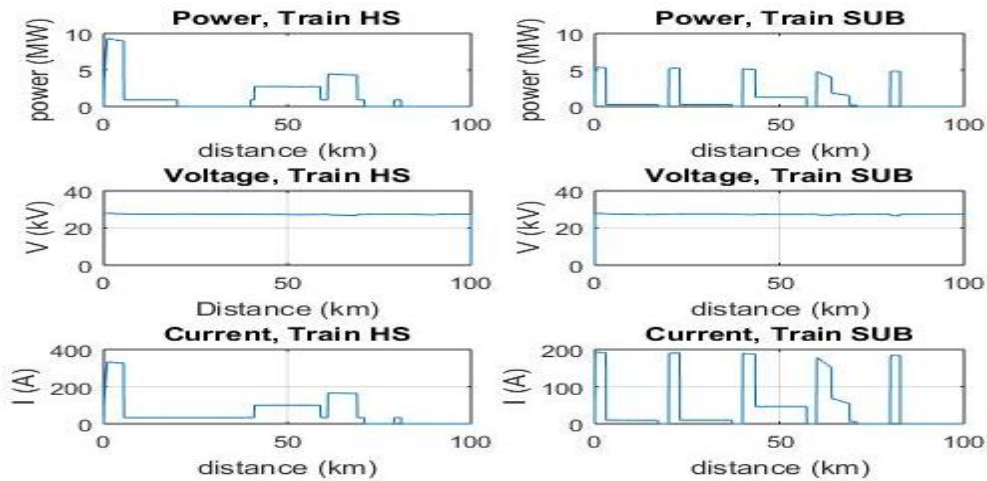
Figure 4-7: Power, voltage and current of the HS and SUB trains
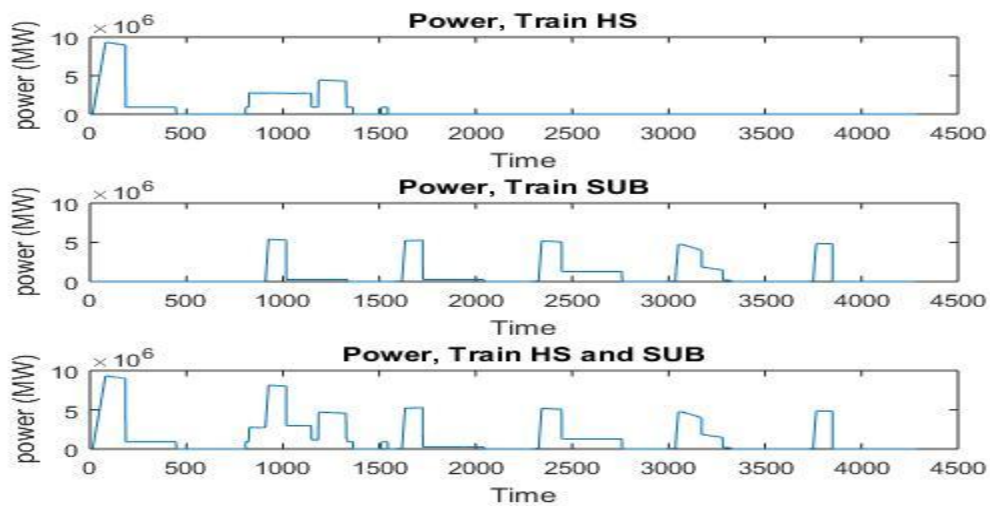
Figure 4-8: Power of the HS and SUB trains in sequence

Figure 4-7 shows the power draw of the HS and SUB trains, which is measured as a function of distance from the SS; power as a function of time for the trains is shown in Figure 4-8. The first train, HS, runs from 1 s, while the second train, SUB, runs 900 s after the HS train.

4.2 Simulation of PV array system

To construct the 1,000 MW PV array used in the smart grid, 741 strings of five series of 330 SPR-305E-WHD-D solar panels constructed by Sun Power are used in the modelling. Table 4-5 shows the input data used in the simulation.

Table 4-5: Input data of a 1,000 MW PV array system simulation

R_s	0.37152 (Ω)	K_i	0.0032 (%/°C)
R_p	269.5934 (Ω)	N_s	96
I_{scn}	5.96 (A)	N_{sm}	5 (Number of series connected modules)
V_{ocn}	64.2 (V)	N_{st}	741 (Number of string connected modules)
V_{mp}	54.7 (V)	A	0.945
I_{mp}	5.58 (A)	E_g	1.12 (eV)
K_v	-0.123 (%/°C)		

The irradiance and temperature are set to reflect characteristic values obtained in central London in August using data obtained from the Joint Research Centre (JRC), the European Commission's in-house science service [85]. Although the JRC data cover 15-min intervals over the course of a day, here the data are broken into 1-s intervals to account for variation. As seen in Figure 4-9, the voltage produced by the MPPT algorithm is stable at around 55 kV but the current fluctuates as a result of the variable irradiance and temperature.

| (a) Voltage | (b) Current | (c) Power |
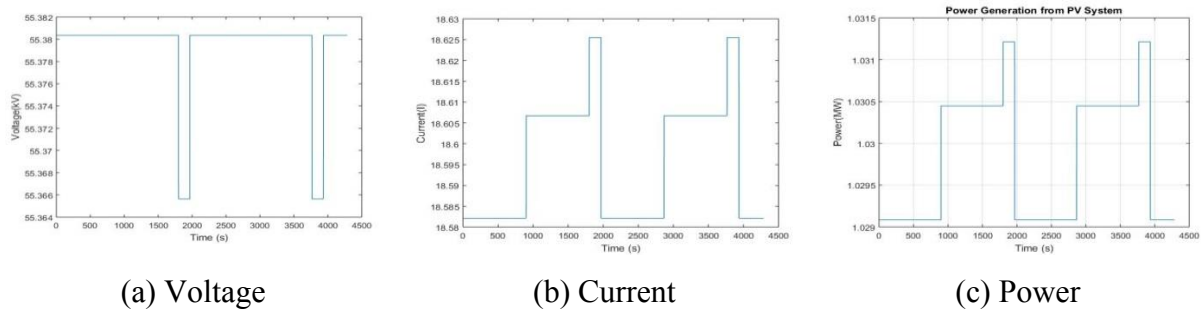
Figure 4-9: The result of a 1000 MW PV array system

4.3   Simulation of wind power system

In the model, 100×25.4-metre radius wind power units are connected to the grid. Table 4-6 shows the input data used in the simulation.

Table 4-6: Input data of a wind power generation simulation

C_p	0.45	ρ	1.225 (kg/m3)
R	50.3 (m)	ω_{blade}	45 (rad/s)
β	0	η	0.85
N	17		

To simplify the simulation, the wind speed is assumed to be random and the pitch angle β is set to zero. In addition, the voltage is set to a constant 55 kV to equalise the shapes of the current and power graphs. As with the modelled PV array system, the MPPT algorithm is applied for power stabilisation. As seen in Figure 4-10, the MPPT algorithm produces a continuous current at 1 MW of power generation.
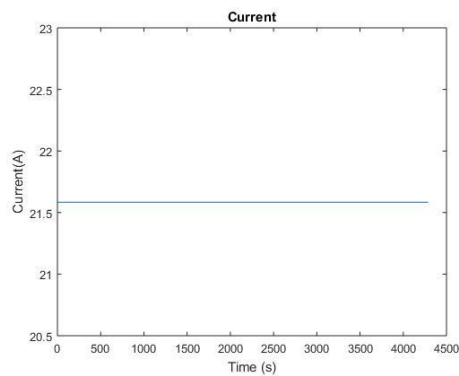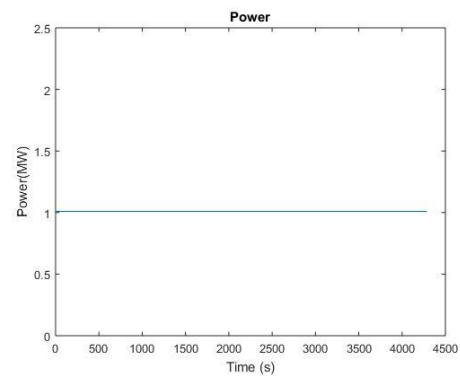
(a) Current   (b) Power

Figure 4-10: The result of 1,000 MW wind power generation with Matlab

4.4   Simulation of ESS

Figure 4-11 outlines the operational flow of the ESS model used in the model. The model ESS follows a very similar flow to that of the ESS model shown in Fig. 3-25. When the DG-produced power exceeds the load, the system enters charging mode and the storage systems are charged until either the load is balanced or all devices are fully charged, in which case power is fed back to the national grid. Conversely, if the load exceeds the power production the storage systems are drained until either the load is balanced or the devices are empty, in which case power is drawn from the grid to balance the load. The system checks the amount of distributed energy and the load at each second to ensure rapid mode reversal if necessary.
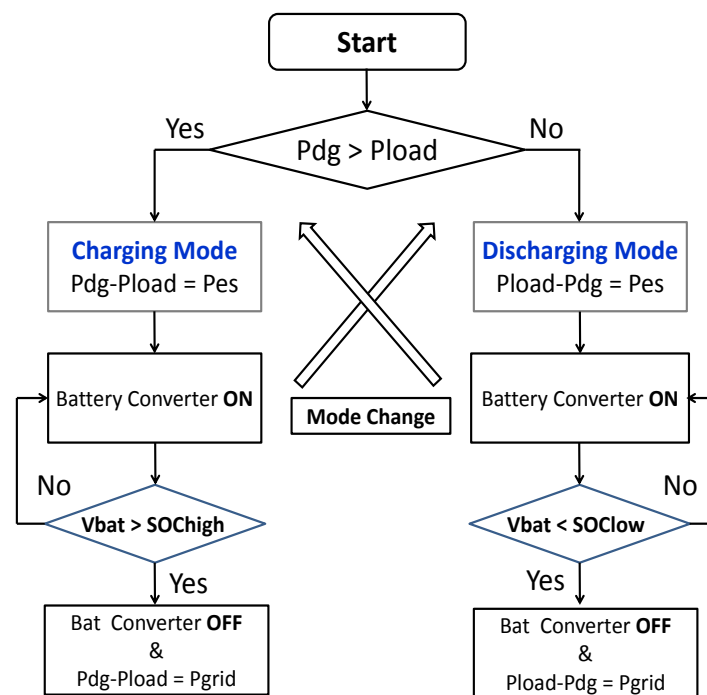
Figure 4-11: The operation method of ESS

4.5 Simulation of a smart grid for a railway

Figure 4-12 shows the complete model railway system comprising two trains moving on a 100-km railway powered by a 1,000 MW PV array system, a 1,000 MW wind power generation system and a 1,000 MW ESS.
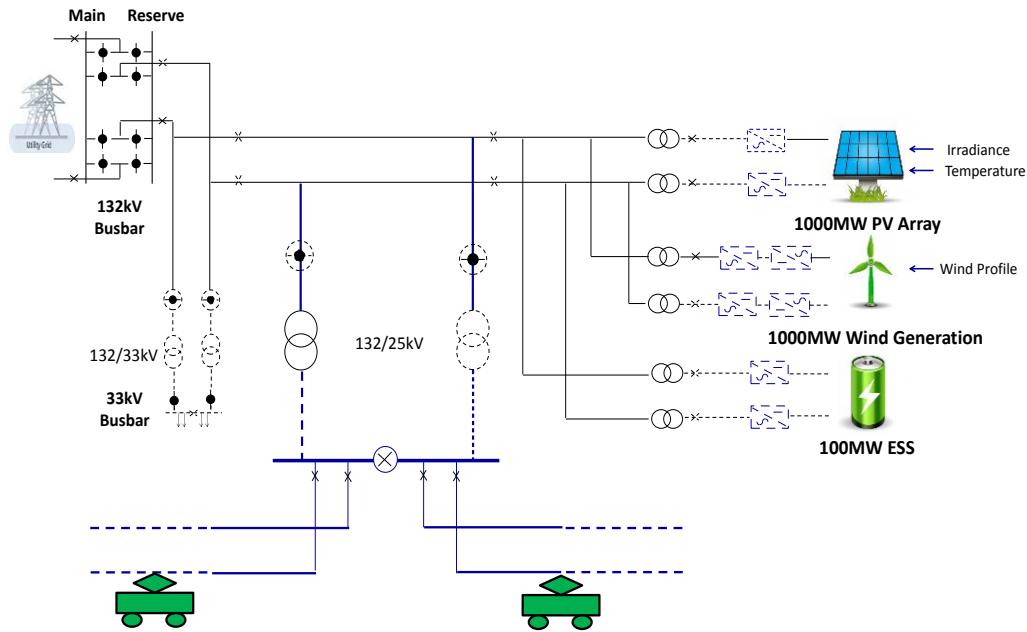
Figure 4-12: Simulation of a smart grid for a railway

Table 4-7 provides the simulation results produced by the management system. The two trains require a total of 6,539 MW; the DGs supply 7,833 MW, the national grid supplies 2,520MW, 3,280 MW is returned to the national grid and 2,216 MW is charged to the ESS. Figure 4-13 (a) shows the power consumption by the loads, which is identical to that in Figure 4-8 (c). Figure 4-13 (b) shows power produced by the DGs comprising the PV array system, the wind power system and the battery. Figure 4-13 (c) shows the difference between the power demand by the loads and the power produced by the DGs; where it is positive, the loads exceed the DG and the national grid must be tapped into to supply power. Figure 4-13 (f) shows the amount of power obtained from the national grid. Figure 4-13 (d) shows the power obtained from the ESS following the process outlined in Figure 4-11. Figure 4-13 (e) shows the power sent back to the national grid; when the DG power exceeds the load, this is positive. Figure 4-14 shows all of the results in Figure 4-13 in a single frame. Figure 4-15 shows the state of charge (SoC) of the battery, which varies between a maximum and minimum of 0.9 and 0.4, respectively, over the life cycle of the battery.

Table 4-7: Results of the simulation of a smart grid for a railway

Traction Power (MW)	Energy Supply (MW)						
	Distributed Generation				Grid		Charging ESS
	Total	PV	Wind	ESS	From	To	
6,539	7,833	4,415	4,326	775	2,520	3,278	2,216
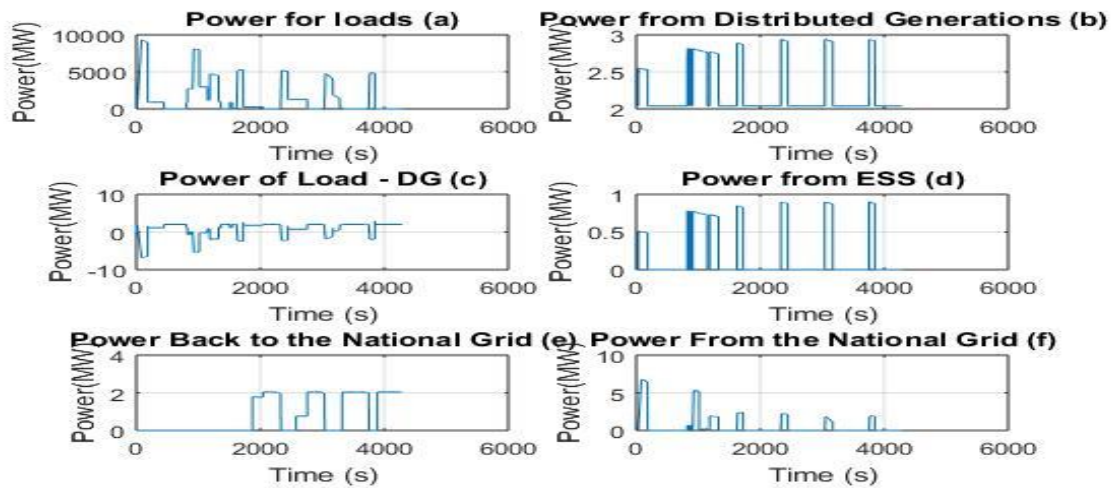
Figure 4-13: Results of the simulation of a smart grid for a railway (1)
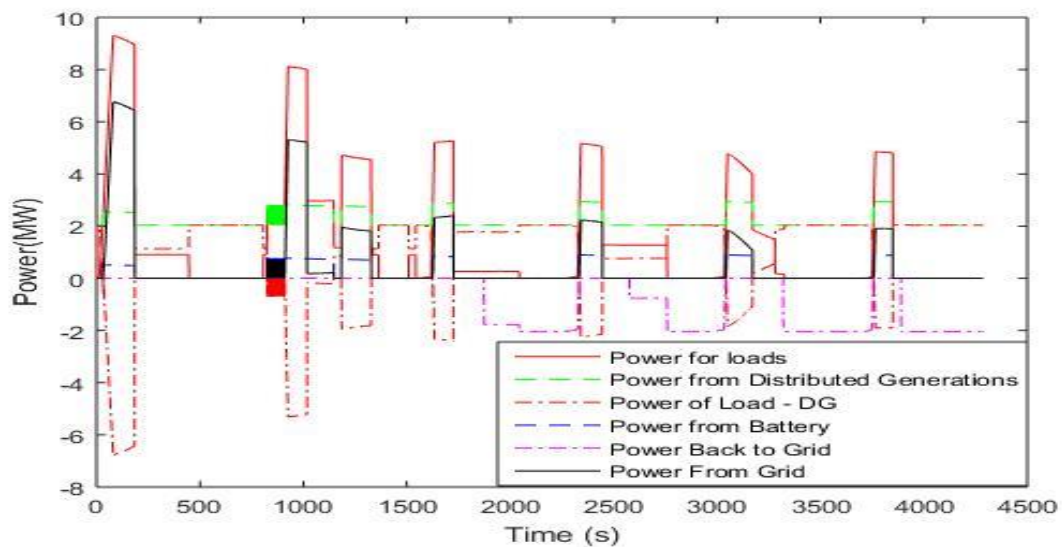
Figure 4-14: Results of the simulation of a smart grid for a railway (2)
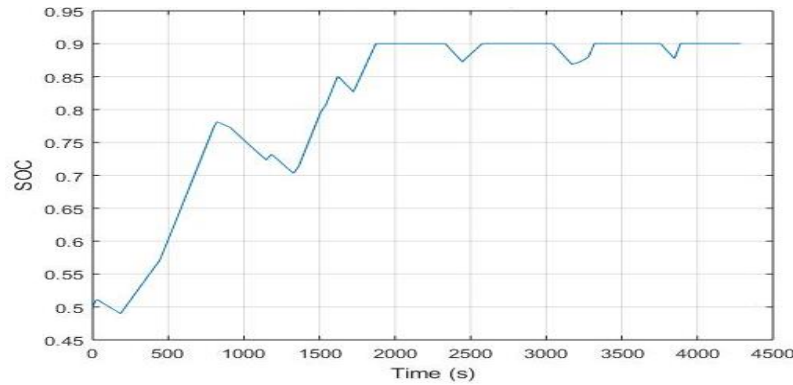
Figure 4-15: SOC of the ESS

In this chapter, the parameters and results of a Matlab-simulated 100-km railway carrying two loads (two trains) powered by DGs comprising a 1,000 MW PV array system, a 1,000 MW wind power system, a 1,000 MW ESS and a management system are presented. The simulation outputs were all within the average voltage over the zone of BS EN 50641 and are therefore acceptable for use in the economic analysis to be carried out in Chapter 5.

5 Economic analysis of smart grid railway

5.1 Levelised Cost of Electricity Generation (LCEG)

Calculating the electricity generation costs of a smart grid is the best way to analyse the relative economic effectiveness of renewable and non-renewable energy generation. Such analysis and comparison is a common tool in arriving at economic decisions regarding how and when to deploy capacity. Table 5-1 lists the factors used in calculation of the levelised cost of electricity generation (LCEG). Several economic analysis methods can be applied to compare renewable and non-renewable energy generation costs, the most popular of which is LCEG, which is therefore applied following the methodology in this study [86]. There are, however, some limitations to the levelised cost approach. First, its estimates are highly sensitive to underlying data and assumptions, including assumptions on capital, fuel and carbon and operating costs as well as operating profile, load factor and discount rates. This thesis uses data produced by the UK's Department of Energy and Climate Change in 2013. It should be noted that the levelised costs are generic rather than site-specific; for instance, land

costs are not included in the estimation and, although use of system charges is included, they are calculated on an average basis [86].

Table 5-1: Calculation of levelised cost of electricity

Step 1 : Gather Plant Data and Assumptions		
Capex Costs	Opex Costs	Expected Generation Data
-Pre-development costs -Construction costs* -Infrastructure costs* (*adjusted over time for leaning)	-Fixed opex* -Variable opex -Insurance -Connection cost -Carbon transport and storage costs -Decommissioning fund costs -Heat revenues -Fuel Prices -Carbon Costs	-Capacity of Plant -Expected Availability -Expected Efficiency -Expected Load Factor(all assumed base load)

Step 2 : Sum the Net Present Value of Total Expected Costs for Each Year
$$\text{NPV of Total Costs} = \sum_n \frac{total\ Capex\ and\ Opex\ costs}{(1 + discount\ rate)^n}$$ $$n = time\ period$$

Step 3 : Sum the Net Present Value of Expected Generation for Each Year
$$\text{NPV of Electricit Generation} = \sum_n \frac{Net\ Electricity\ Generation}{(1 + Discount\ Rate)^n}$$ $$n = time\ period$$

Step 4 : Divide Total Costs by Net Generation
$$Levelised\ Cost\ of Electricity\ Eneration\ Estimate = \frac{NPV\ of\ Total\ Costs}{NPV\ of\ Electricity\ Generation}$$

Second, levelised costs are not strike prices [86] and do not provide any indication of potential future strike prices for a particular technology. If strike prices were to be used, other inputs, including revenue assumptions, land costs, financing costs, and wider policy considerations, could also be used. Timing is also important for the calculation of levelised costs because pre-development and construction timing vary by technology and, therefore, the estimated dates for 'project start' or 'financial close' can vary by technology. To control for this, central estimates for pre-development and construction timings were used to develop the Electricity Generation Costs (Annex 3) applied in this study [86].

Table 5-2 lists the central levelised cost data estimated for a project starting in 2019 under a 10% discount rate [86]. The data contain all capital expenditure (Capex) and operational expenditure (Opex) costs.

Table 5-2: Data of the central levelised cost estimated for projects in 2019

Costs		CCGT	OCGT	Nuclear	CCGT with CCS	Coal(ASC) with CCS	Coal(IGCC) with CCS	Off shore Wind	Large scale Solar PV
		Non-renewable						Renewable	
Capex	Pre-development	0	5	5	1	1	1	4	0
	Capital	9	54	56	21	37	53	83	100
Opex	Fixed O&M	40	23	10	4	8	19	27	23
	Variable O&M	0	0	3	2	2	0	1	0
	Fuel	49	74	5	56	36	36	0	0
	Carbon	24	35	0	4	5	7	0	0
	CO2 Capture and Storage	0	0	0	7	18	17	0	0
	Decommissioning and waste	0	0	2	0	0	0	0	0
Total Levelised Costs		85	190	80	95	107	134	115	123

The study in [86]also produced levelised cost estimates for project commissioning in 2014, 2016, 2020, 2025 and 2030 at a10% discount rate [87], which are listed in Table 5-3.

Table 5-3: Levelised cost estimates for project commissioning in 2014 to 2030

	2014	2016	2020	2025	2030
CCGT	75	77	82	86	88
OCGT	175	179	185	192	195
Nuclear	-	-	93	90	80
CCGT with CCS	-	-	-	95	95
Coal(ASC) with CCS	-	-	107	109	108
Coal(IGCC) with CCS	-	-	-	135	133
Onshore>5MW UK	104	103	100	99	97
Off shore Wind	146	135	122	116	114
Large scale Solar PV	158	144	123	105	90
Biomass	108	108	-	-	-

5.2 Electricity generation cost from the national grid and an ESS

Figure 5-1 shows a simplified profile of the installed generation capacity in the UK obtained from national grid data [88]. The early cost of electricity is calculated based on the percentage breakdown of generation capacity; for instance, the 12.8% share of nuclear capacity in the total 2020 portfolio is multiplied by nuclear power's LCEG for that year to obtain the overall cost of nuclear generation. Applying this calculation to each generation source and summing the results produces the national grid electricity cost (£/MWh) in 2020, as shown in Table 5-4. Similarly, Tables 5-5 and 5-6 show the national grid electricity costs in 2025 and 2030, respectively.
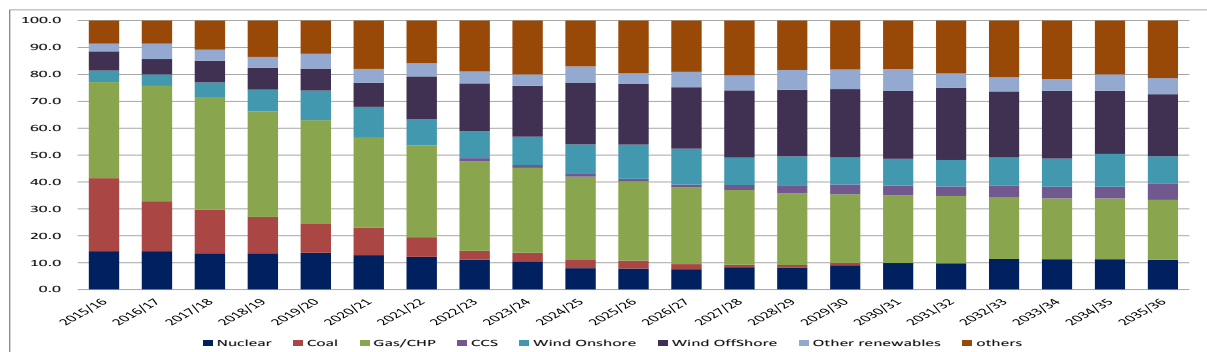
Figure 5-1: Installed capacity of generation in the UK

Table 5-4: The nation grid electricity cost in 2020

	Total	Nuclear	Coal	Gas/ CHP	CCS	Wind Onshore	Wind Offshore	Other renews	Others
% (A)	100	12.8	10.3	33.3	0	11.5	9	5.1	17.9
LCEG in 2020 (B)		93	107	82	0	100	122	123	108
2020 £/MWh (A× B)	**98.316**	11.904	11.021	27.306	0	11.5	10.98	6.273	19.332

Table 5-5: The nation grid electricity cost in 2025

	Total	Nuclear	Coal	Gas/ CHP	CCS	Wind Onshore	Wind Offshore	Other renews	Others
% (A)	100	7.8	2.9	29.4	1	12.7	22.5	3.9	19.6
LCEG in 2025 (B)		90	109	86	95	99	116	105	108
2025 £/MWh (A× B)	**100.351**	7.02	3.161	25.284	0.95	12.573	26.1	4.095	21.168

Table 5-6: The nation grid electricity cost in 2030

	Total	Nuclear	Coal	Gas/ CHP	CCS	Wind Onshore	Wind Offshore	Other renews	Others
% (A)	100	7.8	2.9	29.4	1	12.7	22.5	3.9	19.6
LCEG in 2030 (B)		80	108	88	95	97	114	90	108
2030 £/MWh (A× B)	**98.841**	6.24	3.132	25.872	0.95	12.319	25.65	3.51	21.168

It is very difficult to calculate the levelised cost for an ESS because each has a unique expected life cycle. To make matters worse, the levelised cost is influenced by environmental factors such as weather and temperature and by the frequency of charging and discharging [89]. However, Lizard's Levelised Cost of Storage Analysis (LCOS), introduced in November 2015 [89], can be used to develop estimates. As an ESS, this study uses a micro grid-embedded lithium-ion battery, which is chosen for its long-term competitiveness in terms of energy storage. This battery has an LCOS-listed levelised cost of $369/MWh; following currency conversion (USD/GBP exchange rate of 0.75), £277/MWh is set as a basic life cycle ESS levelised cost. This value is halved for the purposes of this study because

the conditions under which charging and discharging are carried out are very clear; when the ESS serves as a feed for traction energy (through the smart grid), it is discharging, and when it is not serving as a feed, it is charging. Additionally, the ESS values are negative in the charging mode, as the unit is storing energy for later use in this case.

5.3   Economic Analysis for a smart grid

Using the smart grid simulation methodology applied in the preceding chapter, the ESS, wind generation and PV array capacities were varied to create 45 cases for economic analysis, as shown in Table 5-7. Each of the 45 cases was applied to scenarios in which railway system installation is started in 2020, 2025 and 2030. As inputs to these analyses, the LCEG values for PV array and wind power systems for the respective years were adapted from Table 5-3.

Table 5-7: 45 Cases for economic analysis of a smart grid

No	ESS	Wind	PV	No	ESS	Wind	PV
1	1000	0	1000	24	2000	2000	1000
2	1000	0	2000	25	2000	2000	2000
3	1000	0	3000	26	2000	2000	3000
4	1000	1000	0	27	2000	3000	0
5	1000	1000	1000	28	2000	3000	1000
6	1000	1000	2000	29	2000	3000	2000
7	1000	1000	3000	30	2000	3000	3000
8	1000	2000	0	31	3000	0	1000
9	1000	2000	1000	32	3000	0	2000
10	1000	2000	2000	33	3000	0	3000
11	1000	2000	3000	34	3000	1000	0
12	1000	3000	0	35	3000	1000	1000
13	1000	3000	1000	36	3000	1000	2000
14	1000	3000	2000	37	3000	1000	3000
15	1000	3000	3000	38	3000	2000	0
16	2000	0	1000	39	3000	2000	1000
17	2000	0	2000	40	3000	2000	2000
18	2000	0	3000	41	3000	2000	3000
19	2000	1000	0	42	3000	3000	0
20	2000	1000	1000	43	3000	3000	1000

21	2000	1000	2000	44	3000	3000	2000
22	2000	1000	3000	45	3000	3000	3000
23	2000	2000	0				

5.3.1 Project starting in 2020

The LCEGs of projects starting in 2020 based on the 45 cases were calculated and the overall results are listed in Appendix Table A-1. Table 5-8 shows the maximum and minimum LCEG values obtained. The table shows the total energy generated by each type of DG, the energy obtained from and sent to the national grid and the energy charged to the ESS in both cases. Columns I-J shows the cost difference between using only the national grid and using both the smart grid and the national grid; a positive value corresponds to a greater cost for using a smart grid.

Table 5-8: Maximum and minimum different costs in 2020

				LCEG(£)	0.12	0.12	0.14	0.10	-0.09*	-0.14		0.10	
Case No	ESS (MW)	Wind (MW)	PV (MW)		DG		ESS (D)	Grid		Charg ESS(H)	Smart Grid (I=A+B+D +F+G+H)	Traction Power (J)	I-J
					PV (A)	Wind (B)		From (F)	To (G)				
15	1,000	3,000	3,000	MW	13,245	12,977	155	385	18,620	1,596		6,539	
				MWh	15,773	15,453	185	458	22,173	1,901		7,787	
				1000£	1,940	1,885	26	45	-1,962	-263	1,671	781	905
4	1,000	1,000	-	MW	-	4,326	828	3,807	152	2,268		6,539	
				MWh	-	5,152	986	4,534	181	2,701		7,787	
				1000£	-	628	136	446	-16	- 374	821	781	55

*   The cost of energy back to the grid : 90% of generation cost (from the national grid)
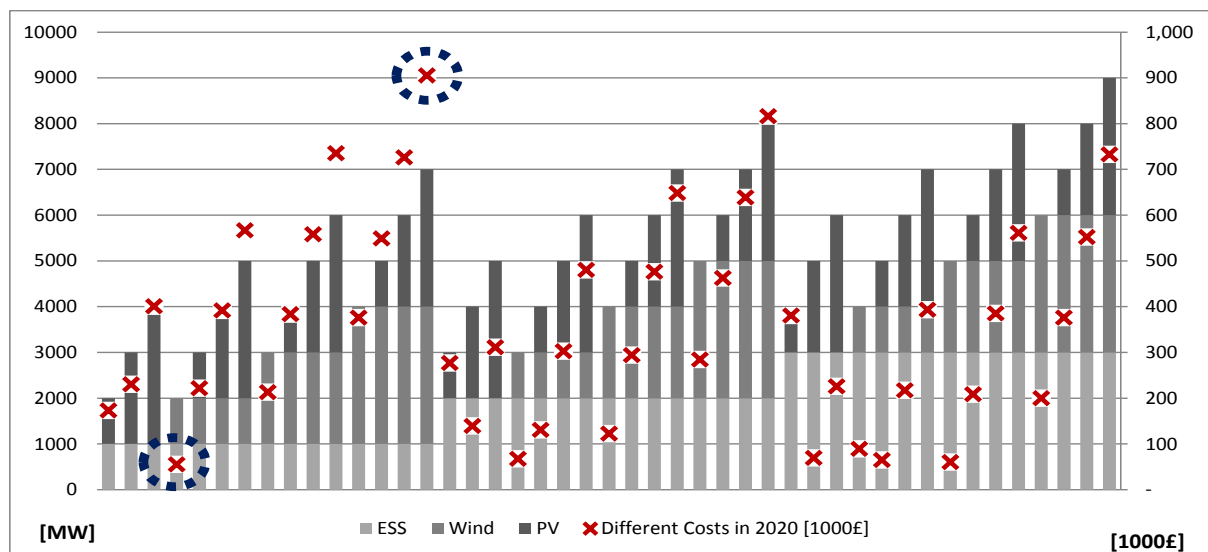
Figure 5-2: The difference in costs between using a smart grid and the national grid for 45 Cases in 2020

Figure 5-2 shows clear differences in cost between using a smart grid and using the national grid alone over all 45 cases. There are no negative values: starting a smart grid project for a railway in 2020 does not generate business profits.

5.3.2 Project starting in 2025

The LCEGs over the 45 cases for a railway project beginning in 2025 were calculated and the results are shown in Appendix Table A-2. Table 5-9 shows the cases with maximum and minimum values; in one of the cases (32), there is a negative value in column I-J.

Table 5-9: Maximum and minimum different costs in 2025

Case No	ESS (MW)	Wind (MW)	PV (MW)	LCEG	0.105	0.116	0.14	0.100	-0.090	-0.14		0.10	
					DG		ESS (D)	Grid		Charg ESS (H)	Smart Grid (I=A+B+D +F+G+H)	Traction Power (J)	I-J
					PV (A)	Wind (B)		From (F)	To (G)				
15	1,000	3,000	3,000	MW	13,245	12,977	155	385	18,620	1,596		6,539	
				MWh	15,773	15,453	185	458	22,173	1,901	-	7,787	
				1000£	1,656	1,793	26	46	- 2,003	- 263	1,255	781	473
32	3,000	-	2,000	MW	8,830	-	1,682	1,706	-	5,676		6,539	
				MWh	10,515	-	2,003	2,032	-	6,759	-	7,787	
				1000£	1,104	-	277	204	-	-935	650	781	-132
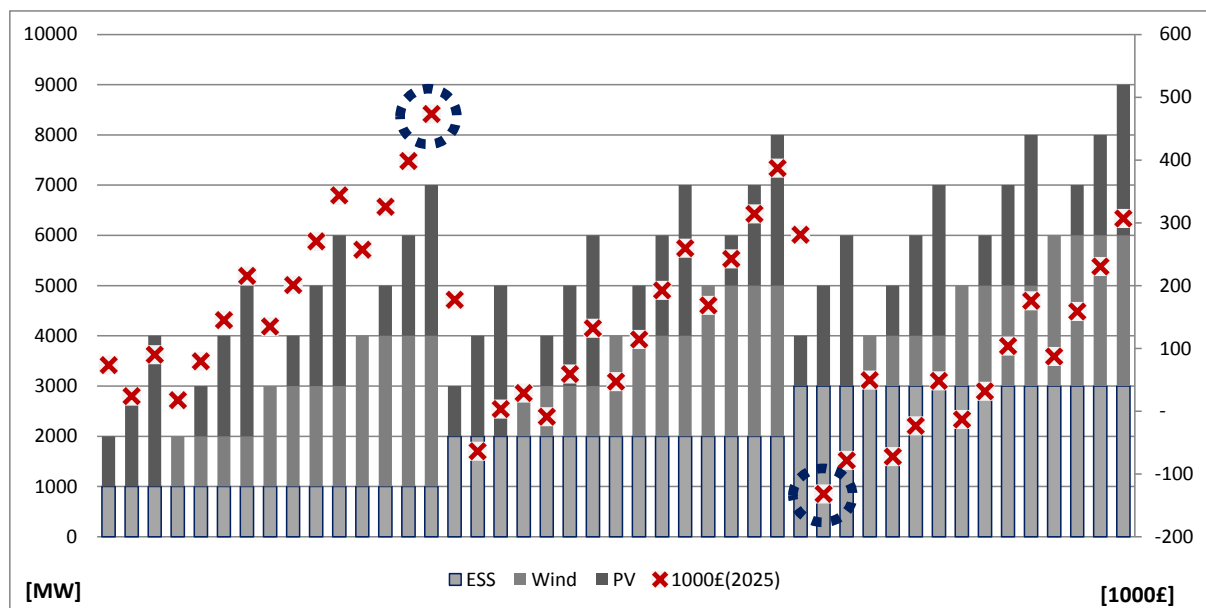
Figure 5-3: The different Costs between a Smart Grid and a National Grid of 45 Cases in 2025

Figure 5-3 shows that there are seven cases with a negative cost differential; these are shown in Table 5-10. In each of these cases, the ESS system capacity is larger than or equal to the DG capacity (the equivalence case occurs where the DG is a PV array system). Thus, a smart grid project for a railway starting in 2025 that has more ESS than DG capacity can generate business profits.

Table 5-10: Cases which have economic profits for a smart grid in 2025

				LCEG	0.105	0.116	0.14	0.100	-0.090	-0.14		0.10	
Case No	ESS (MW)	Wind (MW)	PV (MW)		DG		ESS (D)	Grid		Charg ESS (H)	Smart Grid (I=A+B+D +F+G+H)	Traction Power (J)	I-J
					PV (A)	Wind (B)		From (F)	To (G)				
17	2,000	-	2,000	MW	8,830	-	1,277	2,046	1,454	4,158		6,539	
				MWh	10,515	-	1,521	2,436	1,731	4,951	-	7,787	
				1000£	1,104	-	210	244	-156	-685	717	781	-64
20	2,000	1,000	1,000	MW	4,415	4,326	1,275	2,068	1,386	4,157		6,539	
				MWh	5,258	5,152	1,518	2,463	1,650	4,950	-	7,787	
				1000£	552	598	210	247	-149	-685	773	781	-9
32	3,000	-	2,000	MW	8,830	-	1,682	1,706		5,676		6,539	
				MWh	10,515	-	2,003	2,032	-	6,759	-	7,787	
				1000£	1,104	-	277	204	-	-935	650	781	-132
33	3,000	-	3,000	MW	13,245	-	1,184	1,246	3,626	5,506		6,539	
				MWh	15,773	-	1,410	1,484	4,318	6,557	-	7,787	
				1000£	1,656	-	195	149	- 390	-907	703	781	-79
35	3,000	1,000	1,000	MW	4,415	4,326	1,680	1,728	-	5,607		6,539	
				MWh	5,258	5,152	2,001	2,058	-	6,677	-	7,787	
				1000£	552	598	277	206	-	-924	709	781	- 72
36	3,000	1,000	2,000	MW	8,830	4,326	1,182	1,259	3,552	5,503		6,539	
				MWh	10,515	5,152	1,408	1,499	4,230	6,553	-	7,787	
				1000£	1,104	598	195	150	- 382	-907	758	781	- 23
38	3,000	2,000	-	MW	-	8,652	1,678	1,746	-	5,534		6,539	
				MWh	-	10,303	1,998	2,079	-	6,590	-	7,787	
				1000£	-	1,195	277	209	-	-912	768	781	- 13

5.3.3 Project starting in 2030

The LCEGs over the 45 cases for a railway project beginning in 2030 were calculated and the results are shown in Appendix Table A-3. Table 5-11 shows the cases with maximum and minimum values; as in 2025, one case (33) produces a negative cost differential in column I-J. This highest-margin case, comprising a 3,000 MW ESS and a 3,000 MW PV array system, produces lower costs than the best 2025 case.

Table 5-11: Maximum and minimum different costs in 2030

				LCEG	0.09	0.11	0.11	0.10	-0.09	-0.11		0.10	
					DG		ESS (D)	Grid		Charg ESS(H)	Smart Grid (I=A+B+D +F+G+H)	Traction Power (J)	I-J
Case No	ESS (MW)	Wind (MW)	PV (MW)		PV (A)	Wind (B)		From (F)	To (G)				
15	1,000	3,000	3,000	MW	13,245	12,977	155	385	18,620	1,596		6,539	
				MWh	15,773	15,453	185	458	22,173	1,901	-	7,787	
				1000£	1,420	1,762	26	45	- 1,972	-263	1,017	781	247
33	3,000	-	3,000	MW	13,245	-	1,184	1,246	3,626	5,506		6,539	
				MWh	15,773	-	1,410	1,484	4,318	6,557	-	7,787	
				1000£	1,420	-	195	147	-384	-907	470	781	-300
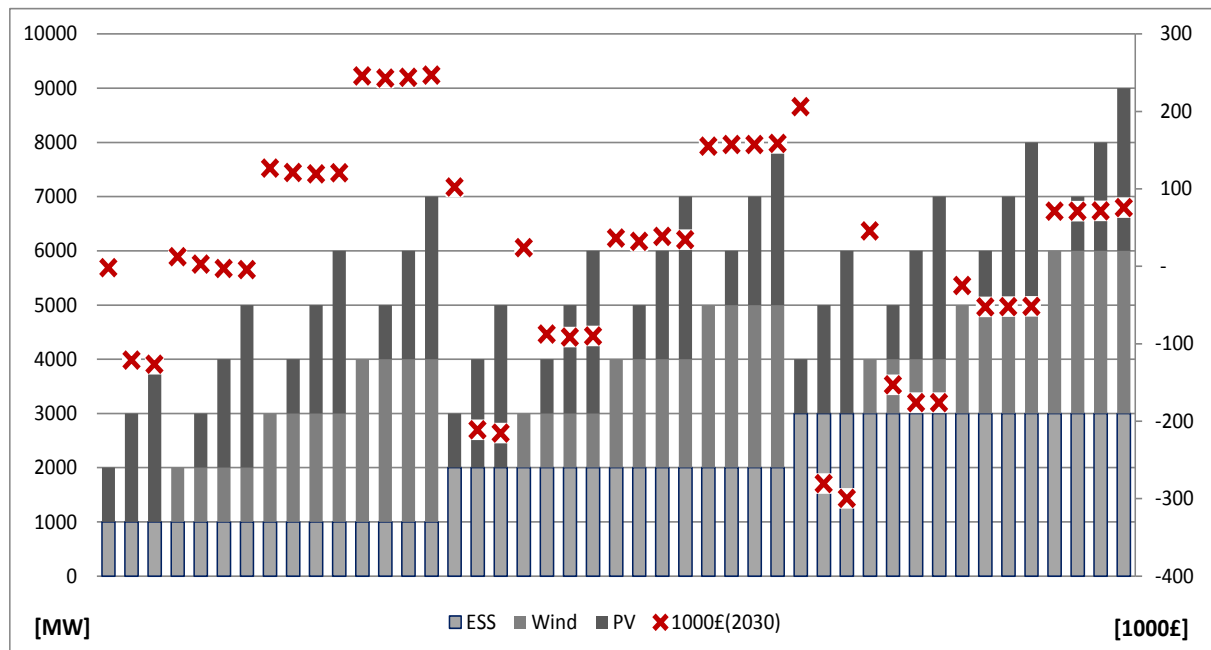
Figure 5-4: The difference in costs between using a smart grid and the national grid for 45 Cases in 2030

It is seen from Figure 5-4 that the number of cases in which there is a negative differential between the smart grid and national grid-only costs has expanded to 19 for projects starting in 2030; these cases are shown in Table 5-12. As in the 2025 results, in many of the viable business cases the ESS capacity is larger than the DG capacity or as large as the PV capacity; however, there are also several cases in which the ESS capacity is less than the DG capacity. In all such cases, the PV array capacity is larger than the wind power capacity. Thus, a smart grid project for a railway that is started in 2030 and has a large ESS and a large PV array system can realise business profits.

Table 5-12: Cases which have economic profits for a smart grid in 2030

Case No	ESS (MW)	Wind (MW)	PV (MW)	LCEG	0.105	0.116	0.14	0.100	-0.090	-0.14	0.10	
					DG			Grid		Charg ESS (H)	Smart Grid (I=A+B+D +F+G+H)	Traction Power (J)	I-J
					PV (A)	Wind (B)	ESS (D)	From (F)	To (G)				
1	1,000	-	1,000	MW	4,415	-	956	4,522	-	2,397		6,539	
				MWh	5,258	-	1,138	5,385	-	2,854	-	7,787	
				1000£	473	-	158	532	-	- 395	768	770	- 2
2	1,000	-	2,000	MW	8,830	-	776	2,497	3,343	2,218		6,539	
				MWh	10,515	-	924	2,974	3,981	2,641	-	7,787	
				1000£	946	-	128	294	- 354	- 365	649	770	-121
3	1,000	-	3,000	MW	13,245	-	669	1,562	6,825	2,109		6,539	
				MWh	15,773	-	797	1,860	8,127	2,511	-	7,787	
				1000£	1,420	-	110	184	-723	-348	643	770	-127
6	1,000	1,000	2,000	MW	8,830	4,326	669	1,579	6,750	2,112		6,539	
				MWh	10,515	5,152	797	1,880	8,038	2,515	-	7,787	
				1000£	946	587	110	186	-715	-348	767	770	-3
7	1,000	1,000	3,000	MW	13,245	4,326	495	978	10,562	1,938		6,539	
				MWh	15,773	5,152	589	1,165	12,578	2,308	-	7,787	
				1000£	1,420	587	82	115	-1,119	-319	765	770	-4
17	2,000	-	2,000	MW	8,830	-	1,277	2,046	1,454	4,158		6,539	
				MWh	10,515	-	1,521	2,436	1,731	4,951	-	7,787	
				1000£	946	-	210	241	-154	-685	558	770	-211
18	2,000	-	3,000	MW	13,245	-	1,042	1,230	5,051	3,924		6,539	
				MWh	15,773	-	1,241	1,465	6,015	4,673	-	7,787	
				1000£	1,420	-	172	145	-535	-647	554	770	-215
20	2,000	1,000	1,000	MW	4,415	4,326	1,275	2,068	1,386	4,157		6,539	
				MWh	5,258	5,152	1,518	2,463	1,650	4,950	-	7,787	
				1000£	473	587	210	243	-147	-685	682	770	-88
21	2,000	1,000	2,000	MW	8,830	4,326	1,041	1,246	4,979	3,921		6,539	
				MWh	10,515	5,152	1,240	1,484	5,929	4,669	-	7,787	
				1000£	946	587	172	147	- 527	- 646	678	770	-91
22	2,000	1,000	3,000	MW	13,245	4,326	792	905	9,049	3,676		6,539	
				MWh	15,773	5,152	943	1,078	10,776	4,378	-	7,787	
				1000£	1,420	587	131	107	-959	-606	680	770	-90
32	3,000	-	2,000	MW	8,830	-	1,682	1,706		5,676		6,539	
				MWh	10,515	-	2,003	2,032	-	6,759	-	7,787	
				1000£	946	-	277	201	-	-935	489	770	-281
33	3,000	-	3,000	MW	13,245	-	1,184	1,246	3,626	5,506		6,539	
				MWh	15,773	-	1,410	1,484	4,318	6,557	-	7,787	
				1000£	1,420	-	195	147	-384	- 907	470	770	-300
35	3,000	1,000	1,000	MW	4,415	4,326	1,680	1,728	-	5,607		6,539	
				MWh	5,258	5,152	2,001	2,058	-	6,677	-	7,787	
				1000£	473	587	277	203	-	-924	617	770	-153
36	3,000	1,000	2,000	MW	8,830	4,326	1,182	1,259	3,552	5,503		6,539	
				MWh	10,515	5,152	1,408	1,499	4,230	6,553	-	7,787	

Case No	ESS (MW)	Wind (MW)	PV (MW)	LCEG	DG PV (A) 0.105	DG Wind (B) 0.116	ESS (D) 0.14	Grid From (F) 0.100	Grid To (G) -0.090	Charg ESS (H) -0.14	Smart Grid (I=A+B+D +F+G+H)	Traction Power (J) 0.10	I-J
				1000£	946	587	195	148	- 376	- 907	594	770	-176
37	3,000	1,000	3,000	MW	13,245	4,326	1,108	798	7,503	5,430		6,539	
				MWh	15,773	5,152	1,319	950	8,935	6,466	-	7,787	
				1000£	1,420	587	183	94	-795	-895	594	770	-176
38	3,000	2,000	-	MW	-	8,652	1,678	1,746	-	5,534		6,539	
				MWh	-	10,303	1,998	2,079	-	6,590	-	7,787	
				1000£	-	1,175	277	206	-	- 912	745	770	-25
39	3,000	2,000	1,000	MW	4,415	8,652	1,184	1,272	3,475	5,506		6,539	
				MWh	5,258	10,303	1,410	1,515	4,138	6,557	-	7,787	
				1000£	473	1,175	195	150	-368	-907	717	770	-53
40	3,000	2,000	2,000	MW	8,830	8,652	1,110	809	7,425	5,431		6,539	
				MWh	10,515	10,303	1,322	963	8,842	6,467	-	7,787	
				1000£	946	1,175	183	95	- 787	-895	718	770	-52
41	3,000	2,000	3,000	MW	13,245	8,652	640	361	11,393	4,959		6,539	
				MWh	15,773	10,303	762	430	13,567	5,905	-	7,787	
				1000£	1,420	1,175	105	42	-1,207	- 817	718	770	-52

The varying results by start year arise from the rapid decrease in the LCEG of PV array systems. Figure 5-5 shows the LCEGs in 2020, 2025 and 2030 by capacity type; it is seen that, while the PV array system rapidly becomes cheaper, the LCEG of wind generation decreases only slightly, and wind generation remains expensive in 2030. Note that a clearer model of ESSLCEG would produce more accurate results.
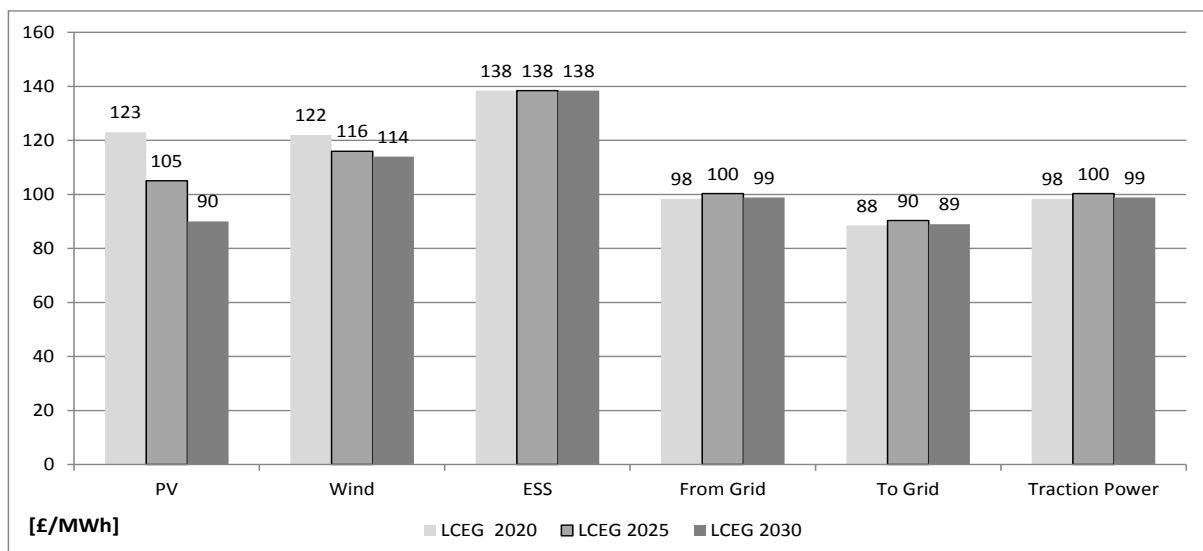
Figure 5-5: The difference in LCEG in 2020, 2025 and 2030
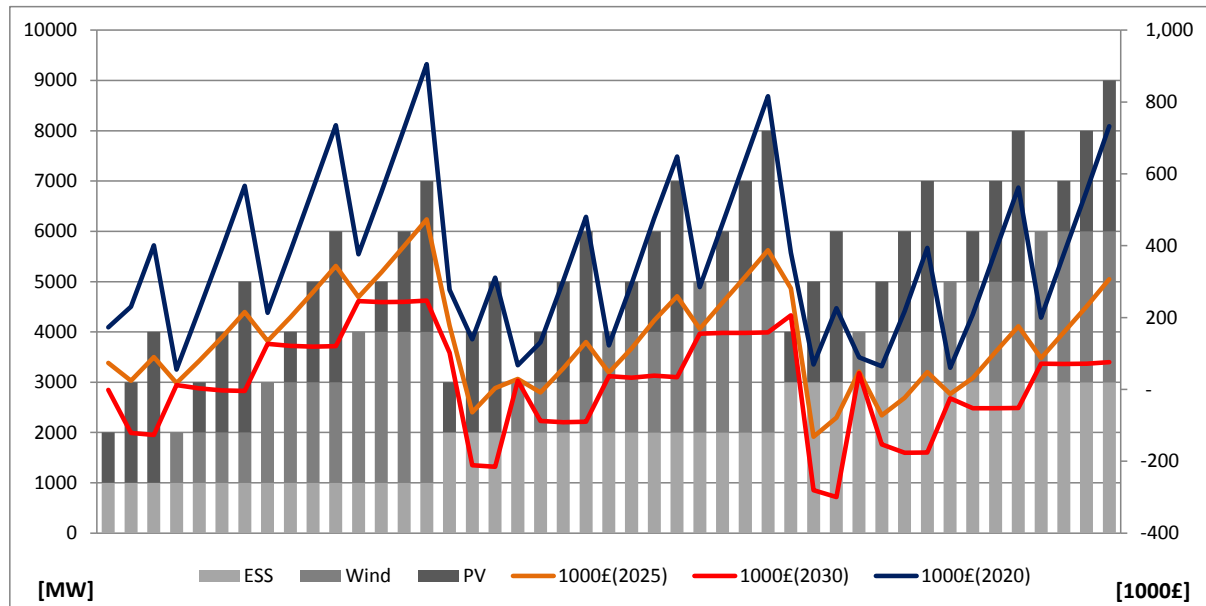
Figure 5-6: The Difference in costs between a smart grid and the national grid in 2020, 2025 and 2030

Figure 5-6 shows the cost differentials between a smart grid and the national grid alone in 2020, 2025 and 2030 as a line graph combining the results in Figures 5-3, 5-4 and 5-5. It implies that, while projects which starting after 2025 will have some advantages, nearly half of the projects starting after 2030 can obtain economic profit depending on the costs of DG and ESS.

In this chapter, a multi-case economic analysis of railway smart grid implementation was undertaken. Business profitability was assessed based on a comparison of smart grid LCEG electricity generation costs with those of the national grid for 45 distinct combinations of ESS and DG capacity for projects starting in 2020, 2025 and 2030. It was found that several smart grid projects starting in 2025with more ESS than DG capacity would realise economic profit, and that nearly half of the cases starting in 2030 - those with high ESS and PV array capacities - would be economical. A more accurate understanding of the LCEG of ESS might increase the number of profitable cases and potentially justify the earlier construction of smart grid rail system projects.

6   Conclusion and future work

6.1   General summary of contents

The contents of this study can be divided into three parts:

- Part one, comprising the first three chapters, presents a background and literature review:

Chapter 1 introduces the definition of smart grids, discusses their historical use and summarises the use of renewable energy worldwide.

Chapter 2 reviews the global trends in smart grid implementation with a focus on Europe, the US and Asia. Government strategies and regulations, along with various definitional frameworks for smart grid policy, are discussed. The chapter also looks at the work done to date in implementing rail system smart grids and the differences between smart grids for the domestic and rail sectors in terms of the unique characteristics of railways. A new definition of and set of criteria for a smart grid railway grid are suggested at the end of this chapter.

Chapter 3 explains the technologies related to smart grids by presenting outlines, theories and methods for calculating the parameters of electrical traction, PV array, wind power, ESSs and management systems. Multi-terminal modelling is introduced as a method for simply determining the power flow of railway traction systems and extracting the precise electrical characteristics of systems with moving load features. The chapter introduces an ESS designed specifically for rail systems and a detailed multi-agent control system to manage a smart grid.

- Part two, which includes Chapter 4, provides the results of Matlab simulations of a system incorporating all of the technology types discussed in the preceding section. The chapter describes the simulation results for a two-train set of loads on a 100-km-long smart grid railway powered by a 1,000 MW PV array system, a 1,000 MW wind power system and a 1,000 MW ESS under a management system. It is found that the two-train system draws 6,539 MW of power. The system DGs and national grid supply 7,833 MW and 2,520 MW, respectively. During operation, 3,280 MW goes back to the national grid and 2,216 MW is charged to the ESS.

- In part three (Chapter 5) a multi-case economic analysis based on the smart grid parameters developed in part two is carried out. The LCEG is introduced as a valid metric for examining the profitability of a business case for developing a smart grid railway system based on the differential between the net cost of construction and operation using electricity generated by the smart grid and backed up by the national grid and the net cost of using national grid electricity alone. 45 cases involving various permutations of 1,000, 2,000 and 3,000 MW PV array and wind power systems and ESSs starting in either 2020, 2025 or 2030 are constructed. It is found that several smart grid projects starting in 2025 in which there is more ESS capacity than DG capacity are profitable, whereas nearly half of the projects starting in 2030, namely, those with large ESS and PV array capacities, result in economic profit. More clearly modelling the LCEG of ESS could expand the number of profitable cases and justify earlier construction dates.

6.2 Future work
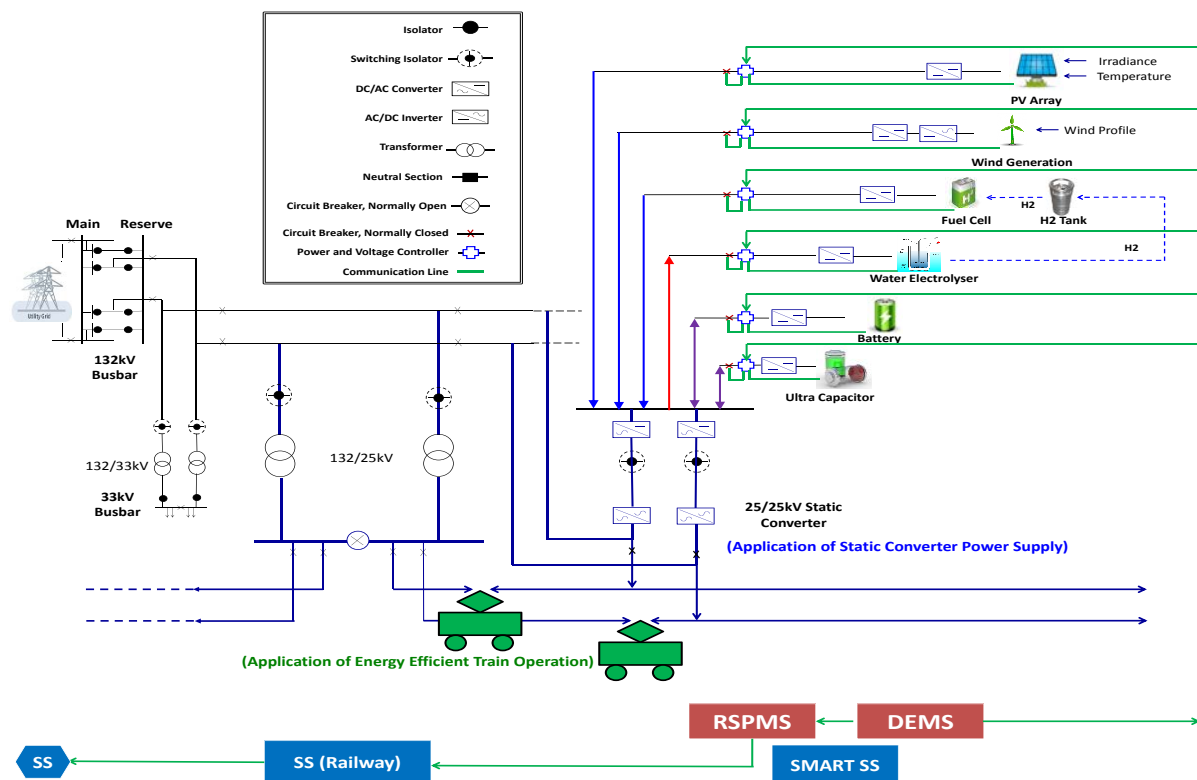
Figure 6-1: The future smart grid for railways with more DGs and multi-agent system

Figure 6-1 shows a schematic of an advanced smart grid railway multi-agent control system. In this scheme, a Railway Smart Power Management System (RSPMS) serves as the control agent, a Distributed Energy Management System (DERMS) serves as the DER agent and an existing Supervisory Control and Data Acquisition (SCADA) system is implemented in the railway SS as a user and database agent. DGs are connected in parallel to a grid site comprising the primary portion of a railway substation main transformer system. Each renewable generation source has its own converter, enabling it to communicate freely with the DERMS. This system differs from a standard micro grid control only with respect to its operation in islanded mode. Although smart and micro grids are generally able to cut all except the most important loads in islanded mode, it is difficult for a railway smart grid to operate in islanded mode if the DG capacity does not cover the peak load. Most loads come from one or more moving trains located within a given section and can change on a second-by-second basis. Although a moving load cannot be cut, in an urgent situation the load amount can be reduced by controlling train speed. Therefore, islanded mode is not used in normal conditions but remains a last resort for use in urgent situations. Work on this advanced smart rail grid will be continued during the author's PhD research.

6.3   Expected effects

6.3.1 Expected amounts of energy saving and electric generation capacity

Whereas a conventional traction system requires a100% power contribution from the existing grid, a traction system with a smart grid requires only 35% from the grid (Figure 6-2). Regenerative braking energy can provide 35% of the energy requirement, with DGs (renewables) and the ESS providing another 30% depending on the available space and energy consumption conditions. In terms of electric energy capacity, if the electric energy capacity of a conventional traction system is defined as 100%, a railway smart grid could achieve a capacity of about 215% in running the same system (Figure 6-3) by adding 35% regenerative braking energy under an optimised driving strategy, 50% using static converter substations and 30% using renewables and ESSs. This would also reduce the scale of a new substation by more than 50%, in turn reducing the land required for the substation and lowering its equipment requirements in terms of circuit breakers, transformers, cables and

protection systems. This would also cut the total initial cost of building one substation by more than half, as doubling the equipment load generally more than doubles the price[90].
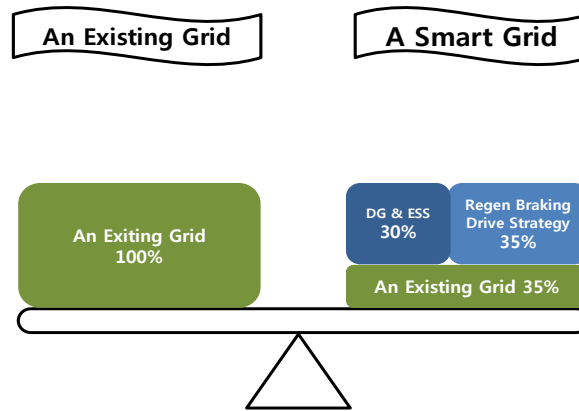
Figure 6-2: The expected amount of energy saving with a smart grid for railways
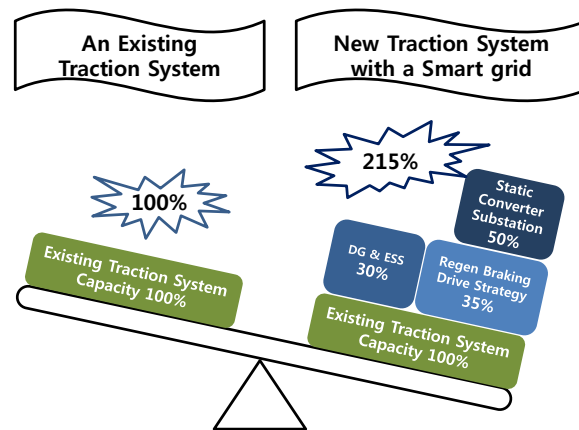
Figure 6-3: The expected electric generation capacity with a smart grid for railways

6.3.2 Expected advantages for railways

With respect to railway technologies, this research presents the following advantages and innovations:

- It presents an approach for securing a stable power supply without incident in a manner that reflects service capacity based on the use of technology for monitoring smart power and distributed energy resource management systems;
- It provides a stable linkage to the development of new renewable energy sources and power storage systems for aiding and managing power generation;
- It helps in the development of key technologies for smart grid for railways;

- It helps in the achievement of electric power industry technology competitiveness;
- It points the way toward the reduction of construction, running and maintenance costs.

This is also an oriented study that can help guide the current industry in the advanced planning of smart grid systems to be implemented in the near future. In addition to contributing to improvements in railway traction systems, implementing the methods and systems in this thesis would be expected to improve international competitiveness in terms of greenhouse gas reduction and to reduce energy imports. This study is vitally connected to the work of the Birmingham Centre for Railway Research and Education (BCRRE) at the University of Birmingham, which has been focussing on various aspects of smart grids for railways, including the optimisation of driving strategies, the use of static converter substations and the development of railway smart grid management systems.

7   References

[1]   MEF Partners Report, "Technology action plan: Smart Grids," *Rep. to Major Econ. Forum Energy Clim. Action Plan Smart Grids Rep. to Major Econ. Forum Energy Clim. Prep. by Italy Korea Consult. with MEF Partners*, 2009.

[2]   M. G. Simoes, R. Roche, E. Kyriakides, S. Suryanarayanan, B. Blunier, K. D. McBee, P. H. Nguyen, P. F. Ribeiro, and A. Miraoui, "A comparison of smart grid technologies and progresses in Europe and the U.S.," *IEEE Trans. Ind. Appl.*, vol. 48, no. 4, pp. 1154–1162, 2012.

[3]   S. M. Amin and B. F. Wollenberg, "Toward a smart grid: power delivery for the 21st century," *IEEE Power Energy Mag.*, vol. 3, no. 5, pp. 34–41, 2005.

[4]   M. Amin, "Balancing market priorities with security issues," *IEEE Power Energy Mag.*, vol. 2, no. 4, pp. 30–38, 2004.

[5]   H. Farhangi, "The path of the smart grid," *IEEE Power Energy Mag.*, vol. 8, no. 1, pp. 18–28, 2010.

[6]   L. I. Minchala-Avila, L. E. Garza-Castañón, A. Vargas-Martínez, and Y. Zhang, "A Review of Optimal Control Techniques Applied to the Energy Management and Control of Microgrids," *Procedia Comput. Sci.*, vol. 52, no. Seit, pp. 780–787, 2015.

[7]   Enerdata, "Global energy statistical yearbook 2015," 2015.

[8]   J. Jung, "A Study on the Analysis of Overseas Smart Grid's Demo Projects and the Future Direction of Integrated EMS Based on Reliable DR with Multi-Energy," Hoseo University, 2015.

[9]   United States Department of Energy, "Grid Modernization Multi-Year Program Plan," 2015.

[10]   ETP SmartGrids, *European technology platform smart grids: vision and strategy for Europe's electricity networks of the future*, vol. 19, no. 3. 2006.

[11]   European Commission, "Green Paper: A European strategy for sustainable, competitive and secure energy." [Online]. Available: http://eur-lex.europa.eu/legal-content/EN/TXT/?uri=URISERV:l27062.

[12]   A. Zervos, C. Lins, and J. Muth, "RE-thinking 2050: a 100% renewable energy vision for the European Union," *Erec*, 2010.

[13]   K. Brice and H. Bazmi, "Smart electricity," *ABB Rev.*, vol. 1, 2010.

[14]   Ofgem, "Network regulation – the RIIO model," 2013. [Online]. Available: https://www.ofgem.gov.uk/network-regulation-riio-model.

[15]   Ofgem, "Creating the right environment for demand-side response: next steps," 2013.

[16]   D. of E. and C. Change, "Smart Grid Vision and Routemap," 2014.

[17]   "What Caused the Power Blackout to Spread So Widely and So Fast? Genscape's Unique Data Will Help Answer That Question," *Cision*, 2003.

[18]   Congress, "American Recovery and Reinvestment Act 2009 Public Law 111–5 111th Congress An Act," p. 1–407 pg. 112 HITECH ACT, 2009.

[19]   Ministry of Trade Industry and Energy, "Smart Grid Roadmap in South Korea," 2010.

[20]   KEPCO, "Jeju Smart Grid Test bed," 2013. [Online]. Available: http://home.kepco.co.kr/kepco/KO/C/htmlView/KOCDHP00502.do?menuCd=FN050 30505.

[21]   "Sejong city supports 10 Millian won for new PV array generation," *Daejeon Today*, 2015.

[22]   Z. R. & Consulting, "Japan: Tsunami Wakens the Smart Grid," no. March, 2012.

[23]   S. F. Programme, "Map of smart grids initiatives : international outreach Revision : Final," 2014.

[24]   D. Xu, M. Wang, C. Wu, and K. Chan, "Evolution of the smart grid in China," *McKinsey Smart Grid*, pp. 18–23, 2010.

[25]   A. Ling, S. Kokichi, and M. Masao, "The Japanese Smart Grid Initiatives, Investments, and Collaborations," *Int. J. Adv. Sci. Appl.*, vol. 3, no. 7, pp. 44–54, 2012.

[26]   J. Zhang, H. Huang, and Y. B. Zhang, "The comparative analysis of foreign smart grid top-level roadmaps," *Power Syst. Technol. (…*, no. Powercon, pp. 20–22, 2014.

[27]   International Energy Agency, "Technology Roadmap - Smart Grids," 2011.

[28]   U.S. Department of Commerce, "2016 Top Markets Report Automotive Parts," 2016.

[29]   Y. Yu, J. Yang, and B. Chen, "The smart grids in China-A review," *Energies*, vol. 5, no. 5, pp. 1321–1338, 2012.

[30]   T. W. Palfreyman, "The smart grid applied to railway traction systems : A vision for integration," *Civil-Comp Press. 2012 Proc.*, pp. 1–21, 2012.

[31]   EU 7th Framework Programme, "Merlin Project." [Online]. Available: http://www.merlin-rail.eu/.

[32]   E. Commission, "Sustainable and intelligent management of energy for smarter railway systems in Europe an integrated optimisation approach B ackground," pp. 1– 145, 2013.

[33]   J. Hyungi and J. Jongduck, "Smart grid for urban railways," *Korean Soc. Railw.*, vol. 4, pp. 21–25, 2014.

[34]   H. Lee, Y. Cho, H. Kim, and H. Jung, "A Study for Power Management System using Regenerative Energy in," vol. 63, no. 1, pp. 191–196, 2014.

[35]   H. Hayashiya, H. Yoshizumi, T. Suzuki, T. Furukawa, T. Kondoh, M. Kitano, T. Aoki, T. Ishii, N. Kurosawa, and T. Miyagawa, "Necessity and possibility of smart grid

technology application on railway power supply system," *Proc. 2011 14th Eur. Conf. Power Electron. Appl.*, pp. 1–10, 2011.

[36] Y. Okada, T. Koseki, and K. Hisatomi, "Power Management Control in DC-electrified Railways for Regenerative Braking Systems of Electric Trains," *WIT Trans. State-of-the-art Sci. Eng.*, 2011.

[37] H. Hayashiya, Y. Watanabe, Y. Fukasawa, T. Miyagawa, A. Egami, T. Iwagami, S. Kikuchi, and H. Yoshizumi, "Cost impacts of high efficiency power supply technologies in railway power supply - Traction and Station - Traction a," *15th Int. Power Electron. Motion Control Conf. Expo. EPE-PEMC 2012 ECCE Eur.*, pp. 1–6, 2012.

[38] lifegate, "7,000 railway stations in India will be powered by solar energy _ LifeGate." .

[39] E. Pilo, S. K. Mazumder, and I. González-Franco, "Smart Electrical Infrastructure for AC-Fed Railways with Neutral Zones," *IEEE Trans. Intell. Transp. Syst.*, vol. 16, no. 2, pp. 642–652, 2015.

[40] F. Schmid and C. J. Goodman, "Electric railway systems in common use," *IET Semin. Dig.*, pp. 6–20, 2009.

[41] C. J. Goodman, "Overview of electric railway systems and the calculation of train performance," *9th IET Prof. Dev. Course Electr. Tract. Syst.*, pp. 13–36, 2006.

[42] Y. Kim, "Study on interconnecting dispered generation system to distribution system," Hanyang University, 2008.

[43] The IEC SG3, "IEC Smart grid standardization roadmap," *IEC*, 2010.

[44] R. E. L. Arnett, J. C.; Schaffer, L. A.; Rumberg, J. P.; Tolbert, "Design, installation and performance of the ARCO Solar one-megawatt power plant," *Photovolt. Sol. Energy Conf. Proc. Fifth Int. Conf. Athens, Greece, Oct. 17-21, 1983 (A85-11301 02-44). Dordrecht, D. Reidel Publ. Co., 1984, p. 314-320.*, 1984.

[45] Press Information Bureau G overnment of India Mi nistry of Heavy Industries & Public, "BHEL signs MoU for setting up an Ultra Mega Solar Power Project at Sambhar in Rajasthan," pp. 10–12, 2014.

[46] S. Jakovljevic and M. Kezunovic, "Advanced substation data collecting and processing for state estimation enhancement," *IEEE Power Eng. Soc. Summer Meet.*, vol. 1, pp. 201–206, 2002.

[47] "World's biggest floating solar farm powers up outside London," *theguardian*, 29-Feb-2016.

[48] KRRI, "Utilization of New Renewable Energy in Railway Areas and Development of Energy Saving Technologies," 2013.

[49] L. S. Piano and K. Mayumi, "Toward an integrated assessment of the performance of photovoltaic power stations for electricity generation," *Appl. Energy*, vol. 186, pp. 167–174, 2017.

[50] T. Yu and Y. Lin, "A Study on Maximum Power Point Tracking Algorithms for Photovoltaic Systems," *Yonghwa Tech. Univ.*, vol. 30.

[51] "History of Wind Energy," *energy.gov*. [Online]. Available: http://energy.gov/eere/wind/history-wind-energy.

[52] "Timeline: The history of wind power," *theguardian*, 17-Oct-2008.

[53] "Wind farm," *Wikipedia*. [Online]. Available: https://en.wikipedia.org/wiki/Wind_farm.

[54] "Wind Turbine Design," *Alternative energy tutorials*. [Online]. Available: http://www.alternative-energy-tutorials.com/wind-energy/wind-turbine-design.html.

[55] Y. P, S. Pivsa-Art, H. Ohgaki, P. Jansuya, and Y. Kumsuwan, "Design of MATLAB/Simulink Modeling of Fixed-pitch Angle Wind Turbine Simulator," *Energy Procedia*, vol. 34, pp. 362–370, 2013.

[56] J. Martinez, "Modelling and Control of Wind Turbines," 2007.

[57] S. W. Mohod and M. V. Aware, "Simulation of wind power with front-end converter into interconnected grid system," *J. Ind. Eng. Manag.*, vol. 2, no. 2, pp. 407–417, 2009.

[58] H. Ahn, "Study on the analysis and improvement of power quality using real-time simulator in distribution system with distributed generation," Sungkyunkwan University, 2013.

[59] IEC, "Electrical Energy Storage," *IEC_White Pap.*, vol. 39, pp. 11–12, 2009.

[60] X. Luo, J. Wang, M. Dooner, and J. Clarke, "Overview of current development in electrical energy storage technologies and the application potential in power system operation," *Appl. Energy*, vol. 137, pp. 511–536, 2015.

[61] RSSB, "Engineering Energy storage systems for railway applications," 2009.

[62] T. Ratniyomchai, S. Hillmansen, and P. Tricoli, "Optimal capacity and positioning of stationary supercapacitors for light rail vehicle systems," *2014 Int. Symp. Power Electron. Electr. Drives, Autom. Motion, SPEEDAM 2014*, pp. 807–812, 2014.

[63] A. Okui, S. Hase, H. Shigeeda, T. Konishi, and T. Yoshi, "Application of energy storage system for railway transportation in Japan," *2010 Int. Power Electron. Conf. - ECCE Asia -, IPEC 2010*, pp. 3117–3123, 2010.

[64] T. Konishi, H. Morimoto, T. Aihara, and M. Tsutakawa, "Fixed energy storage technology applied for DC Electrified railway," *IEEJ Trans. Electr. Electron. Eng.*, vol. 5, no. 3, pp. 270–277, 2010.

[65] P. Radcliffe, J. S. Wallace, and L. H. Shu, "Stationary applications of energy storage technologies for transit systems," *EPEC 2010 - IEEE Electr. Power Energy Conf. "Sustainable Energy an Intell. Grid,"* 2010.

[66] M. Steiner, M. Klohr, and S. Pagiela, "Energy storage system with Ultracaps on board of railway vehicles," *2007 Eur. Conf. Power Electron. Appl. EPE*, 2007.

[67] Bombardier, "MITRAC Energy saver," 2014.

[68] J. Runyon, "Energy Storage Industry Off and Running in January 2016," *Renewable Energy*, 2016. [Online]. Available: http://www.renewableenergyworld.com/articles/2016/01/energy-storage-set-for-record-year-in-2016.html.

[69] B. Seal and R. Uluski, "Integrating Smart Distributed Energy Resources with Distribution Management Systems," *Electr. Power Res. Instiute*, no. September, 2012.

[70] IEC, "Grid integration of large-capacity renewable energy sources and use of large-capacity electrical energy storage," 2012.

[71] S. Ahn, J. Park, I. Chung, S. Moon, S. Kang, and S. Nam, "Power-sharing method of multiple distributed generators considering contril modes and configurations of microgrid," *IEEE Trans. Power Deliv.*, 2010.

[72] C. H. Lo and N. Ansari, "Decentralized controls and communications for autonomous distribution networks in smart grid," *IEEE Trans. Smart Grid*, vol. 4, no. 1, pp. 66–77, 2013.

[73] E. F. Camacho, T. Samad, M. Garcia-Sanz, and I. Hiskens, "Control for Renewable Energy and Smart Grids," *Impact Control Technol.*, vol. 1, pp. 1–20, 2011.

[74] J. M. Guerrero, P. C. Loh, T. L. Lee, and M. Chandorkar, "Advanced control architectures for intelligent microgridsPart II: Power quality, energy storage, and AC/DC microgrids," *IEEE Trans. Ind. Electron.*, vol. 60, no. 4, pp. 1263–1270, 2013.

[75] K. Son and K. Lee, "A trend of control and analysis for a micro grid," *Electr. Electron. J.*, vol. 15, no. 2, p. 30~35, 2010.

[76] CERTS, "The CERTS MicroGrid Concept," 2002.

[77] X. Chen, Y. H. Wang, and Y. C. Wang, "A novel seamless transferring control method for microgrid based on master-slave configuration," *2013 IEEE ECCE Asia Downunder - 5th IEEE Annu. Int. Energy Convers. Congr. Exhib. IEEE ECCE Asia 2013*, pp. 351–357, 2013.

[78] J. Hu, T. Zhang, S. Du, and Y. Zhao, "An overview on analysis and control of micro-grid system," *Int. J. Control Autom.*, vol. 8, no. 6, pp. 65–76, 2015.

[79] K. Lim and J. Choi, "Droop Control for Parallel Inverers in Islanded Microgrid Considering Unbalanced Low-Voltage Line Impedances," *Transacrions Korean Inst. Power Electron.*, vol. 18, no. 4, pp. 387–396, 2013.

[80] V. Verma and G. Gowd Talapur, "Master-slave current control DGs in a microgrid for transient decoupling with mains," *India Int. Conf. Power Electron. IICPE*, pp. 1–6, 2012.

[81] J. M. Guerrero, J. Matas, L. de Vicuna, M. Castilla, and J. Miret, "Decentralized control for parallel operation of distributed generation inverters using resistive output impedance," *Ieee Trans. Ind. Electron.*, vol. 54, no. 2, pp. 994–1004, 2007.

[82] J. M. Guerrero, L. G. De Vicuña, J. Matas, J. Miret, and M. Castilla, "Output impedance design of parallel-connected UPS inverters with wireless load-sharing control," *IEEE Int. Symp. Ind. Electron.*, vol. 2, no. 4, pp. 1123–1128, 2004.

[83] M. Pipattanasomporn, H. Feroze, and S. Rahman, "Multi-agent systems in a distributed smart grid: Design and implementation," *IEEE/PES Power Syst. Conf. Expo. 2009. PSCE '09.*, pp. 1–8, 2009.

[84] BSI Group, "Draft BS EN 50641 Railway applicaions," 2014.

[85] "The European Commission's in-house science service." [Online]. Available: http://re.jrc.ec.europa.eu/pvgis/apps4/pvest.php.

[86] Decc, "Electricity Generation Costs," *Dep. Energy Clim. Chang.*, no. July, p. 68, 2013.

[87] Department of Energy & Climate Change, "Electricity Generation Costs 2013," 2013.

[88] National Grid, "Electricity Ten Year Statement 2015," no. November, p. 138, 2015.

[89] Lazard, "Lazard's levelized cost of storage analysis — version 1.0," no. November, 2015.

[90] Z. Tian, S. Hillmansen, C. Roberts, P. Weston, N. Zhao, L. Chen, and M. Chen, "Energy evaluation of the power network of a DC railway system with regenerating trains," *IET Electr. Syst. Transp. Press*, 2015.

Appendix A

Table A-1: the Results of simulations of 45 cases in 2020

No	ESS (MW)	Wind (MW)	PV (MW)	LCEG 2020	DG PV (A) 0.12	DG Wind (B) 0.12	ESS (D) 0.14	Grid From (F) 0.10	Grid To (G) -0.09	Charg ESS(H) -0.14	Smart Grid (I=A+B+D+F+G+H)	Traction Power (J) 0.10	I-J
1	1,000	-	1,000	MW	4,415	-	956	4,522	-	2,397		6,539	
				MWh	5,258	-	1,138	5,385	-	2,854		7,787	
				1000£	647	-	158	529	-	- 395	939	766	173
2	1,000	-	2,000	MW	8,830	-	776	2,497	3,343	2,218		6,539	
				MWh	10,515	-	924	2,974	3,981	2,641		7,787	
				1000£	1,293	-	128	292	- 352	- 365	996	766	230
3	1,000	-	3,000	MW	13,245	-	669	1,562	6,825	2,109		6,539	
				MWh	15,773	-	797	1,860	8,127	2,511		7,787	
				1000£	1,940	-	110	183	- 719	- 348	1,166	766	401
4	*1,000*	*1,000*	*-*	*MW*	-	*4,326*	*828*	*3,807*	*152*	*2,268*		6,539	
				MWh	-	*5,152*	*986*	*4,534*	*181*	*2,701*		7,787	
				1000£	-	*628*	*136*	*446*	*- 16*	*- 374*	*821*	766	*55*
5	1,000	1,000	1,000	MW	4,415	4,326	775	2,520	3,278	2,216		6,539	
				MWh	5,258	5,152	923	3,001	3,904	2,639		7,787	
				1000£	647	628	128	295	- 345	- 365	987	766	222
6	1,000	1,000	2,000	MW	8,830	4,326	669	1,579	6,750	2,112		6,539	
				MWh	10,515	5,152	797	1,880	8,038	2,515		7,787	
				1000£	1,293	628	110	185	- 711	- 348	1,158	766	392
7	1,000	1,000	3,000	MW	13,245	4,326	495	978	10,562	1,938		6,539	
				MWh	15,773	5,152	589	1,165	12,578	2,308		7,787	
				1000£	1,940	628	82	115	- 1,113	- 319	1,332	766	567
8	1,000	2,000	-	MW	-	8,652	773	2,543	3,213	2,213		6,539	
				MWh	-	10,303	921	3,028	3,826	2,635		7,787	
				1000£	-	1,257	127	298	- 339	- 365	979	766	213
9	1,000	2,000	1,000	MW	4,415	8,652	670	1,596	6,679	2,111		6,539	
				MWh	5,258	10,303	798	1,901	7,954	2,514		7,787	
				1000£	647	1,257	110	187	- 704	- 348	1,149	766	384
10	1,000	2,000	2,000	MW	8,830	8,652	496	990	10,486	1,938		6,539	
				MWh	10,515	10,303	591	1,179	12,487	2,308		7,787	
				1000£	1,293	1,257	82	116	- 1,105	- 319	1,324	766	558
11	1,000	2,000	3,000	MW	13,245	8,652	230	618	14,531	1,670		6,539	
				MWh	15,773	10,303	274	736	17,304	1,989		7,787	
				1000£	1,940	1,257	38	72	- 1,531	- 275	1,501	766	735
12	1,000	3,000	-	MW	-	12,977	671	1,622	6,607	2,111		6,539	
				MWh	-	15,453	799	1,932	7,868	2,514		7,787	
				1000£	-	1,885	111	190	- 696	- 348	1,142	766	376
13	1,000	3,000	1,000	MW	4,415	12,977	497	1,003	10,408	1,941		6,539	
				MWh	5,258	15,453	592	1,194	12,394	2,311		7,787	
				1000£	647	1,885	82	117	- 1,097	- 320	1,315	766	549
14	1,000	3,000	2,000	MW	8,830	12,977	236	625	14,445	1,679		6,539	
				MWh	10,515	15,453	281	744	17,202	1,999		7,787	
				1000£	1,293	1,885	39	73	- 1,522	- 277	1,492	766	726
15	1,000	3,000	3,000	*MW*	*13,245*	*12,977*	*155*	*385*	*18,620*	*1,596*		6,539	
				MWh	*15,773*	*15,453*	*185*	*458*	*22,173*	*1,901*		7,787	
				1000£	*1,940*	*1,885*	*26*	*45*	*- 1,962*	*- 263*	*1,671*	766	*905*
16	2,000	-	1,000	MW	4,415	-	1,586	4,522		2,397		6,539	
				MWh	5,258	-	1,889	5,385		2,854		7,787	
				1000£	647	-	261	529	-	- 395	1,042	766	277
17	2,000	-	2,000	MW	8,830	-	1,277	2,046	1,454	4,158		6,539	
				MWh	10,515	-	1,521	2,436	1,731	4,951		7,787	

No	ESS (MW)	Wind (MW)	PV (MW)
18	2,000	-	3,000
19	2,000	1,000	-
20	2,000	1,000	1,000
21	2,000	1,000	2,000
22	2,000	1,000	3,000
23	2,000	2,000	-
24	2,000	2,000	1,000
25	2,000	2,000	2,000
26	2,000	2,000	3,000
27	2,000	3,000	-
28	2,000	3,000	1,000
29	2,000	3,000	2,000
30	2,000	3,000	3,000
31	3,000	-	1,000
32	3,000	-	2,000
33	3,000	-	3,000
34	3,000	1,000	-
35	3,000	1,000	1,000
36	3,000	1,000	2,000
37	3,000	1,000	3,000

LCEG 2020	DG PV (A)	DG Wind (B)	ESS (D)	Grid From (F)	Grid To (G)	Charg ESS(H)	Smart Grid (I=A+B+D+F+G+H)	Traction Power (J)	I-J
coeff.	0.12	0.12	0.14	0.10	-0.09	-0.14		0.10	
1000£	1,293	-	210	240	- 153	- 685	905	766	139
MW	13,245	-	1,042	1,230	5,051	3,924		6,539	
MWh	15,773	-	1,241	1,465	6,015	4,673		7,787	
1000£	1,940	-	172	144	- 532	- 647	1,077	766	311
MW	-	4,326	1,369	3,362	-	2,517		6,539	
MWh	-	5,152	1,630	4,004	-	2,997		7,787	
1000£	-	628	226	394	-	- 415	833	766	67
MW	4,415	4,326	1,275	2,068	1,386	4,157		6,539	
MWh	5,258	5,152	1,518	2,463	1,650	4,950		7,787	
1000£	647	628	210	242	- 146	- 685	896	766	131
MW	8,830	4,326	1,041	1,246	4,979	3,921		6,539	
MWh	10,515	5,152	1,240	1,484	5,929	4,669		7,787	
1000£	1,293	628	172	146	- 525	- 646	1,069	766	303
MW	13,245	4,326	792	905	9,049	3,676		6,539	
MWh	15,773	5,152	943	1,078	10,776	4,378		7,787	
1000£	1,940	628	131	106	- 953	- 606	1,246	766	480
MW	-	8,652	1,271	2,092	1,322	4,151		6,539	
MWh	-	10,303	1,514	2,491	1,574	4,943		7,787	
1000£	-	1,257	209	245	- 139	- 684	888	766	122
MW	4,415	8,652	1,039	1,264	4,907	3,920		6,539	
MWh	5,258	10,303	1,237	1,505	5,843	4,668		7,787	
1000£	647	1,257	171	148	- 517	- 646	1,060	766	294
MW	8,830	8,652	793	916	8,928	3,674		6,539	
MWh	10,515	10,303	944	1,091	10,632	4,375		7,787	
1000£	1,293	1,257	131	107	- 941	- 605	1,242	766	477
MW	13,245	8,652	450	475	12,947	3,330		6,539	
MWh	15,773	10,303	536	566	15,418	3,965		7,787	
1000£	1,940	1,257	74	56	- 1,364	- 549	1,414	766	648
MW	-	12,977	1,113	1,208	4,763	3,993		6,539	
MWh	-	15,453	1,325	1,439	5,672	4,755		7,787	
1000£	-	1,885	183	141	- 502	- 658	1,050	766	285
MW	4,415	12,977	794	926	8,896	3,674		6,539	
MWh	5,258	15,453	946	1,103	10,594	4,375		7,787	
1000£	647	1,885	131	108	- 937	- 605	1,228	766	463
MW	8,830	12,977	464	479	12,860	3,348		6,539	
MWh	10,515	15,453	553	570	15,314	3,987		7,787	
1000£	1,293	1,885	76	56	- 1,355	- 552	1,404	766	639
MW	13,245	12,977	288	245	17,041	3,180		6,539	
MWh	15,773	15,453	343	292	20,293	3,787		7,787	
1000£	1,940	1,885	47	29	- 1,796	- 524	1,582	766	816
MW	4,415	-	2,216	4,522		2,397		6,539	
MWh	5,258	-	2,639	5,385	-	2,854		7,787	
1000£	647	-	365	529	-	- 395	1,146	766	381
MW	8,830	-	1,682	1,706		5,676		6,539	
MWh	10,515	-	2,003	2,032	-	6,759		7,787	
1000£	1,293	-	277	200	-	- 935	835	766	69
MW	13,245	-	1,184	1,246	3,626	5,506		6,539	
MWh	15,773	-	1,410	1,484	4,318	6,557		7,787	
1000£	1,940	-	195	146	- 382	- 907	992	766	226
MW	-	4,326	1,923	2,906	-	2,615		6,539	
MWh	-	5,152	2,290	3,461	-	3,114		7,787	
1000£	-	628	317	340	-	- 431	855	766	89
MW	4,415	4,326	1,680	1,728	-	5,607		6,539	
MWh	5,258	5,152	2,001	2,058	-	6,677		7,787	
1000£	647	628	277	202	-	- 924	830	766	65
MW	8,830	4,326	1,182	1,259	3,552	5,503		6,539	
MWh	10,515	5,152	1,408	1,499	4,230	6,553		7,787	
1000£	1,293	628	195	147	- 374	- 907	983	766	217
MW	13,245	4,326	1,108	798	7,503	5,430		6,539	
MWh	15,773	5,152	1,319	950	8,935	6,466		7,787	

No	ESS (MW)	Wind (MW)	PV (MW)
38	3,000	2,000	-
39	3,000	2,000	1,000
40	3,000	2,000	2,000
41	3,000	2,000	3,000
42	3,000	3,000	-
43	3,000	3,000	1,000
44	3,000	3,000	2,000
45	3,000	3,000	3,000

LCEG 2020	0.12	0.12	0.14	0.10	-0.09	-0.14		0.10	
	DG		ESS (D)	Grid		Charg ESS(H)	Smart Grid (I=A+B+D+F+G+H)	Traction Power (J)	I-J
	PV (A)	Wind (B)	ESS (D)	From (F)	To (G)	Charg ESS(H)	Smart Grid	Traction Power (J)	I-J
1000£	1,940	628	183	93	- 791	- 895	1,159	766	394
MW	-	8,652	1,678	1,746	-	5,534		6,539	
MWh	-	10,303	1,998	2,079	-	6,590		7,787	
1000£	-	1,257	277	204	-	- 912	826	766	60
MW	4,415	8,652	1,184	1,272	3,475	5,506		6,539	
MWh	5,258	10,303	1,410	1,515	4,138	6,557		7,787	
1000£	647	1,257	195	149	- 366	- 907	974	766	209
MW	8,830	8,652	1,110	809	7,425	5,431		6,539	
MWh	10,515	10,303	1,322	963	8,842	6,467		7,787	
1000£	1,293	1,257	183	95	- 782	- 895	1,151	766	385
MW	13,245	8,652	640	361	11,393	4,959		6,539	
MWh	15,773	10,303	762	430	13,567	5,905		7,787	
1000£	1,940	1,257	105	42	- 1,200	- 817	1,327	766	562
MW	-	12,977	1,184	1,287	3,401	5,505		6,539	
MWh	-	15,453	1,410	1,533	4,050	6,556		7,787	
1000£	-	1,885	195	151	- 358	- 907	966	766	200
MW	4,415	12,977	1,111	820	7,345	5,435		6,539	
MWh	5,258	15,453	1,323	976	8,747	6,472		7,787	
1000£	647	1,885	183	96	- 774	- 896	1,142	766	376
MW	8,830	12,977	658	368	11,307	4,982		6,539	
MWh	10,515	15,453	784	438	13,465	5,933		7,787	
1000£	1,293	1,885	108	43	- 1,191	- 821	1,318	766	552
MW	13,245	12,977	314	263	15,618	4,636		6,539	
MWh	15,773	15,453	374	313	18,598	5,521		7,787	
1000£	1,940	1,885	52	31	- 1,646	- 764	1,498	766	733

Table A-2: the Results of simulations of 45 cases in 2025

No	ESS (MW)	Wind (MW)	PV (MW)	LCEG 2025	DG — PV (A) 0.105	DG — Wind (B) 0.116	ESS (D) 0.14	Grid — From (F) 0.100	Grid — To (G) -0.090	Charg ESS (H) -0.14	Smart Grid (I=A+B+D+F+G+H)	Traction Power (J) 0.10	I-J
1	1,000	-	1,000	MW	4,415	-	956	4,522	-	2,397		6,539	
				MWh	5,258	-	1,138	5,385	-	2,854	-	7,787	
				1000£	552	-	158	540	-	- 395	855	766	74
2	1,000	-	2,000	MW	8,830	-	776	2,497	3,343	2,218		6,539	
				MWh	10,515	-	924	2,974	3,981	2,641	-	7,787	
				1000£	1,104	-	128	298	- 360	- 365	805	766	24
3	1,000	-	3,000	MW	13,245	-	669	1,562	6,825	2,109		6,539	
				MWh	15,773	-	797	1,860	8,127	2,511	-	7,787	
				1000£	1,656	-	110	187	- 734	- 348	871	766	90
4	1,000	1,000	-	MW	-	4,326	828	3,807	152	2,268		6,539	
				MWh	-	5,152	986	4,534	181	2,701	-	7,787	
				1000£	-	598	136	455	- 16	- 374	799	766	17
5	1,000	1,000	1,000	MW	4,415	4,326	775	2,520	3,278	2,216		6,539	
				MWh	5,258	5,152	923	3,001	3,904	2,639	-	7,787	
				1000£	552	598	128	301	- 353	- 365	861	766	79
6	1,000	1,000	2,000	MW	8,830	4,326	669	1,579	6,750	2,112		6,539	
				MWh	10,515	5,152	797	1,880	8,038	2,515	-	7,787	
				1000£	1,104	598	110	189	- 726	- 348	927	766	145
7	1,000	1,000	3,000	MW	13,245	4,326	495	978	10,562	1,938		6,539	
				MWh	15,773	5,152	589	1,165	12,578	2,308	-	7,787	
				1000£	1,656	598	82	117	- 1,136	- 319	997	766	215
8	1,000	2,000	-	MW	-	8,652	773	2,543	3,213	2,213		6,539	
				MWh	-	10,303	921	3,028	3,826	2,635	-	7,787	
				1000£	-	1,195	127	304	- 346	- 365	916	766	135
9	1,000	2,000	1,000	MW	4,415	8,652	670	1,596	6,679	2,111		6,539	
				MWh	5,258	10,303	798	1,901	7,954	2,514	-	7,787	
				1000£	552	1,195	110	191	- 718	- 348	982	766	201
10	1,000	2,000	2,000	MW	8,830	8,652	496	990	10,486	1,938		6,539	
				MWh	10,515	10,303	591	1,179	12,487	2,308	-	7,787	
				1000£	1,104	1,195	82	118	- 1,128	- 319	1,052	766	271
11	1,000	2,000	3,000	MW	13,245	8,652	230	618	14,531	1,670		6,539	
				MWh	15,773	10,303	274	736	17,304	1,989	-	7,787	
				1000£	1,656	1,195	38	74	- 1,563	- 275	1,125	766	344
12	1,000	3,000	-	MW	-	12,977	671	1,622	6,607	2,111		6,539	
				MWh	-	15,453	799	1,932	7,868	2,514	-	7,787	
				1000£	-	1,793	111	194	- 711	- 348	1,039	766	257
13	1,000	3,000	1,000	MW	4,415	12,977	497	1,003	10,408	1,941		6,539	
				MWh	5,258	15,453	592	1,194	12,394	2,311	-	7,787	
				1000£	552	1,793	82	120	- 1,119	- 320	1,107	766	326
14	1,000	3,000	2,000	MW	8,830	12,977	236	625	14,445	1,679		6,539	
				MWh	10,515	15,453	281	744	17,202	1,999	-	7,787	
				1000£	1,104	1,793	39	75	- 1,554	- 277	1,180	766	399
15	*1,000*	*3,000*	*3,000*	MW	*13,245*	*12,977*	*155*	*385*	*18,620*	*1,596*		6,539	
				MWh	*15,773*	*15,453*	*185*	*458*	*22,173*	*1,901*	-	7,787	
				1000£	*1,656*	*1,793*	*26*	*46*	*- 2,003*	*- 263*	*1,255*	766	*473*
16	2,000	-	1,000	MW	4,415	-	1,586	4,522		2,397		6,539	
				MWh	5,258	-	1,889	5,385	-	2,854	-	7,787	
				1000£	552	-	261	540	-	- 395	959	766	177
17	2,000	-	2,000	MW	8,830	-	1,277	2,046	1,454	4,158		6,539	
				MWh	10,515	-	1,521	2,436	1,731	4,951	-	7,787	
				1000£	1,104	-	210	244	- 156	- 685	717	766	- 64
18	2,000	-	3,000	MW	13,245	-	1,042	1,230	5,051	3,924		6,539	
				MWh	15,773	-	1,241	1,465	6,015	4,673	-	7,787	
				1000£	1,656	-	172	147	- 543	- 647	785	766	4
19	2,000	1,000	-	MW	-	4,326	1,369	3,362	-	2,517		6,539	
				MWh	-	5,152	1,630	4,004	-	2,997	-	7,787	

No	ESS (MW)	Wind (MW)	PV (MW)
20	2,000	1,000	1,000
21	2,000	1,000	2,000
22	2,000	1,000	3,000
23	2,000	2,000	-
24	2,000	2,000	1,000
25	2,000	2,000	2,000
26	2,000	2,000	3,000
27	2,000	3,000	-
28	2,000	3,000	1,000
29	2,000	3,000	2,000
30	2,000	3,000	3,000
31	3,000	-	1,000
32	**3,000**	**-**	**2,000**
33	3,000	-	3,000
34	3,000	1,000	-
35	3,000	1,000	1,000
36	3,000	1,000	2,000
37	3,000	1,000	3,000
38	3,000	2,000	-
39	3,000	2,000	1,000

LCEG 2025	0.105	0.116	0.14	0.100	-0.090	-0.14		0.10	
	DG		ESS	Grid		Charg ESS(H)	Smart Grid (I=A+B+D+F+G+H)	Traction Power (J)	I-J
	PV (A)	Wind (B)	(D)	From (F)	To (G)				
1000£	-	598	226	402	-	- 415	810	766	29
MW	4,415	4,326	1,275	2,068	1,386	4,157		6,539	
MWh	5,258	5,152	1,518	2,463	1,650	4,950	-	7,787	
1000£	552	598	210	247	- 149	- 685	773	766	- 9
MW	8,830	4,326	1,041	1,246	4,979	3,921		6,539	
MWh	10,515	5,152	1,240	1,484	5,929	4,669	-	7,787	
1000£	1,104	598	172	149	- 535	- 646	840	766	59
MW	13,245	4,326	792	905	9,049	3,676		6,539	
MWh	15,773	5,152	943	1,078	10,776	4,378	-	7,787	
1000£	-	1,195	209	250	- 142	- 684	828	766	47
MW	-	8,652	1,271	2,092	1,322	4,151		6,539	
MWh	-	10,303	1,514	2,491	1,574	4,943	-	7,787	
1000£	552	1,195	171	151	- 528	- 646	896	766	114
MW	4,415	8,652	1,039	1,264	4,907	3,920		6,539	
MWh	5,258	10,303	1,237	1,505	5,843	4,668	-	7,787	
1000£	1,104	1,195	131	109	- 960	- 605	974	766	192
MW	8,830	8,652	793	916	8,928	3,674		6,539	
MWh	10,515	10,303	944	1,091	10,632	4,375	-	7,787	
1000£	1,656	1,195	74	57	- 1,392	- 549	1,041	766	260
MW	13,245	8,652	450	475	12,947	3,330		6,539	
MWh	15,773	10,303	536	566	15,418	3,965	-	7,787	
1000£	-	1,793	183	144	- 512	- 658	950	766	169
MW	-	12,977	1,113	1,208	4,763	3,993		6,539	
MWh	-	15,453	1,325	1,439	5,672	4,755	-	7,787	
1000£	552	1,793	131	111	- 957	- 605	1,024	766	243
MW	4,415	12,977	794	926	8,896	3,674		6,539	
MWh	5,258	15,453	946	1,103	10,594	4,375	-	7,787	
1000£	1,104	1,793	76	57	- 1,383	- 552	1,096	766	314
MW	8,830	12,977	464	479	12,860	3,348		6,539	
MWh	10,515	15,453	553	570	15,314	3,987	-	7,787	
1000£	1,656	1,793	47	29	- 1,833	- 524	1,169	766	387
MW	13,245	12,977	288	245	17,041	3,180		6,539	
MWh	15,773	15,453	343	292	20,293	3,787	-	7,787	
MW	4,415	-	2,216	4,522		2,397		6,539	
MWh	5,258	-	2,639	5,385	-	2,854	-	7,787	
1000£	552	-	365	540	-	- 395	1,063	766	281
MW	**8,830**	**-**	**1,682**	**1,706**		**5,676**		6,539	
MWh	**10,515**	**-**	**2,003**	**2,032**	**-**	**6,759**	**-**	7,787	
1000£	**1,104**	**-**	**277**	**204**	**-**	**- 935**	**650**	766	**- 132**
MW	13,245	-	1,184	1,246	3,626	5,506		6,539	
MWh	15,773	-	1,410	1,484	4,318	6,557	-	7,787	
1000£	1,656	-	195	149	- 390	- 907	703	766	- 79
MW	-	4,326	1,923	2,906	-	2,615		6,539	
MWh	-	5,152	2,290	3,461	-	3,114	-	7,787	
1000£	-	598	317	347	-	- 431	831	766	49
MW	4,415	4,326	1,680	1,728	-	5,607		6,539	
MWh	5,258	5,152	2,001	2,058	-	6,677	-	7,787	
1000£	552	598	277	206	-	- 924	709	766	- 72
MW	8,830	4,326	1,182	1,259	3,552	5,503		6,539	
MWh	10,515	5,152	1,408	1,499	4,230	6,553	-	7,787	
1000£	1,104	598	195	150	- 382	- 907	758	766	- 23
MW	13,245	4,326	1,108	798	7,503	5,430		6,539	
MWh	15,773	5,152	1,319	950	8,935	6,466	-	7,787	
1000£	1,656	598	183	95	- 807	- 895	830	766	49
MW	-	8,652	1,678	1,746	-	5,534		6,539	
MWh	-	10,303	1,998	2,079	-	6,590	-	7,787	
1000£	-	1,195	277	209	-	- 912	768	766	- 13
MW	4,415	8,652	1,184	1,272	3,475	5,506		6,539	

No	ESS (MW)	Wind (MW)	PV (MW)
40	3,000	2,000	2,000
41	3,000	2,000	3,000
42	3,000	3,000	-
43	3,000	3,000	1,000
44	3,000	3,000	2,000
45	3,000	3,000	3,000

LCEG 2025	DG		ESS (D)	Grid		Charg ESS(H)	Smart Grid (I=A+B+D+F+G+H)	Traction Power (J)	I-J
	PV (A)	Wind (B)		From (F)	To (G)				
	0.105	0.116	0.14	0.100	-0.090	-0.14		0.10	
MWh	5,258	10,303	1,410	1,515	4,138	6,557	-	7,787	
1000£	552	1,195	195	152	- 374	- 907	813	766	32
MW	8,830	8,652	1,110	809	7,425	5,431		6,539	
MWh	10,515	10,303	1,322	963	8,842	6,467	-	7,787	
1000£	1,104	1,195	183	97	- 799	- 895	885	766	104
MW	13,245	8,652	640	361	11,393	4,959		6,539	
MWh	15,773	10,303	762	430	13,567	5,905	-	7,787	
1000£	1,656	1,195	105	43	- 1,225	- 817	957	766	176
MW	-	12,977	1,184	1,287	3,401	5,505		6,539	
MWh	-	15,453	1,410	1,533	4,050	6,556	-	7,787	
1000£	-	1,793	195	154	- 366	- 907	869	766	87
MW	4,415	12,977	1,111	820	7,345	5,435		6,539	
MWh	5,258	15,453	1,323	976	8,747	6,472	-	7,787	
1000£	552	1,793	183	98	- 790	- 896	940	766	159
MW	8,830	12,977	658	368	11,307	4,982		6,539	
MWh	10,515	15,453	784	438	13,465	5,933	-	7,787	
1000£	1,104	1,793	108	44	- 1,216	- 821	1,012	766	231
MW	13,245	12,977	314	263	15,618	4,636		6,539	
MWh	15,773	15,453	374	313	18,598	5,521	-	7,787	
1000£	1,656	1,793	52	31	- 1,680	- 764	1,088	766	307

Table A-3: the Results of simulations of 45 cases in 2030

No	ESS (MW)	Wind (MW)	PV (MW)	LCEG 2030	DG		ESS (D)	Grid		Charg ESS(H)	Smart Grid (I=A+B+D+F+G+H)	Traction Power (J)	I-J
					PV (A) 0.09	Wind (B) 0.11	0.14	From (F) 0.10	To (G) -0.09	-0.14		0.10	
1	1,000	-	1,000	MW	4,415	-	956	4,522	-	2,397		6,539	
				MWh	5,258	-	1,138	5,385	-	2,854	-	7,787	
				1000£	473	-	158	532	-	- 395	768	770	- 2
2	1,000	-	2,000	MW	8,830	-	776	2,497	3,343	2,218		6,539	
				MWh	10,515	-	924	2,974	3,981	2,641	-	7,787	
				1000£	946	-	128	294	- 354	- 365	649	766	- 121
3	1,000	-	3,000	MW	13,245	-	669	1,562	6,825	2,109		6,539	
				MWh	15,773	-	797	1,860	8,127	2,511	-	7,787	
				1000£	1,420	-	110	184	- 723	- 348	643	766	- 127
4	1,000	1,000	-	MW	-	4,326	828	3,807	152	2,268		6,539	
				MWh	-	5,152	986	4,534	181	2,701	-	7,787	
				1000£	-	587	136	448	- 16	- 374	782	766	12
5	1,000	1,000	1,000	MW	4,415	4,326	775	2,520	3,278	2,216		6,539	
				MWh	5,258	5,152	923	3,001	3,904	2,639	-	7,787	
				1000£	473	587	128	297	- 347	- 365	772	766	3
6	1,000	1,000	2,000	MW	8,830	4,326	669	1,579	6,750	2,112		6,539	
				MWh	10,515	5,152	797	1,880	8,038	2,515	-	7,787	
				1000£	946	587	110	186	- 715	- 348	767	766	- 3
7	1,000	1,000	3,000	MW	13,245	4,326	495	978	10,562	1,938		6,539	
				MWh	15,773	5,152	589	1,165	12,578	2,308	-	7,787	
				1000£	1,420	587	82	115	- 1,119	- 319	765	766	- 4
8	1,000	2,000	-	MW	-	8,652	773	2,543	3,213	2,213		6,539	
				MWh	-	10,303	921	3,028	3,826	2,635	-	7,787	
				1000£	-	1,175	127	299	- 340	- 365	896	766	127
9	1,000	2,000	1,000	MW	4,415	8,652	670	1,596	6,679	2,111		6,539	
				MWh	5,258	10,303	798	1,901	7,954	2,514	-	7,787	
				1000£	473	1,175	110	188	- 708	- 348	891	766	121
10	1,000	2,000	2,000	MW	8,830	8,652	496	990	10,486	1,938		6,539	
				MWh	10,515	10,303	591	1,179	12,487	2,308	-	7,787	
				1000£	946	1,175	82	117	- 1,111	- 319	889	766	119
11	1,000	2,000	3,000	MW	13,245	8,652	230	618	14,531	1,670		6,539	
				MWh	15,773	10,303	274	736	17,304	1,989	-	7,787	
				1000£	1,420	1,175	38	73	- 1,539	- 275	890	766	121
12	1,000	3,000	-	MW	-	12,977	671	1,622	6,607	2,111		6,539	
				MWh	-	15,453	799	1,932	7,868	2,514	-	7,787	
				1000£	-	1,762	111	191	- 700	- 348	1,015	766	246
13	1,000	3,000	1,000	MW	4,415	12,977	497	1,003	10,408	1,941		6,539	
				MWh	5,258	15,453	592	1,194	12,394	2,311	-	7,787	
				1000£	473	1,762	82	118	- 1,103	- 320	1,012	766	243
14	1,000	3,000	2,000	MW	8,830	12,977	236	625	14,445	1,679		6,539	
				MWh	10,515	15,453	281	744	17,202	1,999	-	7,787	
				1000£	946	1,762	39	74	- 1,530	- 277	1,014	766	244
15	**1,000**	**3,000**	**3,000**	*MW*	*13,245*	*12,977*	*155*	*385*	*18,620*	*1,596*		*6,539*	
				MWh	*15,773*	*15,453*	*185*	*458*	*22,173*	*1,901*	*-*	*7,787*	
				1000£	*1,420*	*1,762*	*26*	*45*	*- 1,972*	*- 263*	*1,017*	*766*	*247*
16	2,000	-	1,000	MW	4,415	-	1,586	4,522		2,397		6,539	
				MWh	5,258	-	1,889	5,385	-	2,854	-	7,787	
				1000£	473	-	261	532	-	- 395	872	766	102
17	2,000	-	2,000	MW	8,830	-	1,277	2,046	1,454	4,158		6,539	
				MWh	10,515	-	1,521	2,436	1,731	4,951	-	7,787	
				1000£	946	-	210	241	- 154	- 685	558	766	- 211
18	2,000	-	3,000	MW	13,245	-	1,042	1,230	5,051	3,924		6,539	
				MWh	15,773	-	1,241	1,465	6,015	4,673	-	7,787	
				1000£	1,420	-	172	145	- 535	- 647	554	766	- 215
19	2,000	1,000	-	MW	-	4,326	1,369	3,362	-	2,517		6,539	
				MWh	-	5,152	1,630	4,004	-	2,997	-	7,787	
				1000£	-	587	226	396	-	- 415	794	766	24

No	ESS (MW)	Wind (MW)	PV (MW)	LCEG 2030	DG PV (A) 0.09	Wind (B) 0.11	ESS (D) 0.14	Grid From (F) 0.10	To (G) -0.09	Charg ESS(H) -0.14	Smart Grid (I=A+B+D +F+G+H)	Traction Power (J) 0.10	I-J
20	2,000	1,000	1,000	MW	4,415	4,326	1,275	2,068	1,386	4,157		6,539	
				MWh	5,258	5,152	1,518	2,463	1,650	4,950	-	7,787	
				1000£	473	587	210	243	-147	-685	682	766	-88
21	2,000	1,000	2,000	MW	8,830	4,326	1,041	1,246	4,979	3,921		6,539	
				MWh	10,515	5,152	1,240	1,484	5,929	4,669	-	7,787	
				1000£	946	587	172	147	-527	-646	678	766	-91
22	2,000	1,000	3,000	MW	13,245	4,326	792	905	9,049	3,676		6,539	
				MWh	15,773	5,152	943	1,078	10,776	4,378	-	7,787	
				1000£	1,420	587	131	107	-959	-606	680	766	-90
23	2,000	2,000	-	MW	-	8,652	1,271	2,092	1,322	4,151		6,539	
				MWh	-	10,303	1,514	2,491	1,574	4,943	-	7,787	
				1000£	-	1,175	209	246	-140	-684	806	766	37
24	2,000	2,000	1,000	MW	4,415	8,652	1,039	1,264	4,907	3,920		6,539	
				MWh	5,258	10,303	1,237	1,505	5,843	4,668	-	7,787	
				1000£	473	1,175	171	149	-520	-646	802	766	32
25	2,000	2,000	2,000	MW	8,830	8,652	793	916	8,928	3,674		6,539	
				MWh	10,515	10,303	944	1,091	10,632	4,375	-	7,787	
				1000£	946	1,175	131	108	-946	-605	808	766	39
26	2,000	2,000	3,000	MW	13,245	8,652	450	475	12,947	3,330		6,539	
				MWh	15,773	10,303	536	566	15,418	3,965	-	7,787	
				1000£	1,420	1,175	74	56	-1,372	-549	804	766	34
27	2,000	3,000	-	MW	-	12,977	1,113	1,208	4,763	3,993		6,539	
				MWh	-	15,453	1,325	1,439	5,672	4,755	-	7,787	
				1000£	-	1,762	183	142	-505	-658	925	766	155
28	2,000	3,000	1,000	MW	4,415	12,977	794	926	8,896	3,674		6,539	
				MWh	5,258	15,453	946	1,103	10,594	4,375	-	7,787	
				1000£	473	1,762	131	109	-942	-605	927	766	157
29	2,000	3,000	2,000	MW	8,830	12,977	464	479	12,860	3,348		6,539	
				MWh	10,515	15,453	553	570	15,314	3,987	-	7,787	
				1000£	946	1,762	76	56	-1,362	-552	927	766	157
30	2,000	3,000	3,000	MW	13,245	12,977	288	245	17,041	3,180		6,539	
				MWh	15,773	15,453	343	292	20,293	3,787	-	7,787	
				1000£	1,420	1,762	47	29	-1,805	-524	928	766	159
31	3,000	-	1,000	MW	4,415	-	2,216	4,522		2,397		6,539	
				MWh	5,258	-	2,639	5,385	-	2,854	-	7,787	
				1000£	473	-	365	532	-	-395	976	766	206
32	3,000	-	2,000	MW	8,830	-	1,682	1,706		5,676		6,539	
				MWh	10,515	-	2,003	2,032	-	6,759	-	7,787	
				1000£	946	-	277	201	-	-935	489	766	-281
33	**3,000**	**-**	**3,000**	**MW**	**13,245**	**-**	**1,184**	**1,246**	**3,626**	**5,506**		**6,539**	
				MWh	**15,773**	**-**	**1,410**	**1,484**	**4,318**	**6,557**	**-**	**7,787**	
				1000£	**1,420**	**-**	**195**	**147**	**-384**	**-907**	**470**	**766**	**-300**
34	3,000	1,000	-	MW	-	4,326	1,923	2,906	-	2,615		6,539	
				MWh	-	5,152	2,290	3,461	-	3,114	-	7,787	
				1000£	-	587	317	342	-	-431	815	766	46
35	3,000	1,000	1,000	MW	4,415	4,326	1,680	1,728	-	5,607		6,539	
				MWh	5,258	5,152	2,001	2,058	-	6,677	-	7,787	
				1000£	473	587	277	203	-	-924	617	766	-153
36	3,000	1,000	2,000	MW	8,830	4,326	1,182	1,259	3,552	5,503		6,539	
				MWh	10,515	5,152	1,408	1,499	4,230	6,553	-	7,787	
				1000£	946	587	195	148	-376	-907	594	766	-176
37	3,000	1,000	3,000	MW	13,245	4,326	1,108	798	7,503	5,430		6,539	
				MWh	15,773	5,152	1,319	950	8,935	6,466	-	7,787	
				1000£	1,420	587	183	94	-795	-895	594	766	-176
38	3,000	2,000	-	MW	-	8,652	1,678	1,746	-	5,534		6,539	
				MWh	-	10,303	1,998	2,079	-	6,590	-	7,787	
				1000£	-	1,175	277	206	-	-912	745	766	-25
39	3,000	2,000	1,000	MW	4,415	8,652	1,184	1,272	3,475	5,506		6,539	
				MWh	5,258	10,303	1,410	1,515	4,138	6,557	-	7,787	
				1000£	473	1,175	195	150	-368	-907	717	766	-53

No	ESS (MW)	Wind (MW)	PV (MW)
40	3,000	2,000	2,000
41	3,000	2,000	3,000
42	3,000	3,000	-
43	3,000	3,000	1,000
44	3,000	3,000	2,000
45	3,000	3,000	3,000

LCEG 2030	0.09	0.11	0.14	0.10	-0.09	-0.14		0.10	
	DG		ESS (D)	Grid		Charg ESS(H)	Smart Grid (I=A+B+D+F+G+H)	Traction Power (J)	I-J
	PV (A)	Wind (B)		From (F)	To (G)				
MW	8,830	8,652	1,110	809	7,425	5,431		6,539	
MWh	10,515	10,303	1,322	963	8,842	6,467	-	7,787	
1000£	946	1,175	183	95	- 787	- 895	718	766	- 52
MW	13,245	8,652	640	361	11,393	4,959		6,539	
MWh	15,773	10,303	762	430	13,567	5,905	-	7,787	
1000£	1,420	1,175	105	42	- 1,207	- 817	718	766	- 52
MW	-	12,977	1,184	1,287	3,401	5,505		6,539	
MWh	-	15,453	1,410	1,533	4,050	6,556	-	7,787	
1000£	-	1,762	195	151	- 360	- 907	841	766	71
MW	4,415	12,977	1,111	820	7,345	5,435		6,539	
MWh	5,258	15,453	1,323	976	8,747	6,472	-	7,787	
1000£	473	1,762	183	97	- 778	- 896	841	766	71
MW	8,830	12,977	658	368	11,307	4,982		6,539	
MWh	10,515	15,453	784	438	13,465	5,933	-	7,787	
1000£	946	1,762	108	43	- 1,198	- 821	841	766	71
MW	13,245	12,977	314	263	15,618	4,636		6,539	
MWh	15,773	15,453	374	313	18,598	5,521	-	7,787	
1000£	1,420	1,762	52	31	- 1,654	- 764	846	766	76